To my little Alessandro and
my love Diego

Contents

1. Introduction

What is it? Why does it happen? How does it happen? These are the three salient questions biogerontologists continue to ask about the real nature of aging (Martin, 2006). Besides disagreeing on the proper spelling of the word (ag*i*ng or ag*ei*ng?), the scientists don't manage to reach an agreement on the precise meaning of aging, on the difference (if it exists) between aging and senescence, on the principal causes of this phenomenon, and on the possible methods to prevent and/or to eliminate at least some of the deleterious aspects of aging itself.

The lengthening of the average human life span and of the maximum life span, with the consequent increase in the percentage of elderly people, and so in the proportion of the national health expenditures utilized for them, have finally stimulated a boom in biological, epidemiological and demographic studies on aging over the last decades. A lot of different theories, not mutually exclusive and difficult to unravel, have been developed to explain aging and its consequences, leading, after all, to an expanded and complex concept of aging, as a multifactorial process in which several processes may interact at the same time, operating at different levels of functional organization (reviewed in Weinert & Timiras, 2003; see figure 1).

For several researchers, from a conceptual point of view, aging measures the passing of time as minutes, days and years, and all things age, whether living or non-living, but only the living ones can senescence. This is the critical difference adduced by them between senescence and aging: senescent processes are multifactorial and deleterious, and they increase the probability of death, while aging may lead to behavioural, biological and life style changes that can affect people also without bringing risks of death (reviewed in Crews, 2007). Anyway, the core issue is that many physiological decrements, occurring in concert with age, reflect both senescent and disease processes, besides the simply passage of time; really, senescent changes, that are inherent to cells and that alter molecular and physiological processes, even if they are not time-dependent, accumulate over an organism's life span, making it age-related.

Among the different theories summarized in the table of figure 1, what seems to be more important to capture is the idea that the aging process of complex

organisms, as humans, is the result of interactions between intrinsic (genetic and cellular), stochastic (random damage to vital molecules), and extrinsic (environmental) causes. Many social, behavioural and environmental factors affect people as they grow old in a social setting, and, on the other hand, the altered interactions across genetic, protein, cellular, tissue, organ, and organ system levels might contribute to body aging.

To understand and counteract the ultimate causes of the complex process of human aging is, sure enough, far beyond the aim of this Ph.D. thesis. What I hopefully aimed to do, at the beginning of this three years course, was to make my contribution to the experimental research on the aging of a specific tissue, the skeletal muscle, and in particular on the involvement in the aging process of the specific adult stem cell of the skeletal muscle, the satellite cells.

The topic of my personal research is briefly introduced in the next paragraphs, while the basic methods and main results obtained, completed with discussion, are presented subsequently. Finally, in the enclosed appendixes, it is possible to find the final published results.

Table 1. *Classification and brief description of main theories of aging*

Biological Level/Theory	Description
Evolutionary	
Mutation accumulation*	Mutations that affect health at older ages are not selected against.
Disposable soma*	Somatic cells are maintained only to ensure continued reproductive success; after reproduction, soma becomes disposable.
Antagonistic pleiotropy*	Genes beneficial at younger age become deleterious at older ages.
Molecular	
Gene regulation*	Aging is caused by changes in the expression of genes regulating both development and aging.
Codon restriction	Fidelity/accuracy of mRNA translation is impaired due to inability to decode codons in mRNA.
Error catastrophe	Decline in fidelity of gene expression with aging results in increased fraction of abnormal proteins.
Somatic mutation	Molecular damage accumulates, primarily to DNA/genetic material.
Dysdifferentiation	Gradual accumulation of random molecular damage impairs regulation of gene expression.
Cellular	
Cellular senescence-Telomere theory*	Phenotypes of aging are caused by an increase in frequency of senescent cells. Senescence may result from telomere loss (replicative senescence) or cell stress (cellular senescence).
Free radical*	Oxidative metabolism produces highly reactive free radicals that subsequently damage lipids, protein and DNA.
Wear-and-tear	Accumulation of normal injury.
Apoptosis	Programmed cell death from genetic events or genome crisis.
System	
Neuroendocrine*	Alterations in neuroendocrine control of homeostasis results in aging-related physiological changes.
Immunologic*	Decline of immune function with aging results in decreased incidence of infectious diseases but increased incidence of autoimmunity.
Rate-of-living	Assumes a fixed amount of metabolic potential for every living organism (live fast, die young).

Figure1: Theories formulated to explain aging processes (Table 1 from Weinert & Timiras, 2003).

1.1 The skeletal muscle aging

It is difficult to study aging: in fact, the aging process differs considerably in different species, and so it is hard to explicitly correlate human aging to that of most other species usually studied in the researchers' laboratories; moreover, aging occurs at different rates in the various tissues of the body, and age-related changes in one organ may affect the function of other organs and tissues. The multitude of age-related biochemical and structural changes in different tissues lead to the decline in cognitive, sensory and motor abilities, among other general changes that typically occur with age.

With regard to skeletal muscle tissue, studies performed in humans showed an age-related decrease in muscle mass, quality, strength and endurance from the fourth decade of life (reviewed in Nair, 2005). This muscle dysfunctions can affect physical performance and functional status in a lot of activities of daily living of elderly people, such as walking and sitting-to-standing transfers, with risk of falls and fractures, which may get to understand the public health significance of these dysfunctions (Dutta et al., 1997). This age-related muscle deterioration is usually called sarcopenia, from the Greek *sarx* (óÜñî) for flesh and *penia* (ðåíßá) for loss (Rosenberg, 1997); the knowledge accumulated in the last few decades concerning this phenomenon is being used to develop possible therapies to try to retard the age-related loss of muscle functions, and so to improve the physical condition of the elderly.

A variety of factors appear to be involved in the involuntary skeletal muscle wasting that is common in both old humans and animals, and that is often referred to as "sarcopenia of old age" (in Carmeli et al., 2002). Even if the mechanisms of sarcopenia is incompletely understood, a lot of elegant reports and reviews on the possible mechanisms involved are now available (for some recent ones, see Carmeli et al., 2002; Vandervoort, 2002; Doherty, 2003; Greenlund and Nair, 2003; Marcell, 2003; Evans, 2004; Dupont-Versteegden, 2005; Nair, 2005; Di Iorio et al., 2006; Schaap et al., 2006; Solomon and Bouloux, 2006; Edstrőm et al., 2007). To schematically summarize the principal reviewed factors involved in age-related deterioration of muscle mass and strength, it is possible to divide them in:

1. the extrinsic factors, that can be further differentiated in:

- extrinsic to the whole organism, or environmental factors; they include, among others, the individual diet, possible traumatic injuries or diseases, and a sedentary or, on the other hand, an active lifestyle;
- extrinsic to the skeletal muscle, as, for example, changes in the hormonal milieu, alterations in cytokines availability, dysfunctions of central and peripheral nervous system, with a consequent different availability of neurotransmitters and neurotrophic factors;

2. the skeletal muscle intrinsic factors, which include:
   - alterations in the transcriptional profile, due for example to telomere shortening linked to accumulating cell divisions, epigenetic changes, chromatin reorganization and oncogenes activation;
   - changes in protein structure and metabolism;
   - altered redox modulation of muscle contraction and physiology, probably also due to mitochondrial dysfunctions;
   - changes of the sarcolemmal excitability, and alterations of the mechanisms controlling Ca^{2+} handling.

These factors can negatively affect both skeletal muscle fibres and satellite cells, the most specific stem cells available postnatally for skeletal muscle growth and repair (see *Section 1.2*). Indeed, the consequences of these age-dependent alterations are firstly clearly visible in the decrease of muscle mass in older animals and humans, now considered to be in part the result of a loss of mature post-mitotic fibres, and a reduction in their size, mainly of the type 2 fast-twitch ones (in Larsson and Ramamurthy, 2000; for a review see Doherty, 2003 or Greenlund and Nair, 2003). Moreover, in the remaining old fibres, age-related changes in proteins expression and structure, in sarcolemmal excitability and in the mechanisms controlling Ca^{2+} handling are well proved, leading to the deterioration of the two principal contractile parameters, the specific force (force divided by cross-sectional area) and the shortening velocity (in Delbono, 2002 and in Prochniewicz et al., 2007; see *Section 1.3*).

In addition, the capacity of skeletal muscle fibres to properly regenerate is severely impaired in the elderly, mainly because of the decline in the proliferation and differentiation ability of satellite cells, as it will be better described in the next section.

1.2 Satellite cells, muscle regeneration and aging

1.2.1 The satellite cell

Satellite cells were first discovered by Mauro in 1961, and described as intimately associated with the skeletal muscle fibre. In figure 2 it is possible to observe an electron micrograph of a satellite cell, inserted between the plasma membrane of the muscle fibre and the basement membrane, and protruding inward, pushing aside the myofibrils of the fibre.

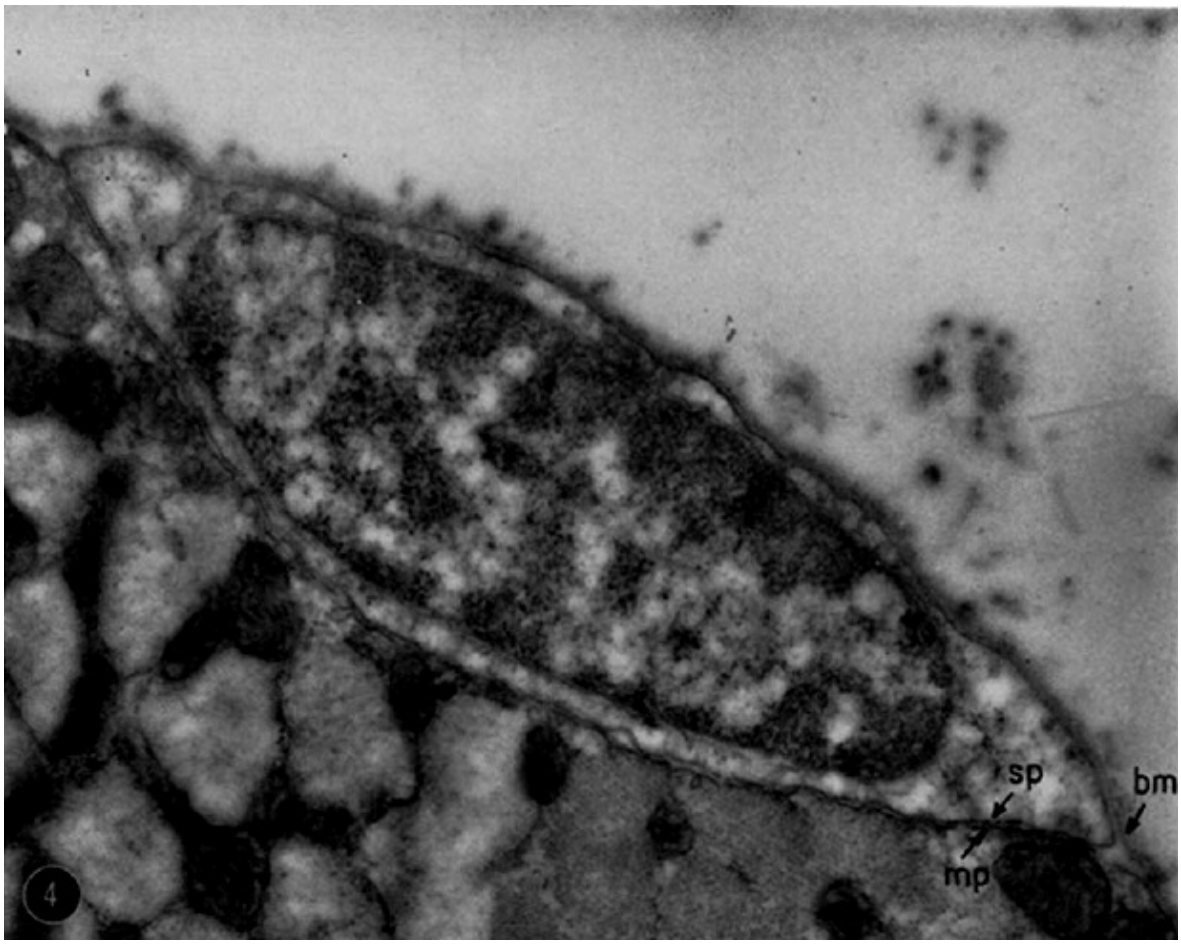

Figure 2: Transverse section of a skeletal muscle fibre from the rat sartorius, in which at the inner border of a satellite cell it is possible to discern the apposing plasma membrane of the satellite cell (sp) and of the fibre (mp), and the basement membrane (bm), extending over the gap between the two membranes (magnification: x 22.000; from figure 1.4, Mauro, 1961).

Already Mauro in 1961 asked himself two important questions about satellite cells: what is their origin? and what is their function? Since 1961 several studies and researches have been adding up to the knowledge of these cells, today universally recognized as the pre-eminent stem cell of the skeletal muscle (for recent reviews

see: Seale and Rudnicki, 2000; Hawke and Garry, 2001; Goldring et al., 2002; Morgan and Partridge, 2003; Dhawan and Rando, 2005; Anderson, 2006).

The embryological origin of satellite cells has been a topic of long-lived debate, and, to date, there is not an end to the matter. Recent evidences pointed out that satellite cells are designated in development by the expression of specific markers, as the transcriptional regulation factors Pax3 and Pax7, appear after primary muscle fibres have formed, and have a somitic dermomyotomal origin (Gros et al., 2005), also if myogenic progenitors from dorsal aorta can also contribute to muscle growth (reviewed in Morgan and Partridge, 2003 and Dhawan and Rando, 2005). Not only there is more than one type of muscle precursor, but quiescent satellite cells, as well as their activated and proliferating progeny, have a complex profile of gene expression, and no single biochemical marker has been found that specifically identifies all satellite cells (in Dhawan and Rando, 2005; Anderson, 2006; Hepple, 2006). To illustrate the complex problem of the origin and the heterogeneity of satellite cells goes beyond the point of this section, while it is preferred to set out a closer examination of the principal functions of satellite cells.

The location beneath the basal lamina of a mature myofiber remains the cornerstone of the identification of satellite cells, and also of their definition, and support the idea that these cells are the primary cells that participate not only in the normal myonuclear turnover, but also in the adaptation, repair and regeneration of the muscle after an injury. In a recent review, Anderson defines satellite cells as the intimate companions of voluntary muscle fibres, and as the major contributors to the plasticity of skeletal muscle. The author elegantly summered the principal roles of satellite cells, by using five metaphors to clarify the nature of satellite cell functions in skeletal muscle plasticity. As schematically showed in figure 3, satellite cells could be seen as the “currency” (1), the “conveyance” (2), the “clue” (3), the “connector” (4) and the “colander” (5) of the skeletal muscle:

1)The “currency” role of satellite cells: satellite cells could be seen as the operational “cash-units” of muscle tissue, the “building blocks”, that, by proliferating and by fusing to the fibre sarcolemma, can support development, adaptation and regeneration. Indeed, a lot of studies (for review see Morgan and

Partridge, 2003; Dhawan and Rando, 2005; Anderson, 2006) have proved that, in response to a stimulus, for example a muscle injury, the satellite cells can exit the quiescence, proliferate, migrate and fuse to form new fibres that elongate between mature fibres and eventually tendons (see figures 4 and 5). These capacities may be reduced or exhausted in severe conditions as dystrophies (Blau et al., 1983), or with age, as it will be described in *Section 1.2.2*.

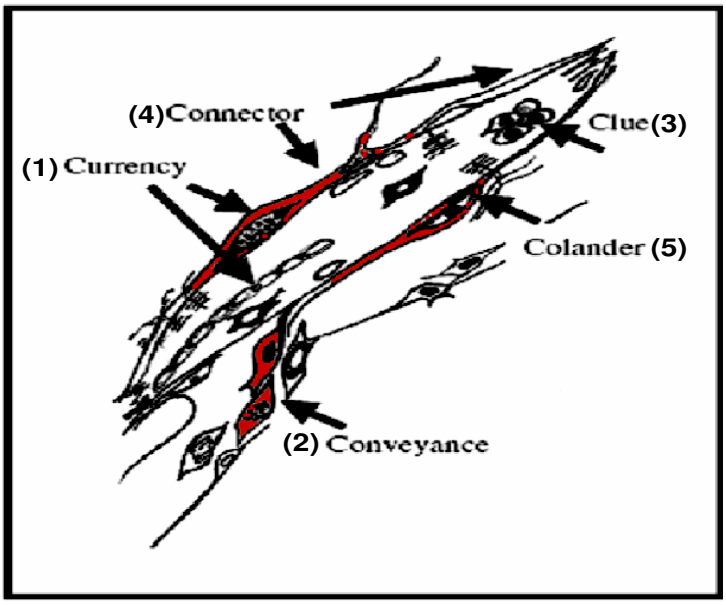

Figure 3: A simple scheme of a regenerating fibre, in which some satellite cells are shown in red, and their five principal roles are indicated: 1)"currency" to make new muscle tissue, 2)"conveyance" to improve muscle plasticity and function, 3)"clue" of development and regeneration in mature muscle, 4)"connector" between fibres and the surrounding environmental of the "myogenic network", 5)"colander" to filter and rework the informations coming from the environment to the fibres (modified from Anderson, 2006).

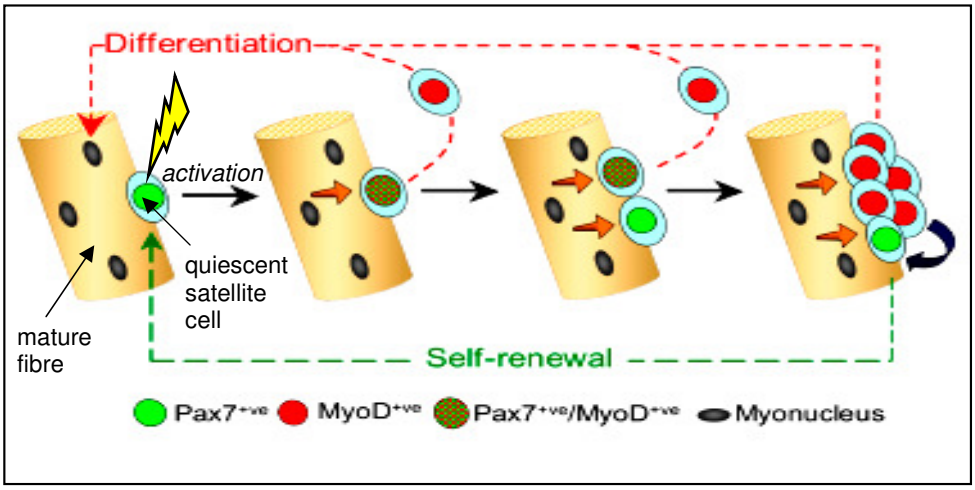

Figure 4: A schematic model of the possible self-renewal or differentiation of a satellite cell: after the activation by an external stimulus, a satellite cell proliferate (green and red pattern), and the progeny can enter the differentiation program (red), or become quiescent (green), thus renewing the satellite cell pool; the different activation of the two transcription factors Pax7 and MyoD is also indicated (modified from Zammit et al., 2004).

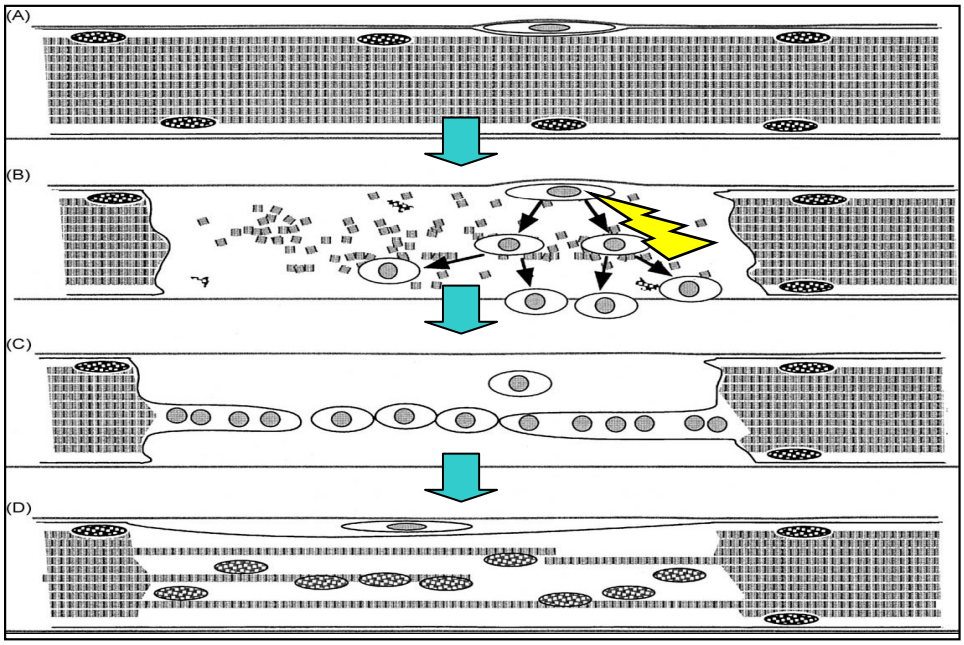

Figure 5: The process of regeneration of an injured skeletal muscle fibre: in (A) a mature fibre with some myonuclei and a sublaminar satellite cell are shown; in (B) the activation of the satellite cell after the injure stimulus, and the consequent proliferation; in (C) the progeny of the satellite cell proceeds in aligning and fusing together, in order to repair the damaged muscle fibre, in (D) the regenerated muscle fibre with a new quiescent satellite cell derived from the self-renewal of the progenitor (modified from Morgan and Partridge, 2003).

2)The "conveyance" role of satellite cells: the satellite cells are seen as "conveyors" of muscle plasticity, that can give to the fibres the "access", *i.e.* a particular phenotype, to new, adapted functions, required to adequately respond to

extrinsic and intrinsic changes, linked to different environmental and muscle tissue conditions (see *Section 1.1*). The “conveyance” role is also revealed by the stem cell nature of satellite cells (see Seale and Rudnicki, 2000; and Dhawan and Rando, 2005), which have been proved to be, at least in part, pluripotent cells that can adapt to demands in other tissues outside skeletal muscle (Jackson et al., 1999). In this optic, satellite cells could be also displayed as “conveyors” in tissue engineering and cell therapy (Irintchev et al., 1997; Wernig et al., 2000, Mouly et al., 2005), or for the expression in loco of different proteins lacked in different pathological statuses, like the hormone IGF-1 in muscle of elderly people (Musarò and Rosenthal, 1999), or dystrophin in Duchenne patients (Gussoni et al.,1999).

3)The “clue” role of satellite cells: in this case the satellite cells have been seen as “clues”, to investigators and researchers, on the nature of the myogenesis and the plasticity of myogenic cell lineages in development and adaption (Anderson, 2006). They are a sort of “markers of events” in mature skeletal muscle, that follow activation and entry into the cell cycle, recapitulating muscle development during embryogenesis (Hawke and Garry, 2001).

4)The “connector” role of satellite cells: satellite cells reside between the sarcolemma of a mature fibre and the basal lamina, thus being part of the environment of the mature fibre. When quiescent, they can receive several signals from the fibre and the surrounding environment; once activated from these signals (for a review see Hawke and Garry, 2001), they may become real “connectors” between the different elements of the “myogenic network”, such as mature fibres, other mononuclear satellite cells, blood vessels, connective tissue, nerve terminals, extra-cellular matrix, immune system cells, and so on (figure 6).

In fact, satellite cells, and their activated progeny, not only express receptors through which they can receive signals from their environment, but are also able to express surface molecules, as M-chaderin, and to produce and release several growth and trophic factors, or gaseous molecules as nitric oxide (reviewed in Anderson, 2006), which enable them to be an active, important participant in the signal trafficking between mature fibres and the environment.

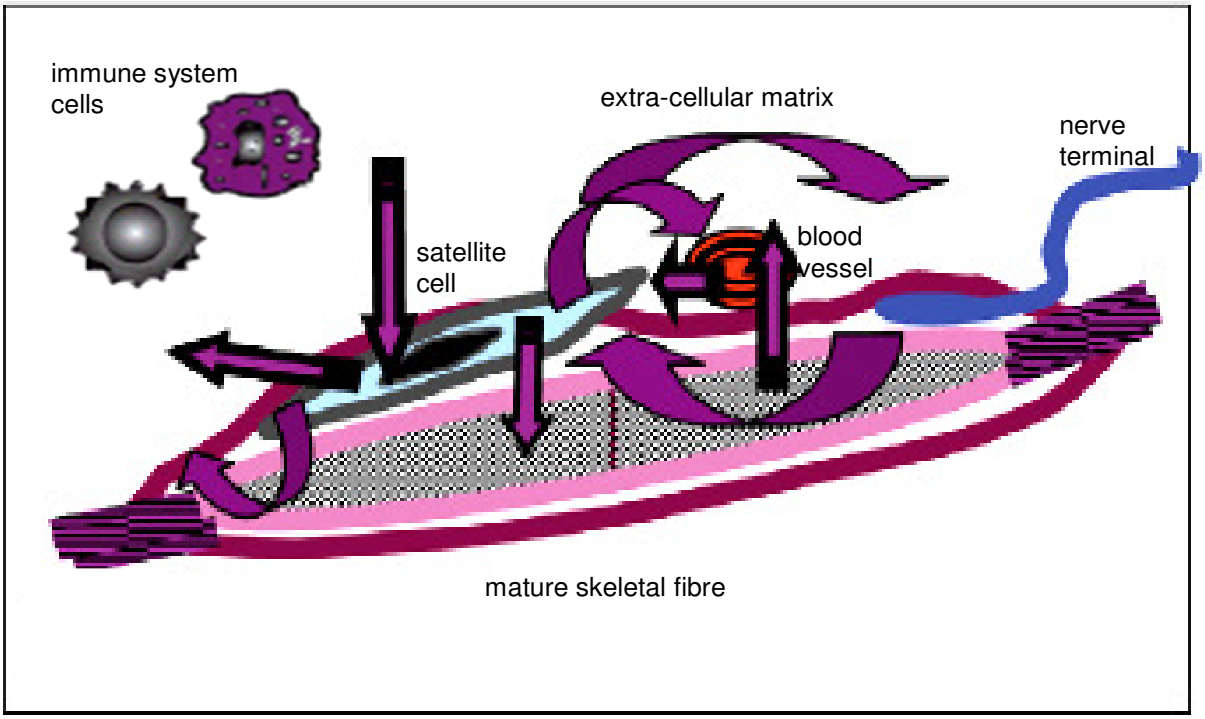

Figure 6: A schematic rapresentation of the "myogenic network", in which the satellite cell is seen as a "connector" between the various elements (modified from Anderson, 2006).

5)The "colander" role of satellite cells: what is highlighted with this last metaphor, is the capacity of satellite cells to "filter" the informations coming from the environment to the fibres. Therefore, the resident satellite cells on a specific region of a myofibre may provide help to this region to discern among different signals and to interpret them in the best way, as an environmental strainer. Moreover, a satellite cell can reside permanently in a region, thanks to interactions through adhesion proteins, or can migrate towards other regions, by releasing specific enzymes; this is an ulterior evidence that satellite cells are active "colanders", that filter the various stimuli related to muscle plasticity (reviewed in Anderson, 2006).

It follows, from what described so far, that, even though skeletal muscle has not a very high range of turnover under usual physiological conditions, it has a great capacity to regenerate in response to different kinds of patho-physiological stimuli, and satellite cells account just for virtually all this regenerative potential (in Conboy and Rando, 2005). This could be of great importance when considering the process of skeletal muscle aging, as it will be explained in the next section.

1.2.2 The myogenic potency in aging skeletal muscle

The senescence process of a body is manifested in every tissue and organ, and can be interpreted as a sign of aging at the level of its somatic stem cells; indeed, we could say that a living organism is as old as its stem cells, since the regenerative potential of a living organism is determined by the possibility and capacity of its stem cells to replace exhausted cells and damaged tissue (Ho et al., 2005).

However, it is very important to note that the already limited regenerative power of mammals of replacing some types of tissue, such as skin and bone marrow, thanks to the resident stem cells, declines with age (Ho et al., 2005). And the same we can say for the skeletal muscle tissue, where, as already anticipated above, it is possible to observe an age-related decline in the effectiveness of the regenerative myogenic response to injury. Being muscle satellite cells the most specific myogenic cells available postnatally for skeletal muscle growth and repair, a consequence of the continuous demand on their activity for muscle tissue regeneration could be the exhaustion of their proliferative ability in aged muscle (Decary et al., 1997; Ranault et al., 2002; Wernig et al., 2005; Shafer et al, 2006).

Indeed, over the last 15 years, an idea is coming out that age-related sarcopenia is associated with an impaired satellite cells regenerative response (reviewed in Hepple, 2006 and Solomon and Bouloux, 2006). Despite some divergent opinions (Hikida et al., 1998; Roth et al., 2000), one of the emerging hypothesis is that increasing human age is accompanied by a reduction in the satellite cells population (Renault et al., 2000; Saiko et al., 2004; Kadi et al., 2004).

This reduction could be based on age-related impaired self-renewal, which could occur, as visualized in figure 7, at three different steps (Shefer et al., 2006):

1) lack of activation of the quiescent satellite cell,

2) fail to undergo clonal expansion after the activation,

3) failure to form reserve cells after the proliferation.

Impaired efficiency in the three steps of self-renewal might be due both by *i*) the age-affected environment and *ii*) by intrinsic changes in the satellite cells themselves (see *Section 1.1*).

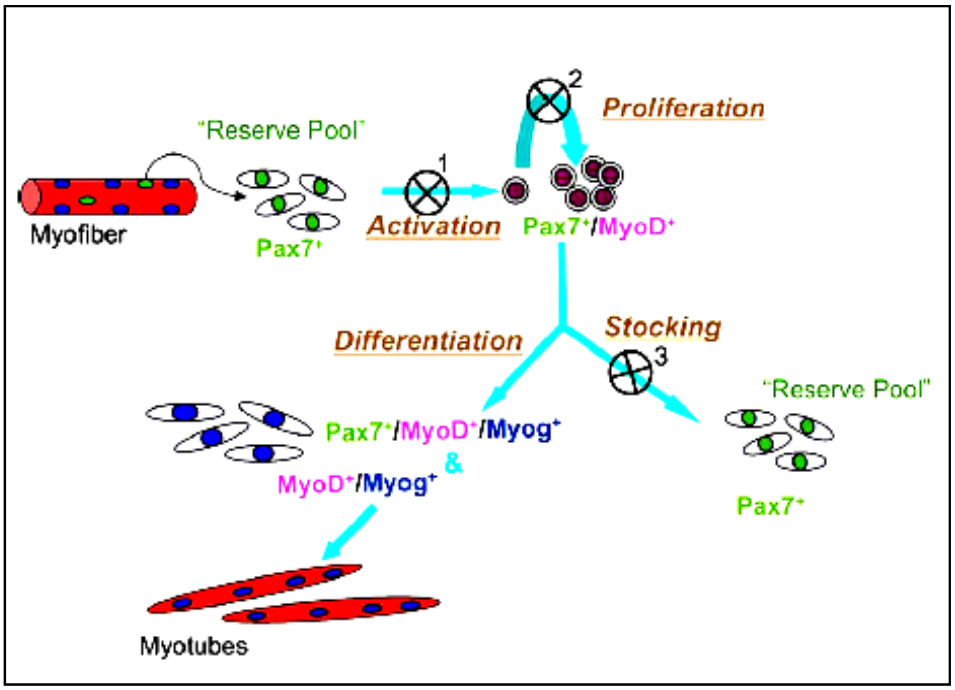

Figure 7: A schematic model representing possible mechanisms for age-related satellite cells pool depletion, in which three different steps that could be impaired in the mechanism of self-renewal of satellite cells are indicated with the symbol ⊗ (the different activation of the transcription factors Pax7, MyoD and myogenin at every step is also indicated; from Shefer et al., 2006).

Focusing the attention on the second point (*ii*), the age-related accumulation of cell generations in a satellite cell may entail, among other things, DNA damage, telomere dysfunction, a different pattern of gene expression, and epigenetic changes, that could lead to an impaired self-renewal and to the so-called cellular senescence, characterized by an irreversible growth arrest and certain altered functions (reviewed in Serrano and Blasco, 2001; Campisi and d'Adda di Fagagna, 2007). Cellular senescence was described firstly as the limited ability of cells to proliferate in culture *in vitro*, and was then proposed to recapitulate the age-related loss of regenerative capacity of cells *in vivo* (in Campisi and d'Adda di Fagagna, 2007); even if the relationship between cell aging *in vivo* and *in vitro* is still matter of debate (reviewed in Rubin, 1997), there are several pieces of evidence showing that senescent cells may persist and accumulate with age *in vivo* and that replicative senescence contributes to aging (Dimri et al, 1995, Campisi, 2001). For these reasons, a useful model of *in vivo* aging of satellite cells may be the aging of the same cells *in vitro* under culture conditions (Decary, 1996); this model would allow to investigate if the replicative senescence affects their regenerating ability (see *Sections 3.1* and *4.1*).

Moreover, senescent satellite cells seem to be to a certain degree resistant to apoptosis, and this might partly explain why senescent cells are stable in culture *in vitro*, and their number increases with age *in vivo*. These senescent cells accumulated during aging *in vivo* are proved to be characterized by striking changes in gene expression, also unrelated to growth arrest, but that can produce, for example, alterations of the skeletal muscle tissue microenvironment, thus contributing to the already mentioned age-related changes in muscle structure and function (in Campisi and d'Adda di Fagagna, 2007, see figure 8).

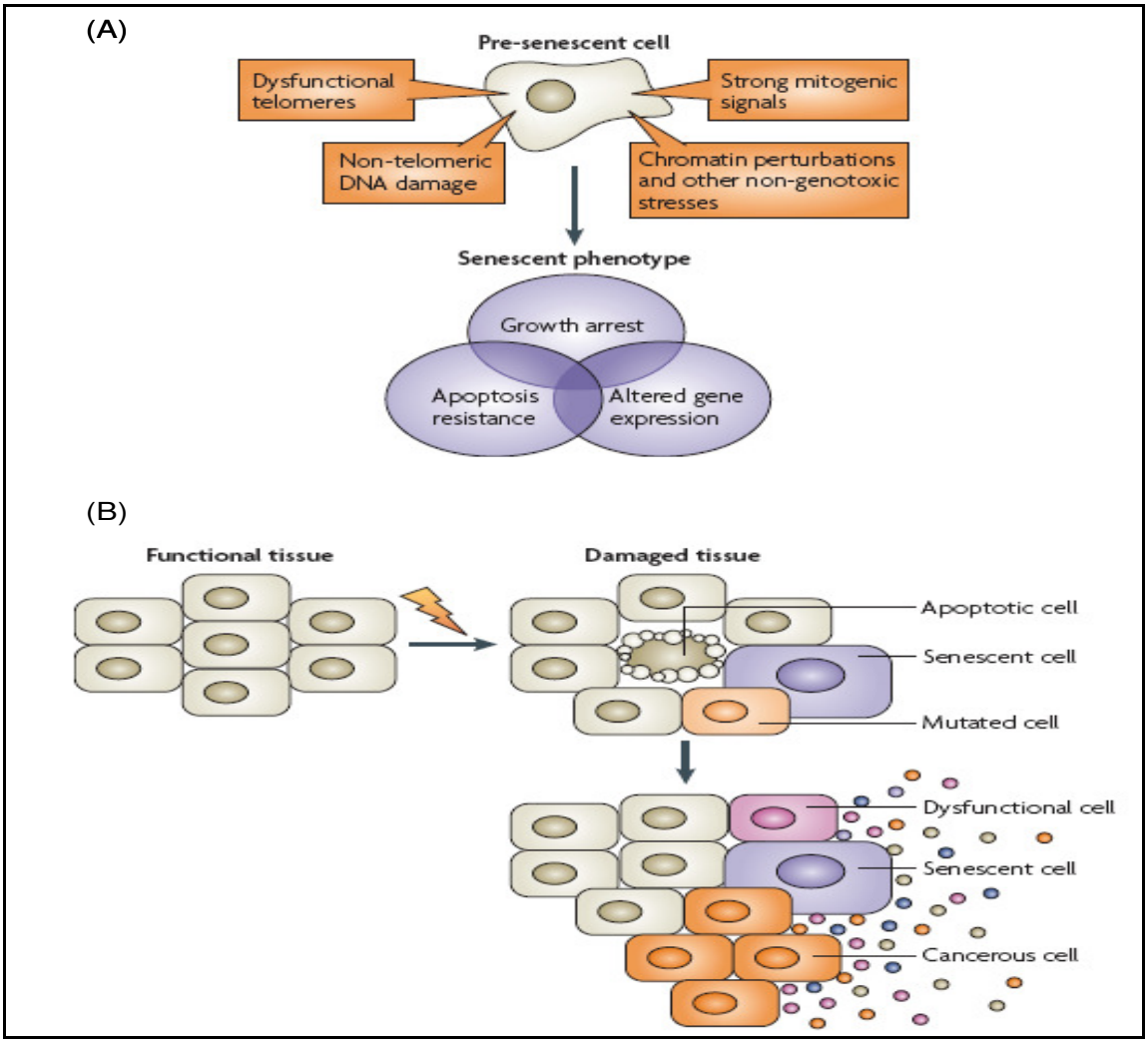

Figure 8: Two simple schemes depicting how satellite senescent cells may persist and accumulate with age *in vivo* and why replicative senescence may contribute to age-related dysfunctions. In (A) the principal age-related intrinsic changes that could lead to the senescent phenotype of a satellite cell; in (B) potential damaging effects of a senescent cell: it could release various factors that may alter the functions of normal neighbouring cells, and, moreover, may stimulate the proliferation and malignant progression of nearby pre-malignant cells (adapted from Campisi and d'Adda di Fagagna, 2007).

On the other hand, the intrinsic aging of the satellite cells could also render them less responsive to environmental stimuli, which are themselves declining with age. Moreover, some researches showed that satellite cells in elderly humans, even if available in a reduced number, are still able to divide enough to promote repair (Thornell et al., 2003). Thus, it seems clear that impaired skeletal muscle regenerative response, seen in elderly mammals, may result from more factors than just declining satellite cell numbers and proliferative ability; among many other already considered general variables (see *Section 1.1*), what seams even more important than the age-related loss of the satellite cells number, is the age-related loss of satellite cells activity and functionality (in Conboy and Rando, 2005). In fact, it was shown for rodent and human satellite cells either aged *in vivo* (*i.e.* isolated from donors of different ages) or aged *in vitro* that there was an age-related decrease in the quality of myoblast fusion, since the myotubes derived from *old* cells in culture were smaller and thinner, and an age-related decrease in the quantity of the fusion, evident from the reduction of the number of myotubes formed in culture and in the number of their nuclei (among others, see Renault et al., 2000; Lorenzon et al., 2004; Machida et al., 2004).

Together with the age-related loss of muscle mass, attributed to the decreasing number and size of muscle fibres and to the inability of satellite cells to perfectly proliferate, differentiate and fuse, the other peculiar aspect of aged skeletal muscle is the decline of muscle contractile force (for a review see Delbono, 2002). In fact, it seems that the age-related impairment in force could be explained only partially by the loss in mass (Brooks and Faulkner, 1994), so other age-associated deficits in the mechanisms underlying the decline in muscle force have been investigated, with particular interest in possible alterations of sarcolemmal excitability and in the mechanisms controlling Ca^{2+} handling. Indeed, these factors form the basis of skeletal muscle functionality, as it will be explain in the next section.

1.3 Skeletal muscle, calcium homeostasis and aging

1.3.1 The calcium homeostasis at the basis of skeletal muscle physiology

A specific Ca^{2+} homeostatic system was most probably crucial already at the very beginning of life, since Ca^{2+} ions interact with many biological molecules, and Ca^{2+} concentration gradient between extracellular and intracellular compartments has both a survival importance and an important signalling function. In fact, even the primitive forms of life required an effective Ca^{2+} homeostatic system, which could maintain Ca^{2+} at low concentrations, around 100 nM, since at high concentrations Ca^{2+} causes aggregation of nucleic acids and proteins, precipitation of phosphates and damage to lipid membranes (reviewed in Case et al., 2007). In the evolution from prokaryotes to eukaryotes, and then to multicellular organisms, the mechanisms of Ca^{2+} handling became even more complex and refined; even if life has allowed the development of a relatively limited number of Ca^{2+} handling systems, as plasmalemmal and intracellular Ca^{2+} channels, membranes Ca^{2+} pumps and exchangers, cytoplasmic and intra-stores buffers, and Ca^{2+} sensitive enzymes, various combinations of these components offer enormous possibilities for creating real "Ca^{2+} signalling toolkits" (Berridge et al., 2003), which allow a great versatility of Ca^{2+} signalling events in various conditions and in diverse cell types (see figure 9). Indeed, a rise in intracellular Ca^{2+} concentrations can give rise to a wide range of cellular events; among others, we can consider the Ca^{2+}-regulated exocytosis of hormones and neurotransmitters (see Katz and Miledi, 1965; Barclay et al., 2005), the regulation of gene expression and tissue development (for reviews see Fields et al., 2005 and Puceat and Jaconi, 2005; see figure 10), the control of cell survival and the triggering of cell death (see for example Hajnoczky et al., 2006; Dargelos et al., 2007).

Certainly, Ca^{2+} is a key signal that play an essential physiological role in muscle (for recent reviews see Berchtold et al., 2000; Martonosi and Pikula, 2003), both in the processes at the basis of its development and regeneration (myogenesis), and in the physiological function of diverse types of adult muscle (see Iino et al., 1993; Endo, 2006; Chakraborti et al., 2007).

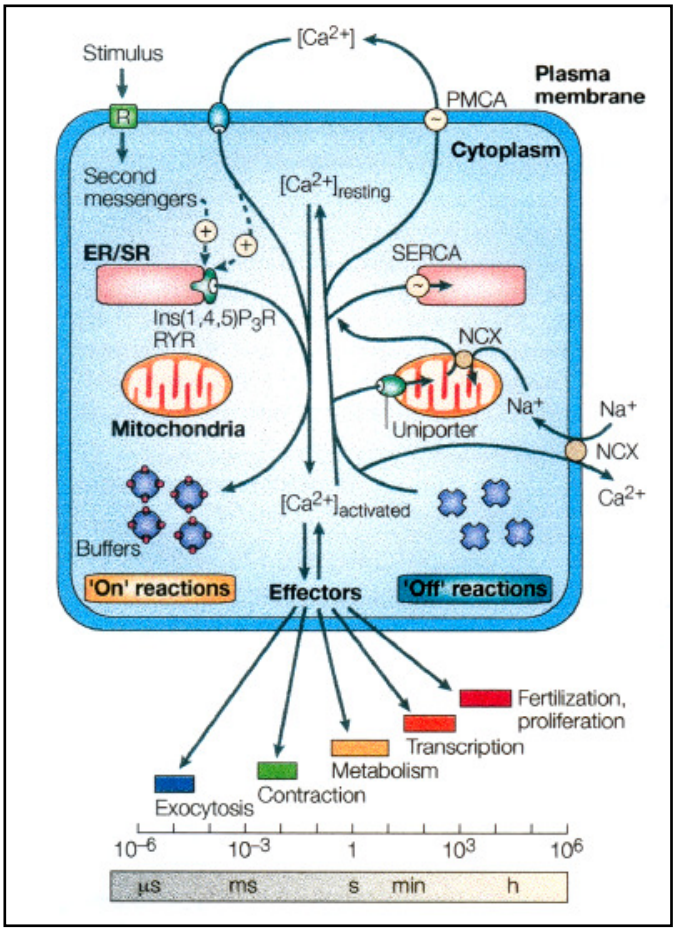

Figure 9: A schematic view of the Ca^{2+} signalling homeostasis. The "on" reactions allow the increase of cytoplasmic Ca^{2+}, while through the "off" reactions the Ca^{2+} can be removed; some of the many divergent processes that can be stimulated by the Ca^{2+} signal are also shown (from Berridge, 2003).

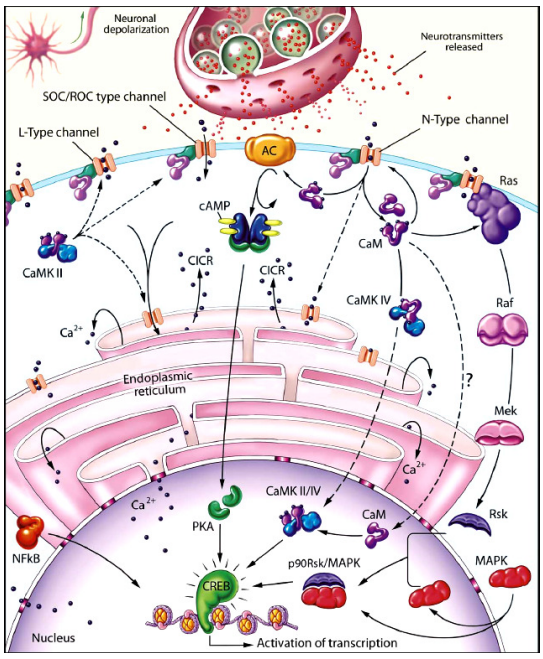

Figure 10: An example of Ca^{2+} mobilization in a post-synaptic cell, to illustrate the complexity of different Ca^{2+} signalling pathways that can be activated to finally regulate gene transcription in the nucleus (from Fields et al., 2005).

In particular, the process of myoblast differentiation and fusion during skeletal muscle myogenesis is Ca^{2+} regulated (Shainberg et al., 1969); in fact, by lowering medium Ca^{2+} concentration it is possible to suppress the fusion of myoblasts into myotubes in culture, and by raising Ca^{2+} concentration again it is possible to re-initiate the process of fusion (Przybylski et al., 1994). The source of the Ca^{2+} signal that triggers the differentiation and fusion of myoblasts into myotubes and its mode of mobilization are still object of discussion; indeed, it seems that myoblasts can change, as required, their preferred Ca^{2+} source for differentiation to take place in culture (Arnadeu et al., 2006). Several researches have also suggested a specific role for the acetylcoline receptor (Ach-R) in myoblasts fusion (see Entwistle et al., 1988 and Krause et al., 1995); one of the hypothesis is that, once activated, AchR can lead to a direct increase in intracellular Ca^{2+} concentration (in Krause et al., 1995), as this channel is permeable to Ca^{2+} ions (reviewed in Fucile, 2004). Moreover, AchR in myotubes, in absence of extracellular Ca^{2+}, can lead to an increase in intracellular Ca^{2+}, through the mobilization from internal caffeine-sensitive and inositoltriphosphate-sensitive stores (Grassi et al., 1994). On the other hand, the direct block of caffeine-sensitive ryanodine receptors, and consequently of Ca^{2+} release from this source, has been found to inhibit fetal myoblast differentiation (Pisaniello et al., 2003).

Interestingly, an involvement of voltage-dependent channels, and specifically of K^+- and of L- and T-type Ca^{2+}-channels, in the crucial process of fusion, in different types of culture, has been proposed by several authors (Beam and Knudson, 1988; Constantin et al., 1996; Seigneurin-Venin et al., 1996; Bijlenga et al., 2000; Bernheim and Bader, 2002; Porter et al., 2002; Liu et al., 2003; Pisaniello et al., 2003; see also next *Section 1.3.2*). Of course, myoblast-myoblast fusion is finely regulated by a great number of cell surface, extracellular and intracellular molecules. Indeed, the mechanisms at the basis of the process of fusion during myogenesis are not yet fully understood, and many of them are Ca^{2+}-regulated; to describe all these mechanisms goes beyond the aim of this thesis, but for reviews the reader could refer to Taylor, 2003, Pavlath and Horsley, 2003 and Chen et al., 2007.

In adult skeletal muscle, among Ca^{2+} triggered events it is particularly important to consider the mechanism controlling the release of calcium from internal stores responsible for fibre contraction, *i.e.* the so-called excitation-contraction coupling

mechanism (E-C coupling). The structural substratum for normal E-C coupling is the mechanical interaction between the dihydropyridine-sensitive voltage-dependent L-type Ca^{2+} channels (dihydropyridine receptors: DHPRs; see next *Section 1.3.2*), organized in tetrads at the sarcolemmal extensions called transverse (T) tubules, and the ryanodine-sensitive Ca^{2+} channels (ryanodine receptors: RyRs) located in the sarcoplasmic reticulum membranes (Block et al., 1988, Rios and Pizarro, 1991; Franzini-Armstrong, 1999). The close apposition of a central transverse tubule and two sarcoplasmic reticulum cisternae forms a triad (Franzini-Amstrong, 1970). This structure allows the intimate interaction, via a direct physical link, between the two types of Ca^{2+} channels, and so the rapid conversion of an electric signal, the sarcolemmal depolarization and the action potential generated at a neuromuscolar junction, detected by the DHPRs which change their conformation, into a chemical signal, the release of Ca^{2+} from the sarcoplasmic reticulum, mediated by the RyRs opening; the consequence is a massive efflux of Ca^{2+} into the myoplasm, available for triggering muscle contraction, and independent from the Ca^{2+} entry from the extracellular compartment (reviewed in Dulhunty et al., 2002; Martonosi and Pikula, 2003; see figure 11).

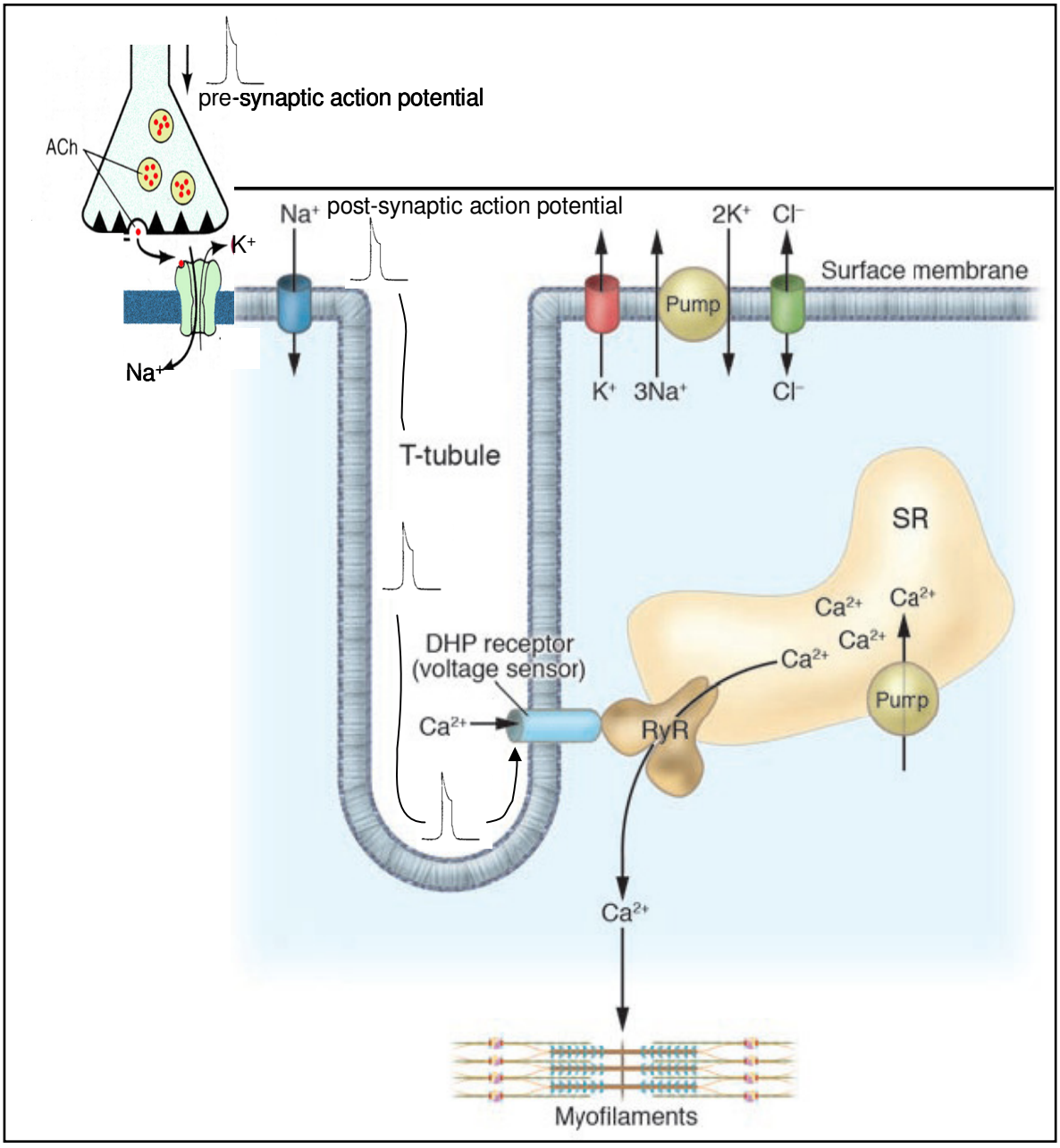

Figure 11: Excitation-contraction coupling mechanism of skeletal muscle. Briefly, a muscle fiber is excited via the motor neuron by an endplate potential and generates an action potential, which spreads out along the sarcolemma and the transverse tubular (T) system, where dihydropyridine (DHP) receptors sense the membrane depolarization, alter their conformation and mechanically allow the opening of the ryanodine receptors (RyRs); consequently the Ca^{2+} is released from the sarcoplasmic reticulum (SR) and can activate the contractile machinery (modified from Jurkat- Rott and Lehmann-Horn, 2005).

1.3.2 The voltage-dependent calcium channels in skeletal muscle

Among the several mechanisms at the basis of Ca^{2+} homeostasis in different types of cell, the voltage-dependent Ca^{2+} channels (VDCCs) are one of the best known tools that allow the enter of Ca^{2+} through membranes into cytoplasm, specifically as a consequence of membrane depolarization. They play an essential role both in the normal functioning and in different pathological conditions that occur in several tissues, in particular in the neuronal and in the muscle ones (for reviews see Catterall, 1991; McDonald, 1994; Catterall, 2000; Perez-Reyes, 2003; Catterall et al., 2005; Dolphin, 2006).

VDCCs were first supposed in crustacean muscle (Fatt and Katz, 1953); since 1953 to these days a lot of electrophysiological, pharmacological, molecular and genetic studies have allowed to classify VDCCs and to divide them in the HVA (high voltage activated) and the LVA (low voltage activated) subfamilies, both further characterized by the presence of different genes encoding molecular subtypes of calcium channels (see figure 12).

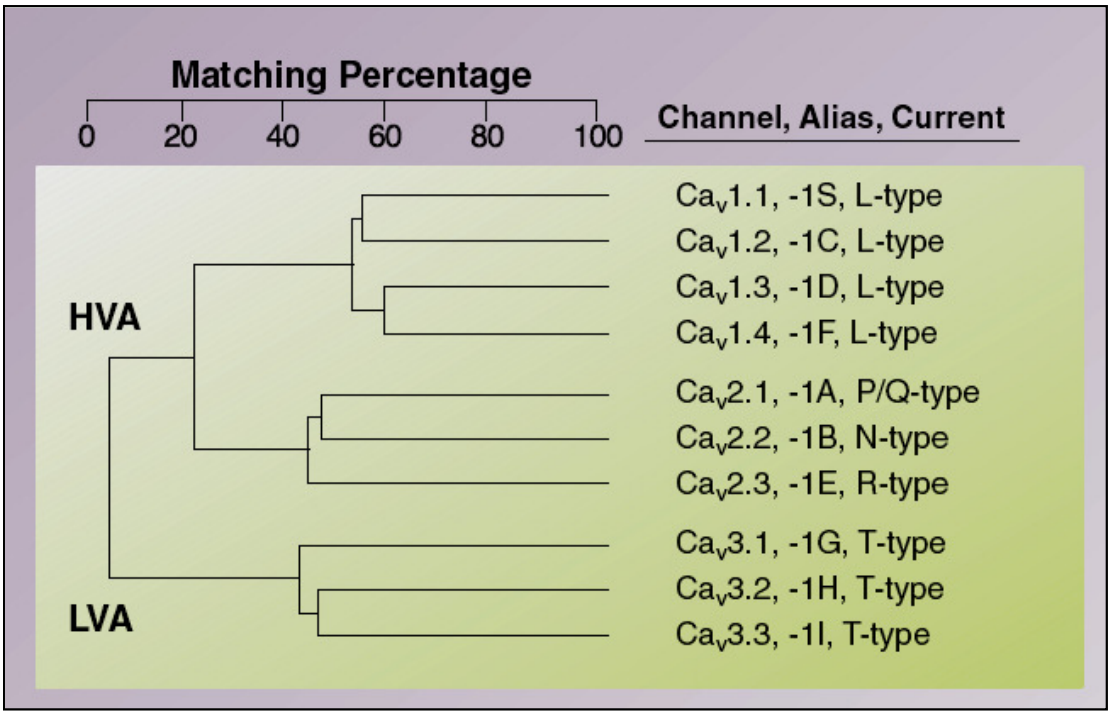

Figure 12: Family tree of voltage-dependent Ca^{2+} channels, based on the full-length human sequences; the present classification is indicated on the right (from Perez-Reyes, 2004).

The classification is based on the sequence of the principal pore-forming subunit of the VDCCs, called α_1-subunit; hydropathy analysis indicated that this subunit has 24 putative transmembrane segments, arranged into four homologous

repeated domains, with extracellular and intracellular linkers and N- and C-termini on the cytoplasmic surface. In common with other voltage-gated channels, the S4 transmembrane segment in each domain is thought to form the voltage-sensor. Moreover, a VDCC was found to usually contain other auxiliary subunits (called respectively β-, α2-δ- and γ-subunit), each encoded by separate genes and expressed in different isoforms, that can regulate the expression and the activation and inactivation kinetics of the channel (for a review see Catterall, 2000, Catterall et al., 2005, and Dolphin, 2006; figure 13).

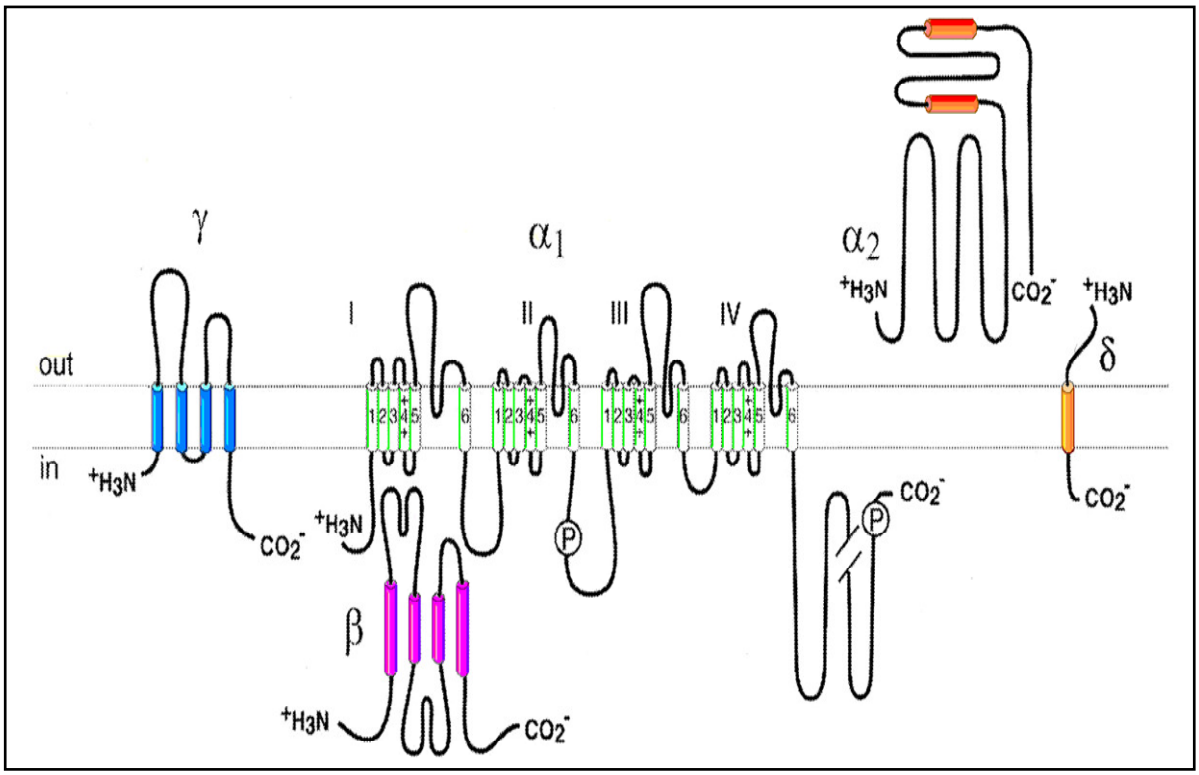

Figure 13: Model of the structure of Ca_V1 channels; this multi-subunits complex contains the α_1 principal pore-forming subunit, with four internal structural repeats (I-IV), each containing six segments (1-6), with the fourth positively charged (voltage sensor) and three auxiliary subunits: the intracellular β subunit, the transmembrane γ subunit, and the transmembrane and extracellular α_2-δ dimer (modified from Catterall et al., 2005).

In humans, the various isoforms of VDCCs are differentially expressed throughout the body, including nervous system, heart, skeletal and smooth muscle, kidney, sperm, oocyte and endocrine organs, and they contribute to specific physiological or pathological processes. What particularly concerns us is that the principal subunits expressed in skeletal muscle cells are (1) the HVA L-type VDCC $Ca_V1.1$ (α_{1S}).and (2) the LVA T-type VDCC $Ca_V3.2$ (α_{1H}).

In adult skeletal muscle, the HVA L-type VDCC $Ca_V1.1$ (α_{1S}) is responsible for carrying the slow, high voltage- activated (HVA) L-type Ca^{2+} current, and for acting as a voltage-sensor to trigger the contractile machinery for EC coupling (see figure 11, *Section 1.3.1*). It is a multi-subunit complex and the general structure is that illustrated in figure 13; in particular, the principal pore-forming α_{1S}-subunit is coded, in humans, by the CACNA1S gene on the 1q31-32 chromosome regions, and provides the basic functional elements of the channel (Ca^{2+} selectivity, voltage-dependent gating, sensitivity to blockers as dihydropyridines and Verapamil, sites of phosphorilation and of interactions with intra-cellular modulators; for reviews see McDonald, 1994; Catterall, 2000). Moreover, the cytoplasmic loop between segments II and III of the α_{1S}-subunit interacts closely with RyRs and is an important determinant of the bi-directional coupling between these two receptors (Nakai et al., 1996; Nakai et al., 1998, Grabner et al., 1999). Regarding the auxiliary subunits, the so called β-subunit interaction domain (BID) binds tightly the α_1-subunit-interaction domain (AID), an intracellular loop joining the I and II repeats, and is proved to be very important for the sarcolemmal expression of the principal subunit and for the regulation of the EC coupling mechanism (Brice et al., 1997; Beurg et al., 1999, Cheng et al., 2005; Hidalgo and Neely, 2007). On the other hand, specific isoforms of α_2-δ-subunit (Shirokov et al., 1998; Nabhani et al., 2005; Obermair et al., 2005) and of γ-subunit (Freise et al., 2000; Ahern et al., 2001, Ursu et al., 2004) are shown to be particularly important in the modulation of the inactivation kinetics.

The L-type Ca^{2+} current is expressed not only in adult skeletal muscle fibres, but also during embryonic and post-natal myogenesis. In fact, the occurrence of this type of HVA voltage Ca^{2+} current has been proved in myotubes isolated from mouse fetuses (Strube et al., 2000) and in myocytes of *Xenopus levis* embryos (Linsdell and Moody, 1995), in cultured myotubes obtained from late-term fetal or newborn rats and mice (Beam and Knudson, 1988; Garcia e Beam, 1994), in primary cultures of satellite cells (Cognard et al., 1993), and in severals cultured muscle cell lines (see Caffrey et al., 1989). Moreover, an involvement of the L-type voltage-dependent Ca^{2+} currents in the crucial process of myoblast differentiation and fusion into myotubes during the process of myogenesis has been also

proposed by several authors in different types of cultures (Seigneurin-Venin et al., 1996; Porter et al., 2002; Bidaud et al., 2006).

On the other hand, during myogenesis, also a LVA Ca^{2+} current was identified as a transiently expressed T-type current, which most likely mediates the influx of Ca^{2+} strictly required to trigger the differentiation and fusion of myoblasts into myotubes (Bijlenga et al., 2000; Bernheim and Bader, 2002; Berthier et al., 2002; Liu et al., 2003, Arnadeu et al., 2006), even if there are some divergent opinions (Bidaud et al., 2006). T-type Ca^{2+} channels, or LVAs, have been firstly distinguished, by electrophysiological studies, from the HVAs by their low voltage thresholds for activation and inactivation, the smaller single channel conductance and the fast inactivation; moreover, among LVAs, three pore-forming subunits have been recently cloned, named α_{1G}, $\alpha_{1H,}$ and α_{1I} (or $Ca_V3.1$-3.3), and they each have several splice variants, showing different molecular, biophysical and biochemical properties, besides being expressed in various cell types (for recent reviews see Perez-Reyes, 2006 and Talavera and Nilius, 2006).

Interestingly, a correlation between LVAs expression and skeletal muscle development has been hypothesized several years ago (Beam and Knudson, 1988; Caffrey et al., 1989; Cognard et al., 1993), but the question about how T-type channels are involved in modulating mammalian, and specifically human, skeletal muscle differentiation has only recently been approached. Several studies aimed at understanding the importance of this source of Ca^{2+} during the initial differentiation of myoblasts and the fusion into myotubes, the precursors of mature skeletal muscle fibres. The only T-type channel principal subunit found both in mouse and human skeletal muscle is the α_{1H} or $Ca_V3.2$ (Bijlenga et al., 2000; Berthier et al., 2002) and the expression of this subunit of the T-type channel in skeletal muscle has been found only during myogenesis in embryonic and newborn muscle and disappears at three weeks of age (Berthier et al., 2002, also reviewed in Perez-Reyes, 2003).

It was shown that the inhibition of T-type current by the T-channel blockers amiloride or Ni^{+} suppressed human myoblast fusion; moreover, it was demonstrated that the T-type channels expressed in fusion-competent myoblasts can give rise to a continuous influx of Ca^{2+} at hyperpolarized potentials (the so called “window current”), large enough to increase intracellular Ca^{2+} and to induce fusion (see Bijlenga et al., 2000 and Bernheim and Bader, 2002; figure 14). Of

course, this is only one of the preferred Ca^{2+} source used by myoblasts for differentiation and fusion to take place in culture (Arnadeu et al., 2006; see previous *Section 1.3.1*).

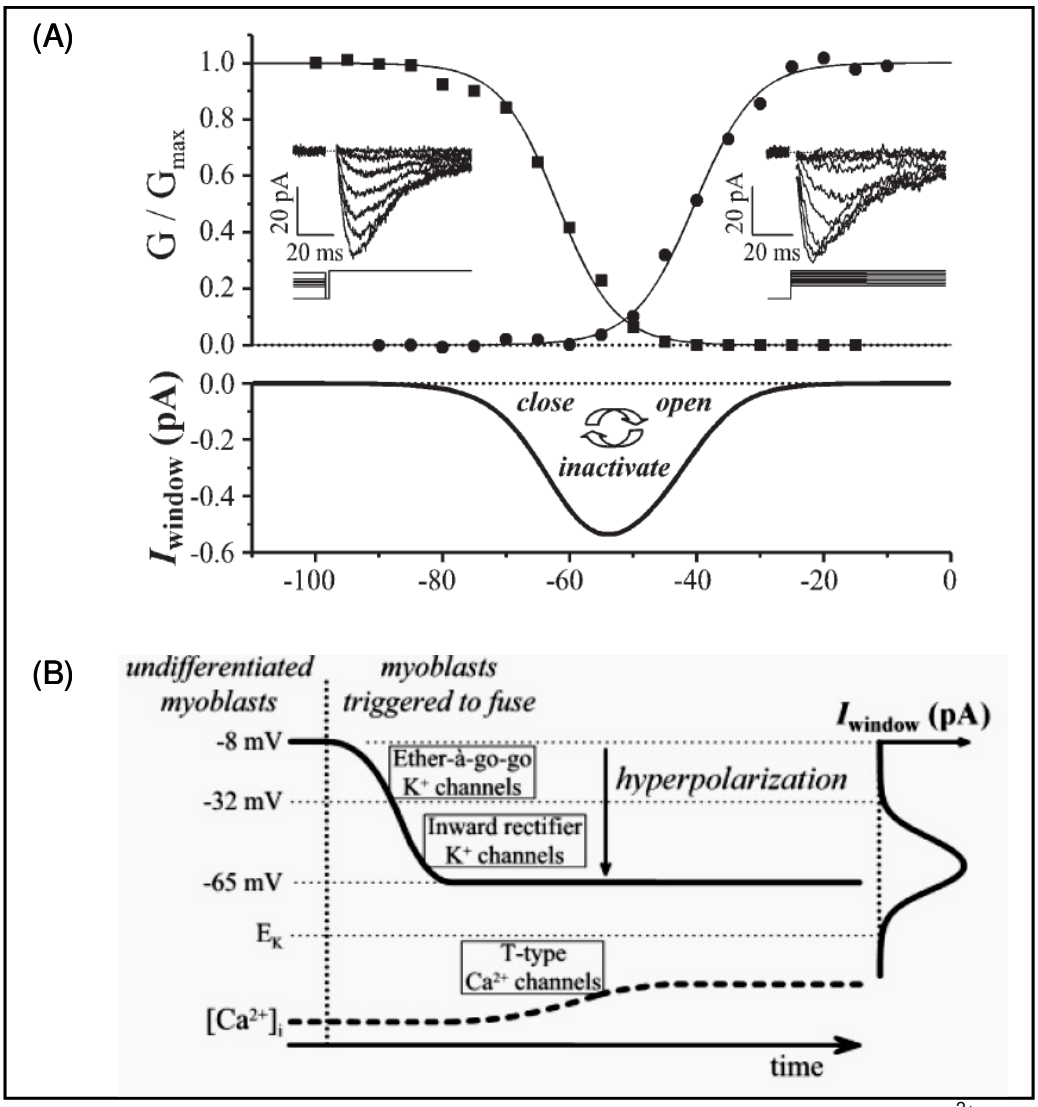

Figure 14: A possible model of the events leading to an increase in intracellular Ca^{2+} via T-type channels in fusing myoblasts. In (A) the T-window Ca^{2+} current, generated by the overlap of the T-channel activation and inactivation voltage-range, in which a fraction of channels results always open. As shown in (B), this window current is situated in the domain of voltages in which myoblasts can fuse, having expressed the two types of K^+ channel indicated, that allow the membrane hyperpolarization. The window current would allow the entry of Ca^{2+} necessary for fusion (modified from Bernheim and Bader, 2002).

1.3.3 Age-related alterations of calcium homeostasis

In the previous two *Sections*, it has been described the importance of Ca^{2+} homeostasis in the skeletal muscle functionality. So, as already anticipated in *Section 1.2*, it is easy to understand that alterations of sarcolemmal excitability and

in the mechanisms controlling Ca^{2+} handling can underlie the age-related decline in muscle force. Indeed, several studies have been showing the contribution of alterations in excitation-contraction (E-C) coupling mechanism to age-related mammalian muscle decline (the so called age-associated *E-C uncoupling* mode; see Delbono et al., 1995; Delbono et al., 1997; Boncompagni et al., 2006; Weisleder et al., 2006). In particular, a significant reduction of maximum of L-type current density, and of peak intracellular Ca^{2+} evoked by sarcolemmal depolarization were found in muscle fibres of old human subjects and of old rodents (Delbono et al., 1995; Renganathan et al., 1997; Wang et al., 2000; Payne et al., 2004). In line with these results, a slower depolarization-induced force response for EDL muscle skinned fibres from old compared with young mice was shown, indicating some level of DHPR-RyR uncoupling (Plant and Lynch, 2002). Moreover, it has already been proposed that defective fibres in old subjects could result from a reduced efficiency of aged satellite cells in properly differentiating into mature skeletal muscle cells with a functional Ca^{2+} handling apparatus. Specifically, human satellite cells aged either *in vitro* or *in vivo* were proved to be unable to differentiate and fuse in culture in functional myotubes with a mature E-C coupling mechanism (Lorenzon et al., 2004; Beccafico et al., 2007).

In figure 15 it is possible to see a simple scheme, that summarize what introduced in the first part of this thesis by putting in relation some extrinsic and intrinsic factors involved in the aging process of skeletal muscle, which could influence both mature muscle fibres and satellite cells, with the failed regulation of Ca^{2+} homeostasis, finally leading to the decline in muscle force evident in elderly subjects.

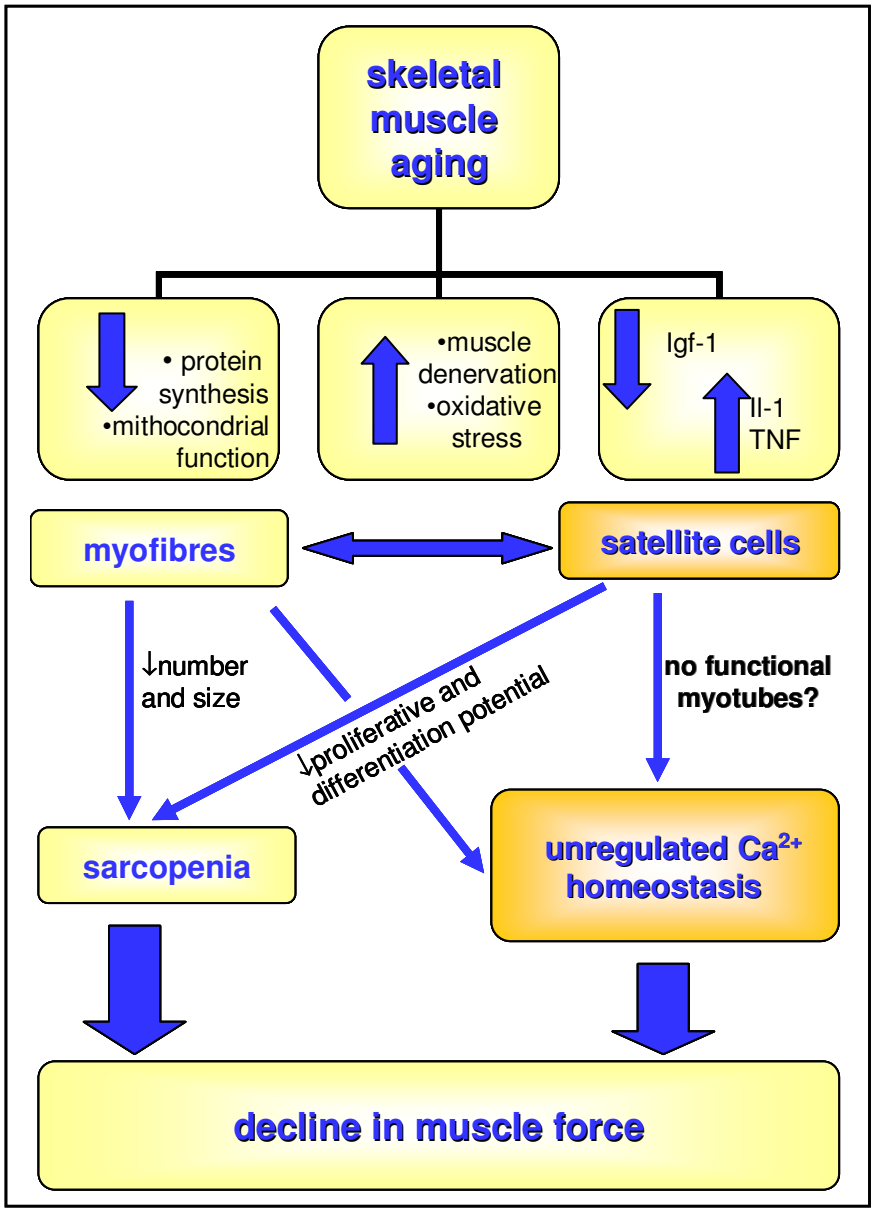

Figure 15: A simple scheme illustrating the principal inter-linked causes of the decline in skeletal muscle mass and strength with advanced age.

2. Aims

As extensively reviewed, the complex process of "sarcopenia of old age", *i.e*. the age-related decline in skeletal muscle mass and strength, is also linked to the modification of mechanisms controlling calcium homeostasis, both in mature skeletal muscle fibres and in satellite cells.

Proceeding from these results, the main goal of the present Ph.D. thesis was to investigate whether the inefficiency of aged satellite cells to generate functional skeletal muscle fibres could be partly due to defective voltage-dependent Ca^{2+} currents.

To this end, two principal experimental steps were developed: *(1)* firstly, to reproduce the physiological muscle aging process that occurs *in vivo* in the useful and simpler model of the *in vitro* aging, by maintaining mouse myogenic cells in culture until the stage of replicative senescence, and to develop in this model the protocols to analyse the properties of voltage-dependent L-and T-type Ca^{2+} currents in myogenic cells and their possible alterations during aging; *(2)* then, to possibly extend, by applying the protocols developed in the first step, the results obtained with the *in vitro* aging of murine satellite cells model to the physiological process of human skeletal muscle aging *in vivo*, *i.e.* to investigate if satellite cells obtained from human old donors could present alterations in calcium homeostasis, and in particular in L-type and T-type Ca^{2+} channels properties.

For this purposes, the whole-cell patch clamp electrophysiology and the videoimaging techniques were employed to measure respectively Ca^{2+} currents and transients in myoblasts and/or myotubes derived from murine and human satellite cells, obtained respectively from young murine skeletal muscle and then aged *in vitro* under culture conditions, and from human skeletal muscle tissue of different aged donors.

3. Materials and methods

3.1 Muscle samples and satellite cell culture

All the experiments, which will be explained further in this Ph.D. thesis (see *Section 4*), were performed on myoblasts and myotubes derived from the *in vitro* proliferation and, whenever necessary, differentiation and fusion of (1) murine and (2) human satellite cells (both kindly supplied by Dr A. Wernig, Department of Physiology and Medical Policlinic, University of Bonn, Germany), shipped seeded in growth medium in culture flasks, or frozen in cryogenic vials on dry ice. The protocols to obtain the desmin positive-enriched culture of satellite cells, from murine and human skeletal muscle tissue (used according to the Protocol of the Ethics Commission of the Medical Faculty of the University of Bonn and the Declaration of Helsinki), are described respectively in Irintchev et al. (1997) and in Shafer et al. (2006).

(1) Mouse satellite cells, isolated from the hind leg muscles of 7-day-old male Balb/c mice and called i28 (see Irintchev et al., 1997), could be expanded and maintained in culture as exponentially-growing myoblasts in the presence of HAM'S F-10 growth medium (GM) plus 20% fetal calf serum (FCS), L-glutamine (2 mM), penicillin (100 units/ml), and streptomycin (100 µg/ml). The myoblasts were plated at a density of about 35000 cells in 90 mm Petri dishes. The cells were sub-cultured in 35 mm matrigel-coated Petri dishes at different seeding densities, depending on the experiments: to prevent myoblasts fusion into multinucleated myotubes, mononucleated myoblasts were plated at a density of 10000 cells; on the other hand, to induce cell fusion, the myoblasts were plated at a density of 70000 cells. In both cases, to induce the beginning of the differentiation program, 1 day after plating the growth medium was replaced with a differentiation medium (DM) consisting of DMEM supplemented with 2% horse serum and L-glutamine, penicillin and streptomycin as above.

(2) Human satellite cells were obtained from healthy donors aged 2, 12, 76 and 86 years (see Shafer et al., 2006). They were then maintained as growing myoblasts, in 90 mm Petri dishes, in HAM'S F-10 growth medium (GM) plus 20% fetal calf

serum (FCS), L-glutamine (1 mM), penicillin (100 units/ml), and streptomycin (100 µg/ml). Whenever necessary, the mononucleated cells were sub-cultured and plated on matrigel-coated coverlips at a density of 100000 cells in 35 mm Petri dishes; to induce cell differentiation and fusion into multinucleated myotubes, 3 days after plating the growth medium was replaced with a differentiation medium consisting of DMEM supplemented with 10 µg/ml of insulin, 100 µg/ml of apotransferrin, penicillin (100 units/ml), and streptomycin (100 µg/ml).

Murine and human cultures were maintained at 37°C in a humid air atmosphere containing 5% CO_2, and the growth medium and the differentiation medium of both cultures were renewed every two-three days, to avoid loss of nutrients and growth factors.

Moreover, as already explained in the introduction of this thesis (see *Section 1.2*), by maintaining myogenic cells in culture we had to take into consideration the fact that they had a limited ability to proliferate, because of the so-called replicative senescence, or *in vitro* aging.

The proliferative capacity of both murine and human myoblasts was evaluated by counting the number of cells in culture at seeding and at harvesting. At each cell passage, the mean population doubling (MPD) was calculated using the formula:

$MPD=[\log (N_h/N_s)]/\log 2]$

where N_h is the harvested cell number and N_s the seeded cell number per Petri dish. The number of total divisions reached by the cell culture was derived from the sum of MPD calculated at each passage.

The murine myogenic cells were maintained in culture until the stage of replicative senescence, determined by examining the effect of *in vitro* aging on the morphology of the plated myoblasts and the failure of such cells to differentiate, align and start to merge into multinucleated myotubes within 4 days in differentiation medium, renewed every two days of culture. The experiments on murine mononucleated myoblasts, or on 3-6 days differentiated multinucleated myotubes (see *Section 4.1*), were performed at different MPDs, thus at different degrees of replicative senescence.

On the other hand, the experiments on human cells (see *Section 4.2*) were conducted on multinucleated myotubes after 3-6 days of differentiation, obtained from the differentiation and fusion of different age donors myogenic cells. The cells

used were all at the very beginning of the proliferative phase of the various cultures, between 3-20 (younger donors) and 6-10 (older donors) MPDs, well before the end of their replicative lifespan (proliferative senescence), in order to consider potential differences derived only from aging *in vivo*, by avoiding the aging *in vitro* of the cells in culture.

3.2 Cyto- and immunocyto- chemistry experiments

3.2.1 The differentiation index

The efficiency of differentiation of murine myogenic i28 cultures was quantified by counting the percentage of myotubes and the mean number of nuclei per myotube. Nuclei were revealed under fluorescence microscopy by DAPI (4,6-diamino-2-phenylindole) staining; the cells, plated on matrigel-coated coverslips, were first fixed at room temperature in freshly prepared 3.7% paraformaldehyde in a phosphate buffer solution (PBS) for 15 min, permeabilized by a 5 min incubation in 100% methanol and then stained for 10 min with DAPI (10 µM in PBS). The fluorescence images of the cells rinsed in normal external solution (NES) were compared to the corresponding bright-field images in order to identify the multinucleated myotubes. In particular, 10 randomly chosen optical fields per coverslip were analysed. Fluorescence and bright-field images were collected by a CCD camera (SensiCam; PCO Computer Optics, Kelheim, Germany) connected to an inverted microscope (Zeiss Axiovert 100) and the analog output was digitized and integrated in real time by an image processor.

Specifically, the efficiency of differentiation of murine myoblasts was tested in two cases:

1) at different population doublings, in order to explore the differentiation and fusion capacity of two different classes of cells, *young* and *old*, with less than 30 and more than 50 divisions respectively;

2) after some days of differentiation in the presence of a specific blocker for different voltage-dependent Ca^{2+} channels (precisely Nickel 200 µM, Nickel 50 µM, Verapamil 20 µM, see *Section 4.1*), in order to prove a possible involvement of these types of channels in the process of differentiation and fusion into myotubes.

3.2.2 The desmin staining protocol

Murine and human myogenic cells express, among others, a specific cytoskeleton protein called desmin (Kaufman and Foster, 1988). This property had been used to investigate the degree of purity of the cells maintained in culture, by assaying the desmin-positive cells using the mouse monoclonal anti-desmin antibody D33 (1/50 in carrageenan, DAKO, Denmark).

Specifically, the cells for the immunofluorescence assay, grown on glass coverslips coated with matrigel, were firstly fixed in freshly prepared paraformaldehyde in PBS for 15 min and then permeabilised by 100% methanol for 5 min, always in the darkness at room temperature. Then, after a pre-incubation for 30 min with normal goat serum (NGS), the cells were incubated with the primary monoclonal anti-desmin antibody for 60 min at 37°C. Following, after several washings in PBS, cells were incubated with the secondary polyclonal Rhodamin Red-conjugated antibody (1/200 in carrageenan, Jackson Immunoresearch Laboratories, USA) for 60 min at room temperature. Nuclei were finally revealed by staining with bis-Benzimide H-33258 (1/1000 in distilled water) for 5 min at room temperature. Fluorescence images were collected by a videocamera (Nikon DXM1200, Nikon- Italia srl, Firenze, Italia) connected to an inverted microscope (Nikon E800), used by courtesy of Dr. Enrico Tongiorgi (Laboratory of Cellular and Molecular Neuroanatomy, University of Trieste, Trieste). At least 10 randomly chosen optical fields per coverslip were analysed, and the percentage of desmin positive cells was calculated as the number of stained cells *vs* the total number of cells observed.

3.2.3 The β-galactosidase assay

In recent years a possible biomarker associated with the senescent phenotype was described (Dimri et al., 1995); it was a “senescence associated” β-galactosidase, which could be detected by staining the cells using the artificial substrate 5-bromo-4-chloro-3-indolyl-β-D-galactoside (X-gal) at pH 6.

Specifically, I used a senescent cells staining kit (CS0030, developed by Sigma) based on a histochemical stain for β-galactosidase activity at pH 6, which was considered to be unique to senescent cells, and undetectable in quiescent,

immortal or tumor cells (Dimri et al., 1995). Briefly, the cells for the β-galactosidase assay, grown in 35 mm Petri dishes coated with matrigel, were firstly fixed in freshly prepared paraformaldehyde in PBS for 15 min in the darkness at room temperature, then washed in PBS, and finally incubated with freshly prepared senescence associated β-galactosidase stain solution (ph 6), containing X-gal (1 mg/ml), at 37°C in a stove without CO_2 (for details see Dimri et al., 1995). Staining was evident in about 24 hours (see *Section 4.1*).

3.3 The electrophysiology and videoimaging experimental protocols

3.3.1 Electrophysiology recordings

The electrophysiology protocols were first developed on murine myoblasts and myotubes and then adapted to the experiments on human myotubes.

In general, besides the mononucleated myoblasts, the 3 to 6 days murine or human multinucleated myotubes with a compact shape, a smooth cell membrane appearance, without branches and not too large were selected for the experiments, to avoid problems of space- and voltage- clamp.

Calcium currents were recorded at room temperature (20-24°C) by means of the whole-cell configuration of the patch-clamp technique using an Axopatch 200B amplifier (Axon Instruments, Union City, CA, USA). Patch pipettes were fabricated from borosilicate glass and fire-polished to a final tip resistance, when filled with intracellular solution (see below), of 5-7 MΩ or 3-5 MΩ, respectively for the murine and human cells. Data acquisition and command voltage pulse generation were performed with a Digidata 1320 interface controlled by pCLAMP 8 software (Axon Instruments). Currents were filtered at 1 kHz and sampled at 5 kHz. The analog circuitry of the amplifier was used to reduce the capacitive transients as much as possible and to compensate the series resistance close to the point of amplifier oscillation. For subtraction of remaining linear leak and capacity, a standard P/4 protocol (leak holding potential –90 mV) was used in all measurements. Cell membrane capacitance (C) was determined by integration of the capacity transient elicited in response to a 10 mV hyperpolarizing pulse from a holding potential of -60 mV and was also used to calculate the calcium current density of each cell (I/C). The time constant for charging membrane capacity of each cell was calculated by fitting the capacity transient by a single exponential function.

Both T- and L-type Ca^{2+} currents were activated from a holding potential of –60 mV, after a 750 ms hyperpolarizing stimulus (-90 mV) to remove inactivation. 500 ms test pulses were applied in 10 mV increments, ranging from –70 to +40 mV. L-type currents were isolated by using a 750 ms depolarizing (-30 mV) conditioning prepulse, that inactivated the T-type currents. T-type currents were then obtained by the subtraction of the recordings obtained with the prepulse from those obtained without it. In a few cases, only one of the two types of current was elicited, by blocking or L-type currents with the specific L-channel blocker verapamil (20 μM), or T-type currents with Nichel (50μM), both applied when necessary by a gravity-driven perfusion system.

To determine current density-voltage (I/C-V) relationships, the peak T-type current, or the peak L-type Ca^{2+} current, normalised to the C, was measured as a function of test potential.

Data were also transformed to a conductance-voltage [G-V] curve using the following equation:

$G(V) = I(V)/(V-E_{rev})$,

where E_{rev} is the reversal potential for the T-type, or for L-type Ca^{2+} current respectively, estimated by linear extrapolation of the I-V curve.

To compare the activation kinetics of the two types of Ca^{2+} current in myotubes derived from the differentiation and fusion of young and *in vitro* (murine) or *in vivo* (human) aged satellite cells, the [G-V] curves of each group were normalised to the maximum conductance value (G_{max}), averaged and then fitted with the Boltzmann function

$G(V)/G_{max} = 1/(1+\exp[-(V-V_{1/2})/k])$

where $V_{1/2}$ is the voltage at which the conductance is half maximal and k describes the steepness of activation.

To promote and measure L-type current inactivation, cells were held at –60 mV, then *i*) stepped using a series of 1500 ms depolarizing voltages from –70 to +40 mV in 10 mV increments (prepulses) to promote inactivation, *ii*) stepped to –60 mV for 100 ms to close non-inactivated channels, *iii*) stepped for 500 ms to the test

potential of +10 mV (in the murine model) or of +20 mV (in the human model) and finally *iv*) turned back to –60 mV to permit recovery from inactivation.

To elicit and measure T-type current inactivation, we used a series of 300 ms conditioning voltages from -80 to -10 in 5 mV increments (prepulses), and a fixed test pulse of 500 ms to -30 mV.

To determine voltage-dependent inactivation, the peak L-type, or T-type Ca^{2+} current respectively, was normalised to the maximal current (I_{max}, generally observed with the prepulse at -80 or -70 mV) and measured as a function of prepulse potential. To compare *young* and *old* myotubes, the inactivation curves within each group were averaged and then fitted with the Boltzmann equation

$$I(V)/I_{max} = 1/(1+\exp[(V-V_{1/2})/k])$$

with $V_{1/2}$ being the voltage of half-inactivation and k a measure for the steepness.

In some cases, also the time course of inactivation of the L-type current, during the 1500 ms depolarization to 0 mV, was measured. It could usually be well fitted by a single exponential component, but in a few myotubes a double exponential time course was observed.

Moreover, to further analyze L-type Ca^{2+} current inactivation, recordings from double-pulse experiments, at the prepulse potential (usually usually 0 or +10 mV in the murine model, +20 mV in the human model) which lead to maximal *prepulse* peak current and maximal *test pulse* current inactivation, were pooled and analysed to obtain other two indexes of inactivation: 1) the rate of the L-type Ca^{2+} current inactivation (r_{1500}, or residual current at 1500 ms), expressed as the percent current reduction at the end of the *prepulse* (I_{1500}) compared to the peak *prepulse* current (I_{peak})

$$r_{1500}\,[\%]=(I_{1500}/\ I_{peak})*100$$

and 2) the degree of maximal voltage-dependent inactivation (called r_{inact}), determined as the ratio of the *test* current (at +10 or +20 mV) and the highest current measured during the set of test pulses (I_{max})

$$r_{inact}[\%]=(I_{(10\text{-}20mV)}/\ I_{max})*100.$$

3.3.2 Videoimaging experiments

Videoimaging experiments were carried out on myotubes plated on matrigel - coated coverlips loaded with the Ca^{2+} indicator Fura-2 pentacetoxymethylester (fura-2 AM). Cells were incubated for 30 min in the dark at room temperature in a physiological solution (NES, see below) supplemented with 10 mg ml^{-1} bovine serum albumin and 5 μM fura-2 AM; after wash-out, cells were maintained in NES for 15 min in the dark at room temperature to allow de-esterification of the probe. All the experiments were performed at room temperature. Cells were alternatively excited at 340 and 380 nm selected by a monochromator (Polychrome II T.I.L.L. Photonics GmbH, Martinsried, Germany) and fluorescence images were collected by a CCD camera (SensiCam; PCO Computer Optics, Kelheim, Germany) at image acquisition rate of 1 image /750 ms.

Intracellular Ca^{2+} ($[Ca^{2+}]_i$) transients in *coupled* myotubes were elicited by cell depolarisation with high $[K^+]$ (40 mM; 5 s superfusion by a gravity-driven perfusion system) in a Ca^{2+}-free solution (see below). The ratio was calculated off-line. The corresponding temporal plots (*i.e.* the variations in the mean value of fluorescence intensity) were calculated from ratio images in the areas of interest, and the fluorescence ratio at rest was conventionally assumed to be 1. Three experimental parameters were evaluated: *i*) the number of responsive myotubes, expressed as a percentage (%), *ii*) the peak of $[Ca^{2+}]_i$ transient , expressed as the maximum difference between the fluorescence ratio at rest and after the stimulus (ΔR), *iii*) the area of $[Ca^{2+}]_i$ transient, determined by integration of the transient itself.

3.4 Chemicals and statistical analysis

As regards the <u>cyto- and immunocyto- chemistry experiments</u>, the phosphate buffered saline solution (PBS) contained (in mM): 10.6 Na_2HPO_4, 1.83 NaH_2PO_4, 145 NaCl, and the physiological solution (NES) contained (in mM): 2.8 KCl, 140 NaCl, 2 $CaCl_2$, 10 Hepes, 2 $MgCl_2$, 10 glucose (pH 7.3).

As regards the <u>electrophysiological experiments</u>, solutions to record T- and L-type Ca^{2+} currents were as follows, with the values in brackets referring to the different

concentrations used during the experiments on the human cells. The bath extracellular solution contained, in mM: 135 (145) TEA-Cl, 2.5 (10) $CaCl_2$, 0.8 $MgCl_2$, 5.6 glucose and 10 Hepes; pH adjusted to7.4 with TEA-OH. The pipette intracellular solution contained (in mM): 130 (140) CsCl, 0.005 $CaCl_2$, 1 $MgCl_2$, 5.6 glucose, 10 Hepes, 1 (0.1) EGTA and 2 ATP; pH adjusted to 7.2 with TEA-OH.

During the videoimaging experiments the physiological solution (NES), used for the Fura-2 loading of the cells, was as above stated; the experiments were then performed in a Ca^{2+}-free solution containing (in mM): 140 NaCl, 2.8 KCl, 5 $MgCl_2$, 2 EGTA, 10 glucose, 10 Hepes (pH adjusted to7.4 with Na-OH).

Fetal calf serum was purchased from Mascia Brunelli (Milano, Italy) and Matrigel from Becton-Dickinson (NJ, USA). All the other chemicals, unless otherwise stated, were from Sigma (St Louis, MO, USA).

For electrophysiological data acquisition and analysis, the pCLAMP software package (v. 8.0, Axon Instruments, Foster City, CA) was used, while fluorescent signals were acquired with a conventional system driven by Imaging Workbench software (v. 2.2, Axon Instruments). For further data analysis, Origin software (v. 7.0, Microcal Software, Northampton, MA) and Prism software (v. 3.0, Graph Pad Software, State of California, USA) were routinely used. All data, whenever possible, are presented as mean ± *SEM*. Differences between data group means were evaluated by Student's t-test and a *P* value <0.05 was considered statistically significant.

4. Results

4.1 Ca^{2+} currents and homeostasis during the in vitro aging of i28 murine satellite cells

As previously introduced in *Section 1.2.2*, a useful model of *in vivo* aging of satellite cells is the aging of the same cells *in vitro* under culture conditions; this model would allow to investigate if the replicative senescence affects the regenerating ability of these cells.

The main goals of the first step of my research were therefore:

(1) to reproduce the physiological muscle aging process that occurs *in vivo*, by maintaining mouse *i28* myogenic cells (see *Section 3.1*) in culture until the stage of replicative senescence, determined by examining the effect of *in vitro* aging on their ability to differentiate and fuse into myotubes, and

(2) to analyse the properties of L-and T-type Ca^{2+} currents in these myogenic cells during *in vitro* aging, in order to study their possible involvement in age-associated alteration in Ca^{2+} homeostasis.

To this end, the *i28* cells were maintained as exponentially-growing myoblasts in culture until the state of 'replicative senescence' (about 90 cell divisions) and two different classes of cells, *young* and *old*, with less than 30 and more than 50 divisions respectively, were taken into consideration.

The principal results obtained are shown in the next paragraphs; the published results, completed with a specific discussion, are presented in the enclosed *Appendix 1* (pag. 83).

4.1.1 The purity of i28 cells maintained in culture:

In order to investigate the degree of purity of i28 cells maintained for several passages in culture, the desmin-positive cells were assayed (for details see *Section 3.3.2*) at two different stages of *in vitro* aging (*young* cells, with less than 30 divisions, and *old* cells, with more than 50 divisions). At least 10 randomly chosen optical fields for every stage were analysed. The percentage of desmin positive cells, calculated as the number of stained cells *vs* the total number of cells observed, was very high at every stage of replicative senescence (99 % of both

young and old cells were desmin positive; figure 16); on the other hand, there was an evident age-related change in the morphology of *old* myoblasts, and also their capacity to fuse appeared compromised, as it will be better explained in the next paragraph.

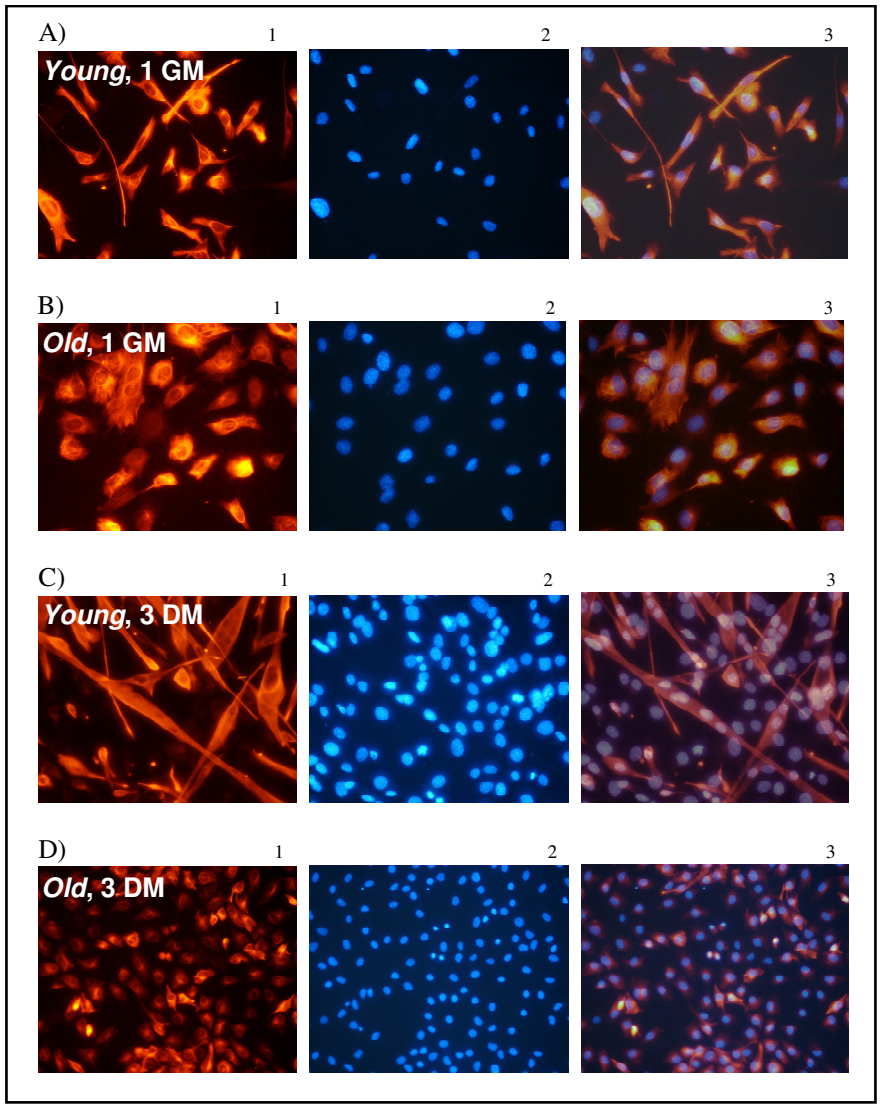

Figure 16: Representative fluorescence photomicrographs of *young* (less than 30 divisions) and *old* (more than 50 divisions) i28 cells after desmin labelling (red, column 1) and bis-Benzimide staining (nuclei in blu, column 2; the column 3 shows the superimposing of column 1 and 2). (A) and (B) show undifferentiated myoblasts at 1 day in growth medium (GM), while (C) and (D) cells differentiated, and eventually fused into myotubes, at 3 day in differentiation medium (DM). Note the difference in the morphology and in the capacity to fuse between *young* (A and C) and *old* (B and D) cells (A), B), and C): 40X magnification; D): 20X magnification).

4.1.2 Impaired differentiation and fusion of i28 cells during in vitro aging

In order to investigate if the process of myogenesis in i28 culture would have been affected by the *in vitro* aging, the differentiation and fusion capacity of two different

classes of cells, *young* (less than 30 divisions) and *old* (more than 50 divisions), were taken into consideration. Myotubes at three and six days in differentiation medium (DM) were analysed for each group (see figure 17A).

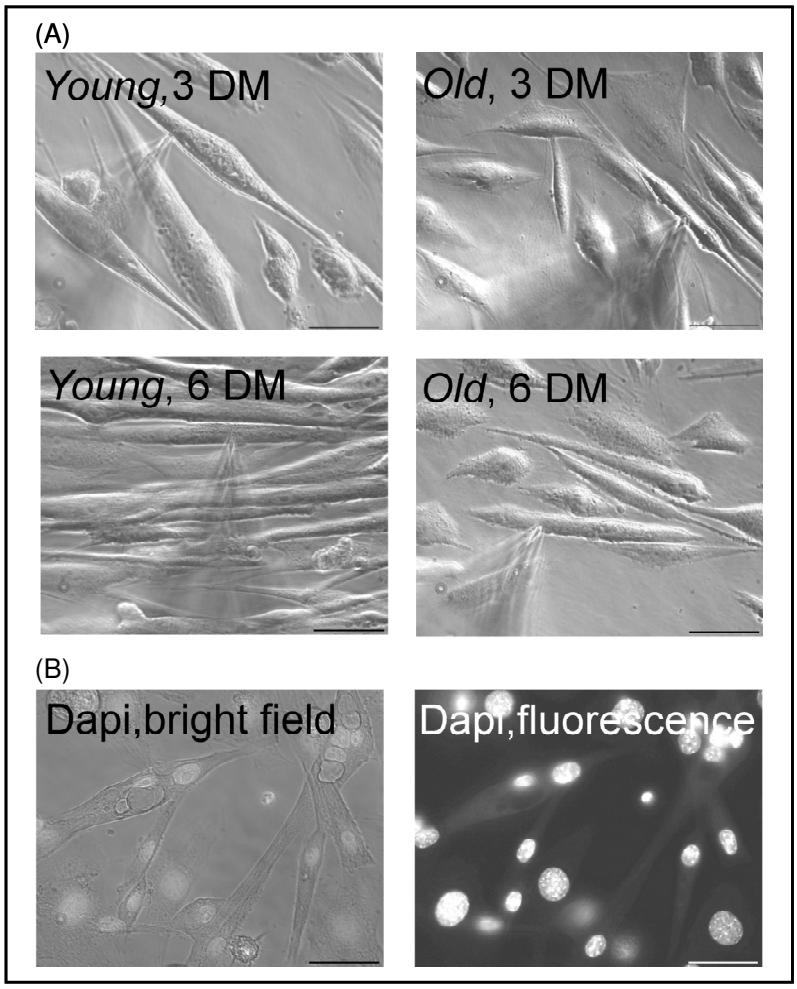

Figure 17: (A) shows representative photomicrographs of patched myotubes, at 3 and 6 days in differentiating medium (DM), originating from the fusion of competent *young* (< 30 divisions) and *old* (> 50 divisions) myoblasts, and (B) shows representative fluorescence and bright-field images of the same optical field (*old* cells, 3 days in DM) after DAPI staining (scale bar, 35 µm).

By maintaining the cells in culture for several passages, it was possible to observe the gradual changes in morphology and shape of myotubes derived from myoblasts approaching the so-called 'replicative senescence'. At later passages, i28 cells were not able to fuse as efficiently as in earlier passages. Indeed, by revealing the nuclei by DAPI (see figure 17B and *Section 3.2.1*), it was found that both *young* and *old* myotubes during their time in DM increased in dimension and in differentiation, judged by the increase in the nuclei per myotube ratio. Nevertheless, during the *in vitro* aging, the differentiation and fusion appeared defective. Both at three and six days in DM, a drastic loss of multinucleated cells

and in the number of nuclei was observed (see figure 18). Moreover, the myotubes originating from *old* satellite cells, approaching the stage of cellular senescence, appeared smaller and thinner, in comparison to *younger* cells at the same day in DM (see representative photomicrographs in figure 17A), and the small myotubes originating from *old* satellite cells rarely had branches, contrary to what was observed in myotubes derived from *young* cells.

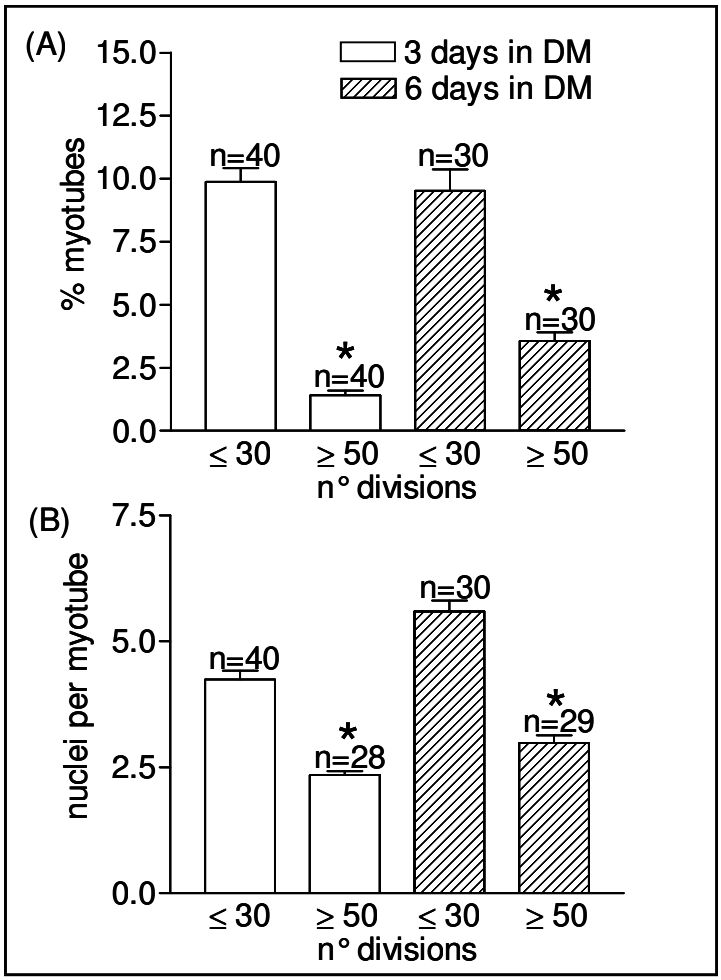

Figure 18: The histogram in (A) shows the drastic aging-related loss of multinucleated cells, and in (B) the aging-related decrease of the number of nuclei per myotube, both comparing cells at the same day in DM (3 and 6 days) (n=number of optical fields, *= statistically extremely significant, *P*<0.001).

4.1.3 Changes in the expression and density of L- and T-type currents in myoblasts and myotubes during in vitro aging

L-type and T-type voltage-dependent Ca^{2+} currents were evoked in myoblasts and in 3-6 days differentiated myotubes using the protocols described in *Section 3.3.1*.

To verify the presence of L-type and T-type currents in differentiated fusion-competent mononucleated myoblasts, the cells were plated at a density of 10000 per Petri dish, to prevent fusion into multinucleated myotubes, and 1 day after plating the growth medium was replaced with a differentiation medium (see *Section 3.1* and figure 19A).

In *young* fusion-competent myoblasts (3-16 days in differentiation medium) both T- and L-type Ca^{2+} currents were detected in 16% of cells; in *old* myoblasts the occurrence of T-type current decreased to 3%, while L-type current was never detected (figure 19C). It is interesting to notice that the two types of current have been never detected simultaneously in the same myoblast. The density of the L-type current ($I_{L,max}/C$, see *Section 3.3.1*) was 4.57±2.94 pA/pF (n=5), and that of T-type current (I_{Tmax}/C) was 1.05±0.39 pA/pF (n=5) in *young* myoblasts.

Surprisingly, the only T-type current detected in an *old* myoblast revealed a current density higher than that found in *young* myoblasts (I_{Tmax}/C = 2.75 pA/pF).

To analyse the expression and the properties of the same currents in multinucleated myotubes, the cells, at different stages of *in vitro* aging, were plated at a density of 70000 per Petri dish, to allow fusion, and 1 day after plating the growth medium was replaced with a differentiation medium (see *Section 3.1*). L-type and T-type currents were evoked in 3- and 6-days differentiated myotubes, using an activation protocol with 500 ms test pulses in 10 mV increments ranging from -70 to +40 mV (see *Section 3.3.1*).

In myotubes derived from *young* cells L-type Ca^{2+} currents were detected in almost 100% of myotubes, but the occurrence decreased to 75% (n=29) in three-day differentiated myotubes originating from the fusion of *old* cells (more than 50 divisions). However, it seemed that there was an age-related delay in maturation; in fact, if we took into consideration the six-day differentiated myotubes derived from *old* cells, I_L was again present in almost all cells (figure 20B).

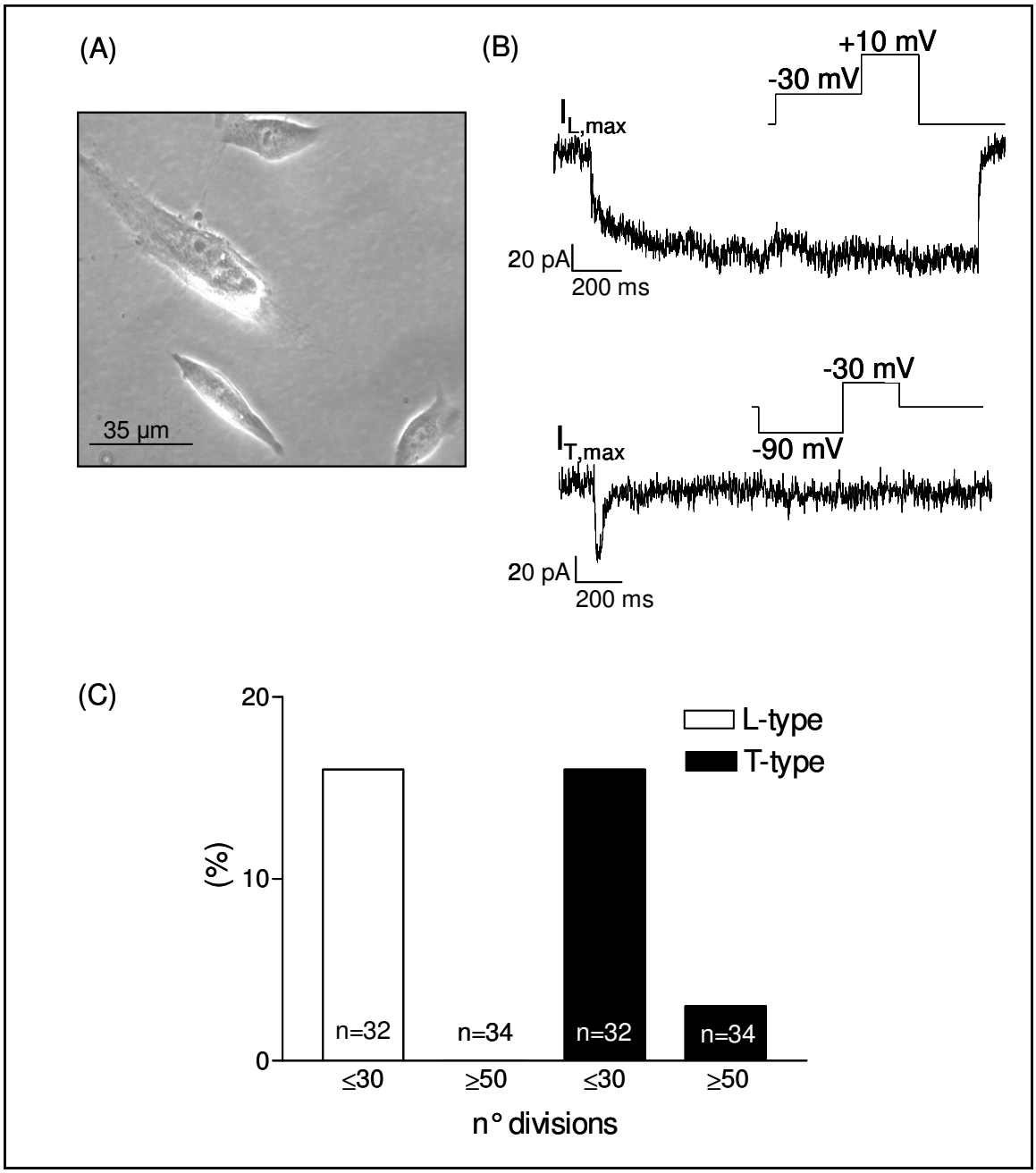

Figure 19: L- and T-type Ca^{2+} currents measured in mononucleated myoblasts during *in vitro* aging. In (A) a photomicrograph of *young* myoblasts; in (B) representative maximum I_L and I_T currents recorded using the stimulation protocol indicated in the inset; in (C) the percentage (%) of cells exhibiting L-type and T-type currents at different stages of replicative senescence.

On the other hand, at 3 and 6 days in DM, T-type Ca^{2+} currents were expressed only in 11 and 56 % respectively of myotubes originated from *young* cells, and the presence clearly decreased to 7 and 9 % in myotubes derived from *old* cells (figure 21B). Moreover, none of the cells tested displayed only I_T, which is probably never expressed before I_L.

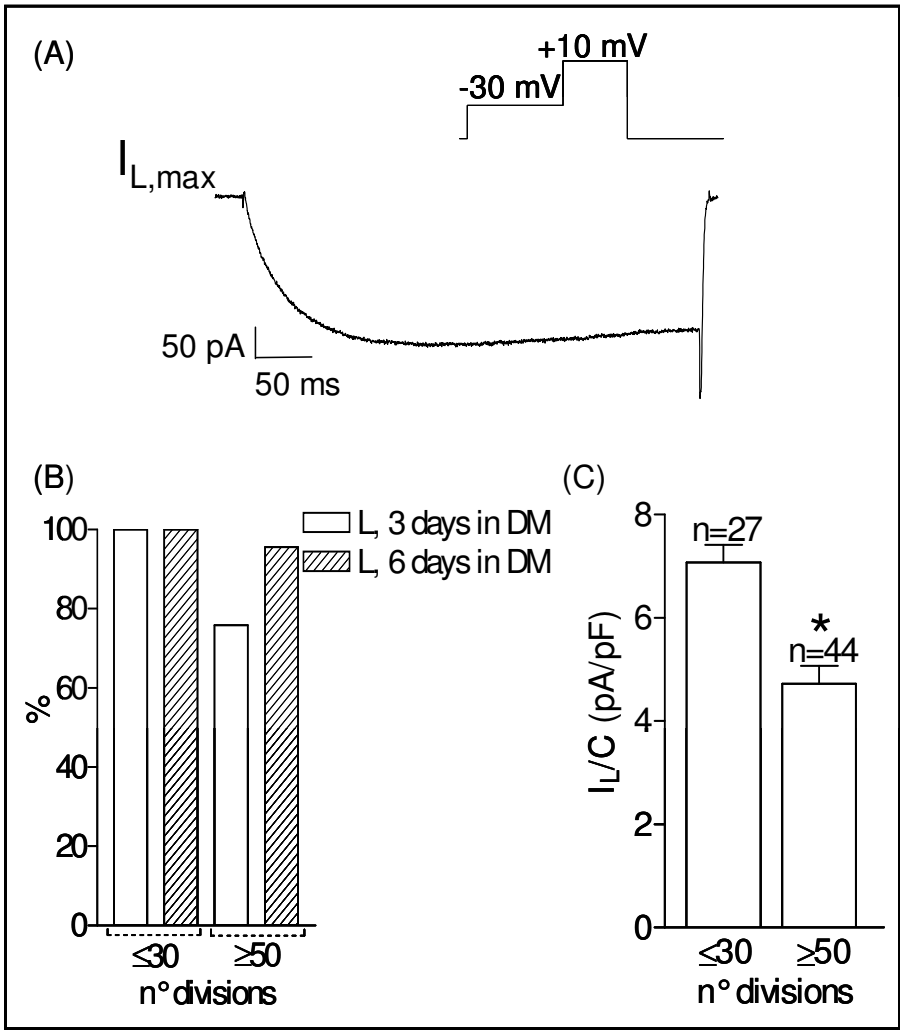

Figure 20: L-type Ca^{2+} currents (I_L) measured in myotubes during *in vitro* aging of i28 cells. In (A) representative maximum I_L current recorded using the stimulation protocol indicated in the inset. In (B) the current expression, *i.e.* the percentage of cells exhibiting I_L at different days in differentiation medium (DM). In (C) the decreasing current density of I_L with aging is shown (3- and 6-day differentiated cells were grouped because of no significant differences; n=number of myotubes, *=statistically extremely significant, $P<0.001$).

In all the cells, the densities of L-type and T-type Ca^{2+} currents were calculated taking into account the maximum peak current value (I_{max}), generally observed at 0 or +10 mV for L-type and at –30 mV for T-type current (see figures 20A and 21A), normalised to the effective cell capacitance. As shown in figure 20C, the L-type current density significantly decreased during the *in vitro* aging of i28 cells. Moreover, a decreasing trend of T-type current density was also evident, even if the reduction was not statistically significant (figure 21C). Here and later, three- and six-day differentiated i28 myotubes were grouped together because of no significant differences in L-type and T-type current density and kinetics (see below) taking into consideration different days in the differentiation medium.

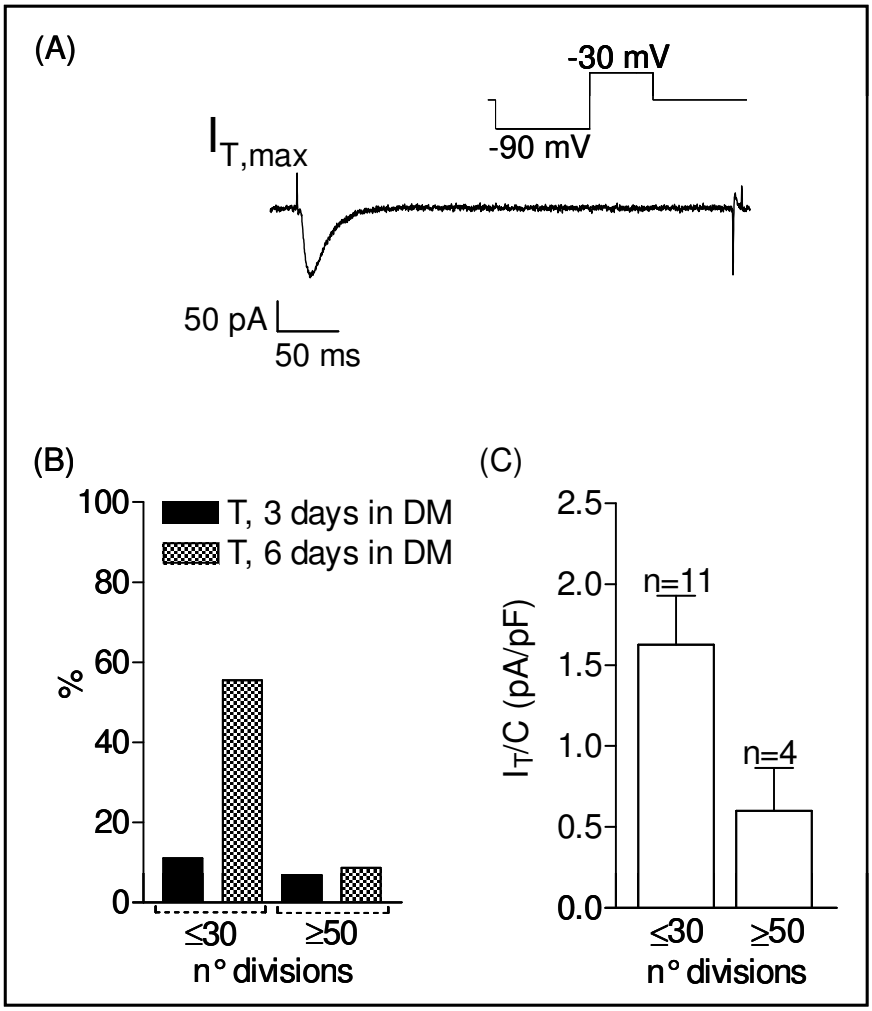

Figure 21: T-type Ca^{2+} currents (I_T) measured in myotubes during *in vitro* aging of i28 cells. In (A) representative maximum I_T current recorded using the stimulation protocol indicated in the inset. In (B) the current expression, *i.e.* the percentage of cells exhibiting I_T at different days in differentiation medium (DM). In (C) the current density of I_T at different stages of replicative senescence is shown (3- and 6-day differentiated cells were grouped because of no significant differences; n=number of myotubes).

Considering that the process of myogenesis in i28 culture was affected by the *in vitro* aging, as shown in *Section 4.1.2*, and that both *old* myoblasts and myotubes displayed an age-related decrease in the occurrence of T- and L-type currents, I decided to test the efficiency of differentiation of *young* cells in the presence of specific blockers for the T- and L voltage-dependent Ca^{2+} channels (precisely Nickel 200 µM, Nickel 50 µM, Verapamil 20 µM), in order to prove the correlation between the expression of these types of channels and the process of differentiation and fusion into myotubes. The cells were initially plated at a density of 70000 per Petri dish, and 1 day after plating the growth medium was replaced with the differentiation medium (DM) alone (control), or with DM added with one of

the specific blockers. After 3 days, the cells were fixed and Dapi stained and the mononucleated myoblasts and the multinucleated myotubes were identified (figure 22A; for details, see *Section 3.2.1*).

The inhibition of T-type current by Ni^+ (200 and more specifically 50 µM) suppressed very significantly i28 myoblast fusion, supporting the hypothesis that *young* cells fuse better because they have higher T-type current density (figure 22). The fusion was also sensitive to the specific L-type current blocker Verapamil (20 µM), also if less significantly (see figure 22B and 22C), suggesting that this type of current is not the principal source of Ca^{2+} required for fusion (see *Section 1.3.1*).

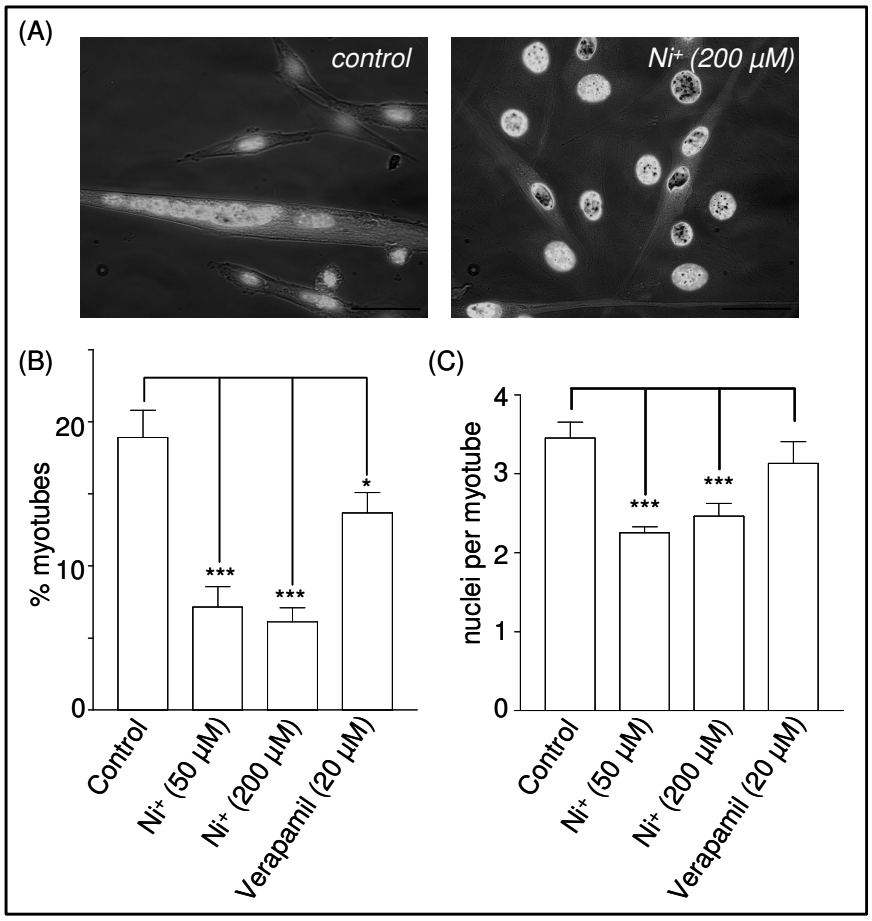

Figure 22: The suppression of i28 myoblast fusion by voltage-dependent Ca^{2+} channels blockers. In (A) representative fluorescence images of *young* cells at 3 days in differentiation medium (DM), on the left, and in Nickel 200 µM in DM, on the right (DAPI staining; scale bar, 35 µm).The histogram in (B) shows the loss of multinucleated cells, and in (C) the decrease of the number of nuclei per myotube, both comparing cells at 3 days in DM with cells at 3 days in DM added with the different blockers indicated (every bar represents the mean of 20 optical fields, *= statistically significant, $P<0.05$; ***= statistically extremely significant, $P<0.001$).

4.1.4 Changes in the L-type current kinetics during i28 in vitro aging

To further investigate the properties of the slow L-type Ca^{2+} current (isolated from T-type as described in *Section 3.3.1*; compare figure 23A and 23B) in myotubes derived from i28 cells at different stages of replicative senescence, I studied the activation and inactivation kinetics. The I-V relationship, determined by measuring the peak L-type Ca^{2+} current as a function of test potential (see figure 23B) was examined, and no significant differences were found when comparing the normalized and averaged I-V curves from cells of different age (figure 23C).

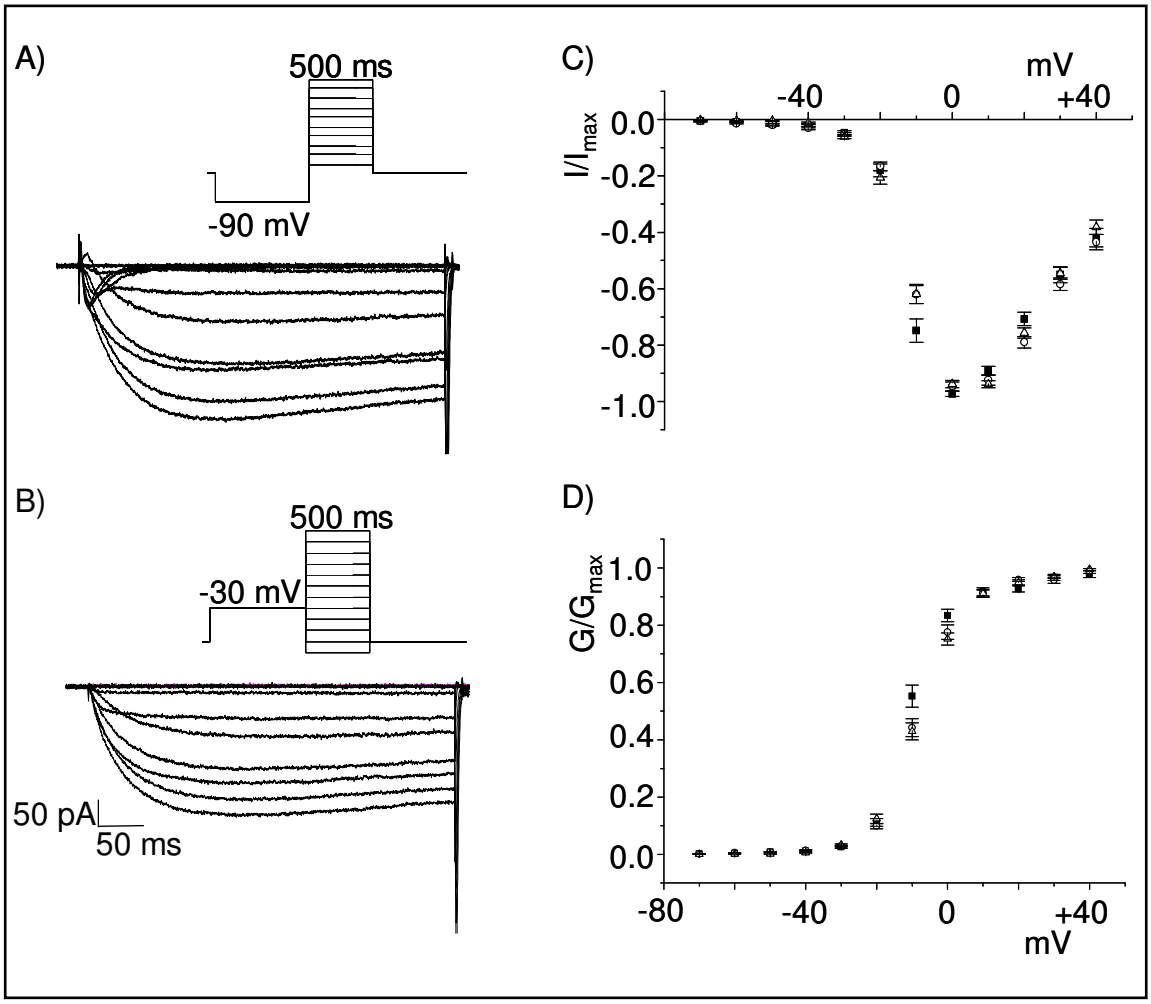

Figure 23: Activation of L-type Ca^{2+} currents in i28 myotubes (A) shows representative L- and T-type Ca^{2+} currents evoked in myotubes by the standard voltage protocol in the inset, and in B) the L-type current was isolated by applying a 750-ms prepulse to -30 mV. C) shows the averaged normalised L-type current-voltage (I-V) relationship and D) the activation curves in myotubes derived from i28 cells at different stages of replicative senescence (■= < 30 divisions; ○= 30< divisions <50; Δ= >50 divisions). Each point is the mean ± SEM and the best fitting parameters (see *Section 3.3.1*) and the number of tested cells are summarised in Table 1. Note little or no change in the shape of the I-V or activation curves due to aging.

Also, the best fitting parameters for $V_{1/2}$ and k, determined from the mean data points of the activation and inactivation curves (see *Section 3.3.1*) showed no significant differences (taking also into account the voltage error due to series resistance) comparing myotubes derived from *young* cells and those derived from *old* ones (see figure 23D and Table 1).

	Activation			Inactivation		
n° of cell divisions	$V_{1/2}$ (mV)	k	n	$V_{1/2}$ (mV)	k	n
n°<30	-11.17±0.45	4.88±0.41	27	-19.50±0.75	7.79±0.67	21
30<n°<50	-8.54±0.35	5.87±0.31	29	-15.18±0.53	7.82±0.47	19
n°>50	-8.15±0.27	6.59±0.23	44	-16.04±0.48	7.35±0.42	29

Table 1: Kinetic parameters of L-type Ca^{2+} current activation and inactivation in murine myogenic i28 cells during *in vitro* aging in culture (n°= number of cell divisions; n=number of cells; data are presented as mean ± SEM, note no significant changes due to aging).

Interestingly, alterations in the kinetics of inactivation of L-type Ca^{2+} currents could be observed in aged i28 satellite cells. To measure I_L inactivation, the current was evoked with two depolarizing voltage steps from the holding potential (-60 mV) in double-pulse experiments; the first pulse (*prepulse*) ranged from -70 to +40 mV and the second (*test pulse*), given after a 100 ms interpulse interval, was held at +10 mV (see *Section 3.3.1* and figure 24A). The greater resistance to inactivation of *old* cells was evident by comparing the *young* and *old* voltage-dependent inactivation curves (figure 24B).

In fact, when comparing myotubes derived from *young* and *old* cells, at least two different inactivation behaviours were observed for L-type current, as illustrated in figure 25. The first one was peculiar for myotubes derived from *young* cells, which usually displayed a rapid phase of inactivation followed by a slower phase; the second one was typically observed in myotubes derived from *old* cells, which showed a very slow decay of the current. In both cases, the time course of inactivation, during the 1500 ms depolarization to 0 mV, could usually be well fitted by a single exponential component (figure 25A); statistical analysis of the data (figure 25B) indicated a significantly different mean for the time constant of

inactivation (ζ_i) found in myotubes derived from the fusion of *young* cells ($\zeta_{i,mean}$= 0.89±0.13 s, n=7) and *old* cells ($\zeta_{i,mean}$= 2.47±0.30 s, n=13). In some cases however, a double exponential time course was observed in myotubes derived from *young* cells.

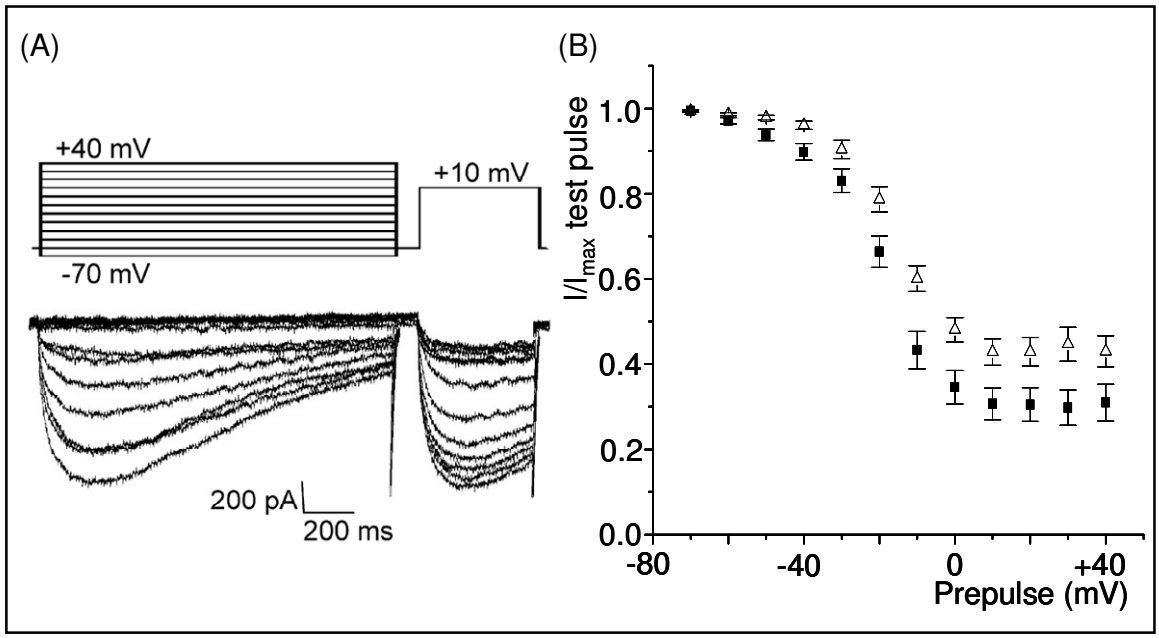

Figure 24: The voltage-dependent inactivation curves. A) Sample I_L traces from a double-pulse experiment covering the range of command potentials shown in the protocol above. B) The averaged relative voltage-dependent inactivation curves (data points are means ± SEM) in myotubes derived from *young* (■) and *old* (Δ) satellite cells (data means are significantly different, paired t-test with $P< 0.05$). Note upward shift of curve with aging.

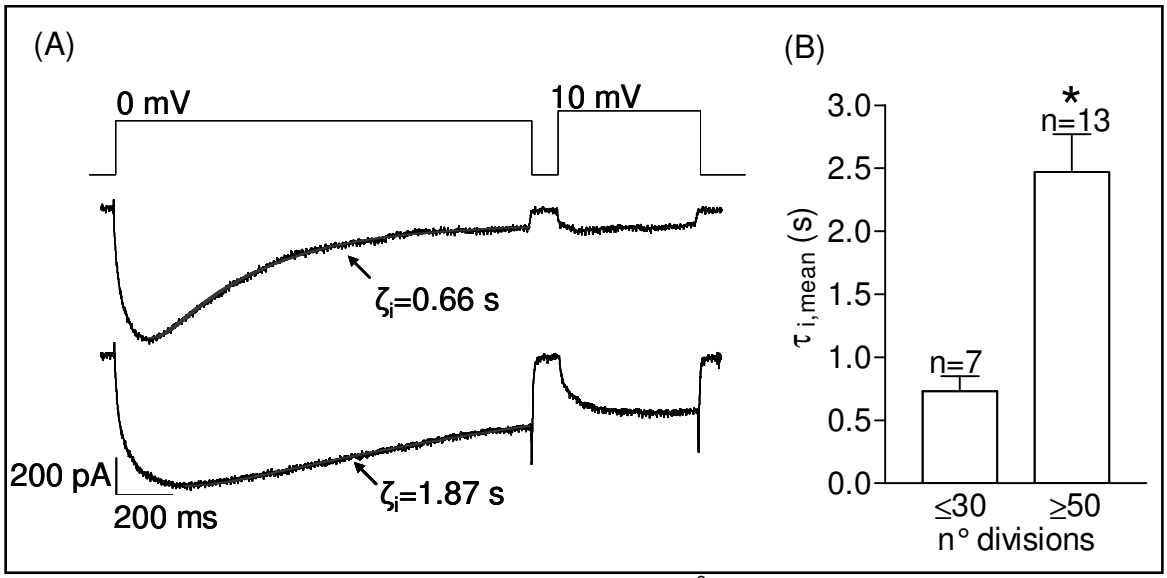

Figure 25: The time course of inactivation of L-type Ca^{2+} currents**.** A) Sample I_L traces from double-pulse experiments from myotubes derived from *young* (upper trace) and *old* (lower trace) i28 satellite cells displaying a different time course and voltage-dependent inactivation at a prepulse potential of 0 mV; superimposed are the exponential fits to the time course of inactivation, and the time constants of inactivation (ζ_i) of the sample currents are indicated. B) The mean ζ_i found in myotubes during aging (*=difference statistically extremely significant, t-test, $P<0.001$).

Moreover, recordings from double-pulse experiments, at the prepulse potential (usually 0 or +10 mV) which lead to maximal *prepulse* peak current and maximal *test pulse* current inactivation, were pooled and analysed to obtain other two indexes of inactivation: 1) the rate of the Ca^{2+} current inactivation (r_{1500}), and 2) the degree of maximal voltage-dependent inactivation (r_{inact}; for details see *Section 3.3.1*). In accordance with the results obtained for ζ_i, data analysis, this further analysis indicated that r_{1500} increased during aging in a significant way. On the other hand, r_{inact} was also significantly higher in *old* cells (figure 26). The correlation between these two indexes of inactivation was highly significant (ρ=0.89; P<0.001).

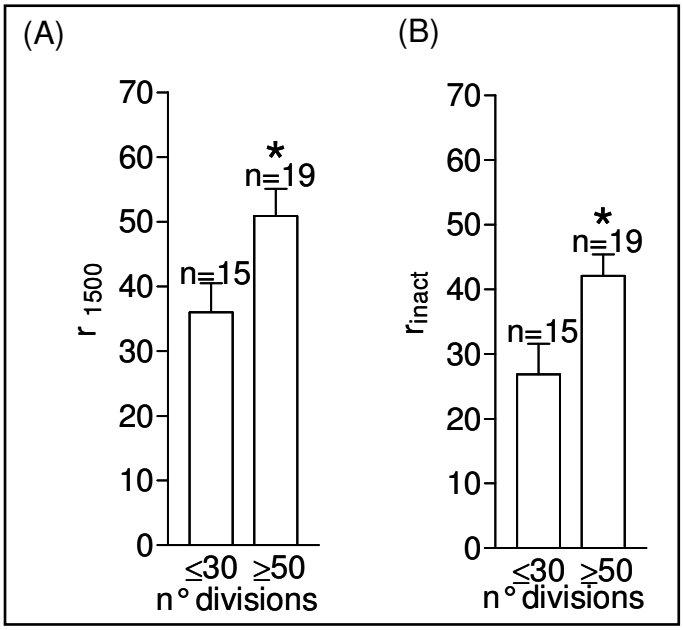

Figure 26: (A) The averaged prepulse residual current at 1500 ms (r_{1500}) and (B) the averaged voltage-dependent inactivation parameter (r_{inact}) during the *in vitro* aging (*=difference statistically significant, t-test, P<0.05).

4.1.5 Is the β-galactosidase a possible biomarker associated with senescence?

As introduced in *Section1.2.2*, cells cutured *in vitro* (and most likely also *in vivo*), after accruing a certain number of cell divisions, undergo cellular senescence, and this state is characterized by some altered functions. After having shown that the *in vitro* aged i28 satellite cells were characterized by inability to fuse into myotubes with functional voltage dependent Ca^{2+} currents (see previous *Sections 4.1.2-*

4.1.4), I decided to verify if the senescence of this type of cells was associated also with the detection of the beta-galactosidase activity at pH 6 (see *Section 3.2.3*). Indeed, this enzyme has been hypothesized as a biomarker associated with the senescent phenotype of fibroblasts in culture (Dimri et al., 1995).

Young (with less than 30 divisions) and *old* (with more than 50 divisions) i28 myoblasts, previously fixed in paraformaldeyde, were stained for β-galactosidase activity at pH 6 (for details see *Section 3.2.3*). At least five randomly chosen optical fields per coverslip were analysed, and the percentage of β-galactosidase positive cells was calculated as the number of cells stained after 24 hours *vs* the number of total cells observed in the optical field. Considering both *young* and *old* cells, the majority of them resulted not stained for β-galactosidase activity at pH 6; in fact, only a small percentage of cells were stained, and there is not a significant difference among the two classes of cells (see figure 27). Moreover, as a positive control, some cells were stained for β-galactosidase activity with the buffer adjusted at pH 4, without modifying the procedure otherwise; since β-galactosidase is normally active in lysosomes at pH 4 also in presenescent cells, all of them proved to be clearly stained. Also, different plating density and different times of incubation were tested, without discovering significant differences in the results (data not shown).

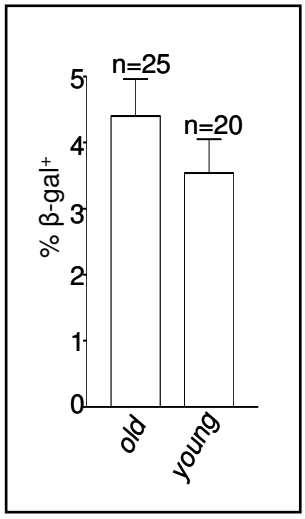

Figure 27: Percentage of cells exhibiting the β-galactosidase activity at pH 6 at different stages of replicative senescence. Note no significant differences (n=number of optical fields).

4.2 Ca^{2+} currents and homeostasis during the in vivo aging of human satellite cells

The latter part of my Ph.D. research has been focussed in particular on exploring the possibility to extend the results obtained with the *in vitro* aging of i28 murine satellite cells model to the physiological process of human aging *in vivo*, *i.e.* to investigate if satellite cells obtained from old donors could present the same or other important age-related alterations in voltage-dependent L-type and T-type Ca^{2+} channel properties that I showed to occur in murine muscle satellite cells aged *in vitro*.

The principal results obtained on human cultures are introduced in the next paragraphs; the results, completed with a specific discussion, at present accepted with minor revisions by the journal Cell Calcium, are presented in the enclosed *Appendix 2* (pag. 84).

4.2.1 Human muscle satellite cells and in vivo aging: myogenic purity and beta-galactosidase activity

Electrophysiological and videoimaging experiments (see next *Sections 4.2.2-4.2.4*) were performed on cultured multinucleated myotubes derived from young donors (2 and 12 years, called “young myotubes”) and old donors (76 and 86 years of age, “old myotubes”). These myotubes derived from the differentiation and fusion in culture of human myogenic satellite cells, all at the very beginning of the proliferative phase of the various cultures, *i.e.* well before the proliferative senescence, in order to avoid problems linked to aging *in vitro* (for details, see *Sections 1.2.2* and *3.1*).

These human satellite cells were obtained from desmin positive-enriched cultures (for details, see Shafer et al., 2006). Moreover, some immunocyto-chemistry experiments were made to control the purity of the culture, by examining the presence of desmin positive cells (figure 28; for details see *Section 3.2.2*). Only cultures with a percentage of desmin positive cells higher than 70% were used in the electrophysiological and videoimaging experiments. Moreover, all the experiments were performed only on young and old multinucleated myotubes,

after 3-6 days in differentiation medium (DM), and not on mononucleated cells, thus being sure of working on myogenic cells.

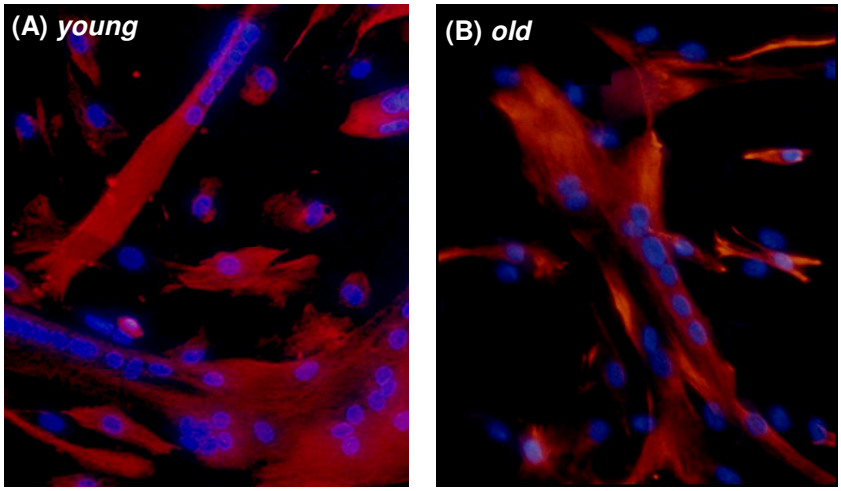

Figure 28: Representative fluorescence photomicrographs of human cells, from (A) 12 years old and (B) 76 years old donors (red: desmin positive cells, blu: bis-Benzimide stained nuclei; 20X magnification).

It is important to note that aging likely influences the human satellite cells differentiation and fusion; in fact not only an age-related loss of multinucleated cells was evident, but also old myotubes were smaller and thinner than young myotubes, as shown in representative examples in figure 28 and 29, and already known from previous works (see *Section 1.2.2*).

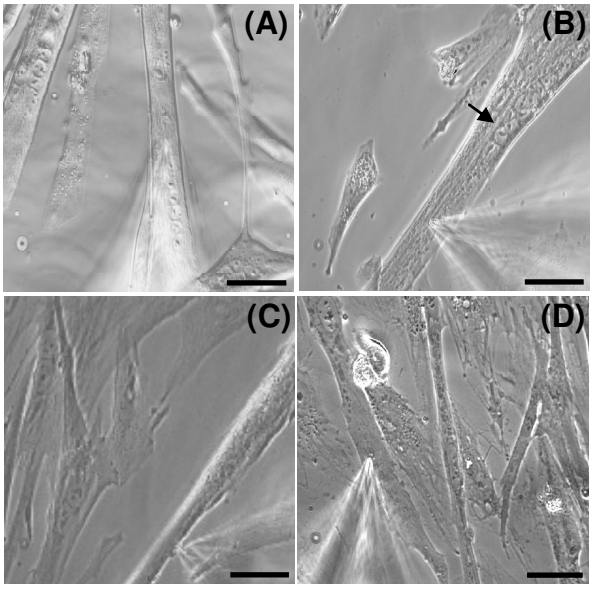

Figure 29: Representative photomicrographs of young and old human patched multinucleated myotubes, derived from the differentiation and fusion in culture of satellite cells of (A) 2 years old, (B) 12 years old, (C) 76 years old, and (D) 86 years old donors (The arrow in (B) indicate some well evident nuclei; scale bar, 35 µm).

Furthermore, I tested the possible link between the beta-galactosidase activity at pH 6 (see *Section 3.2.3*) and the *in vivo* aging of human satellite cells, as previously made for murine satellite cells aged *in vitro* (see *Section 4.1.5*). Unfortunately, the results obtained were confusing and inconclusive. Briefly, the staining were very variable both in percentage and in intensity depending on the donor and on the specific subculture, and this seemed to be unrelated to the age. Also the density of the cells attached to the coverslip, the percentage of desmin positive cells, the passage of the culture, the time of the staining and the field selection seemed to have a certain importance in the detection of the beta-galactosidase activity.

Clearly, these difficulties made impossible a correct comparison between different age groups. A better determination of the possible age-related beta-galactosidase activity at pH 6 and a standardization of the protocol used would be really necessary to obtain clear results.

4.2.2 Age-related changes in T-type Ca^{2+} currents in human myotubes

T-type Ca^{2+} currents (I_T; figure 30A) were evoked from -60 mV holding potential and isolated from L-type Ca^{2+} currents as explained in *Section 3.3.1* (see also figure 31A-C).

I_T were detected in about 90% of the young human myotubes, but only in about 50% of the old myotubes analysed (figure 30B).

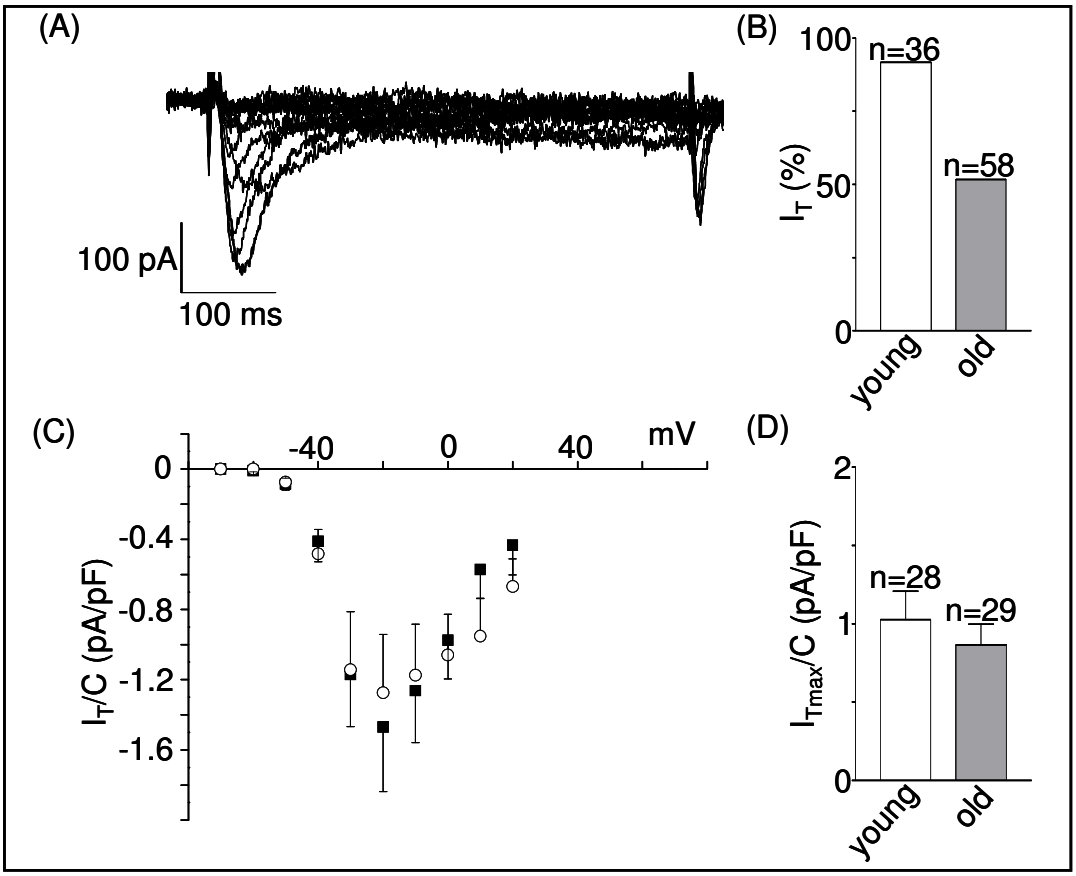

Figure 10: T-type Ca^{2+} current (I_T) occurrence and density in human myotubes during the aging process: (A) shows representative I_T currents recorded in a young human myotube. The histogram in (B) shows the percentage of young and old myotubes exhibiting I_T current (n=number of tested myotubes). In (C) the averaged current density-voltage (*(I_T /C)-V*) curves from young and old myotubes (each point is the mean ± *SEM*; ■= young, n=12; ○=old, n=8, and in (D) the histograms of T-type current density during aging, using only the maximum peak current value ($I_{Tmax,}$ n=number of tested myotubes).

The current density (I_T/C), calculated from the peak current values at different test potentials, was similar in both groups as judged from comparing the normalized and averaged (*I_T /C)-V* curves (Fig. 30C). Similarly, maximum peak current values (I_{Tmax}), generally detected at -30 or -20 mV holding potential, and normalized to the cell capacitance, were similar, thus confirming that there was no significant age-related decrease in T-type current density (Fig. 30D).

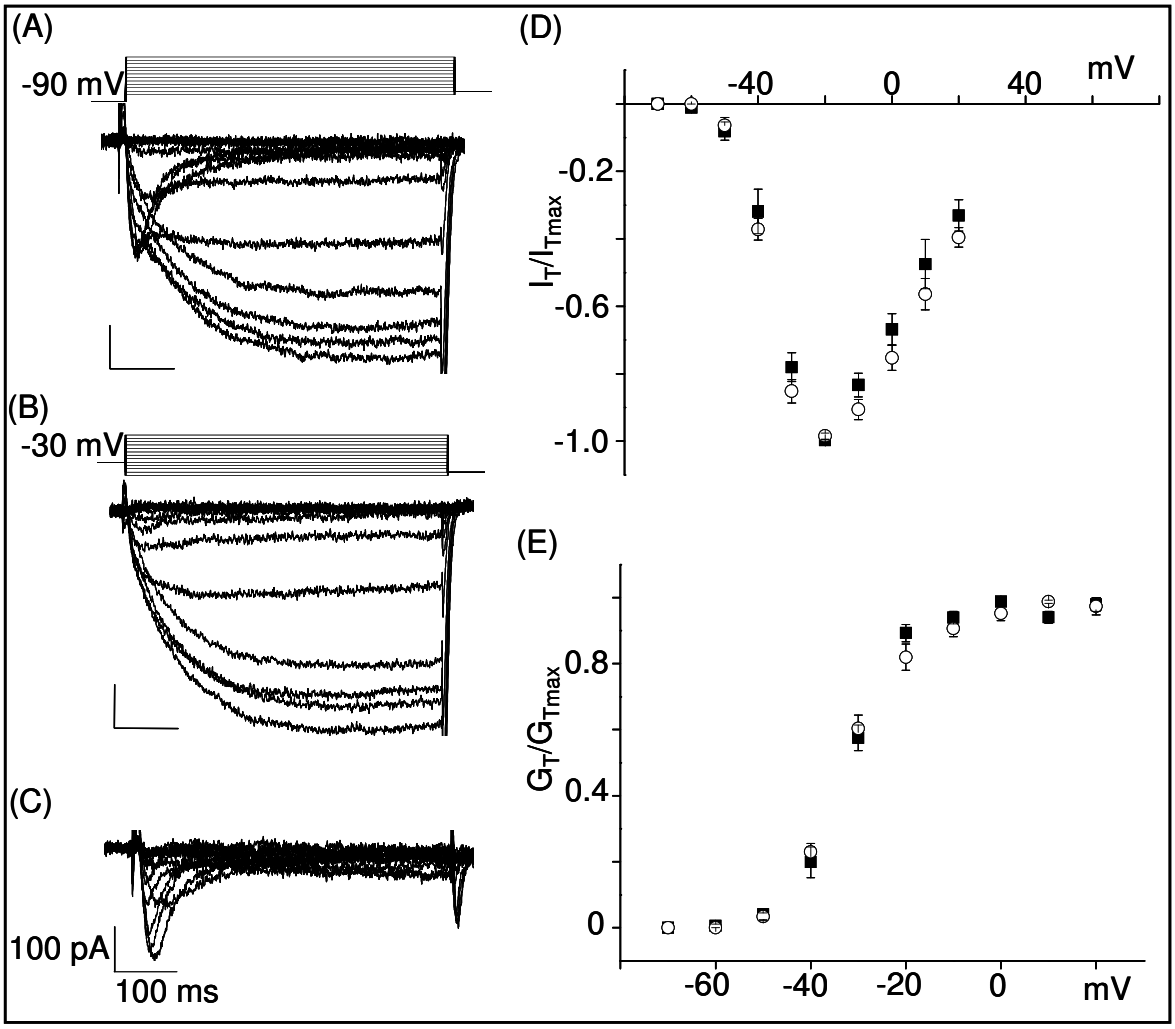

Figure 31: Total Ca^{2+} currents, isolation of T-type (I_T) and voltage-dependent activation kinetics in human myotubes during the aging process: in (A) representative I_T and I_L currents evoked in a young myotube by the standard voltage protocol in the inset; in (B), the same I_L currents, isolated by applying a 750-ms prepulse to -30 mV, and in (C) the I_T currents obtained by the subtraction of the recordings with the prepulse (B) from those obtained without it (A). (D) shows the averaged normalised T-type current-voltage (I-V) relationship and (E) the activation curves in young and old myotubes (each point is the mean ± *SEM*; ■= young, n=10; ○=old, n=8); the best fitting parameters are summarised in Table 2. Note very little or no age-related change in the shape of the I-V or activation curves.

I next examined the voltage dependence of the activation and inactivation of T-type Ca^{2+} currents. Using the subtraction method (figure 31A-C), it was possible to separate the T-type current from the L-type current, and to determine the I_T-V relationship. The value of E_{rev} calculated for each myotube was used to estimate the voltage dependence of activation (G, conductance), and, then, the normalized and averaged I_T-V and G_T-V curves were examined to compare the activation kinetics of T-type current (for further details see *Section 3.3.1*). The voltage-dependence of the T-type current is shown in Figs. 31D and E; no significant

differences were found on comparing the two age groups, and this was also true for the best fitting parameters for $V_{1/2}$ and k, determined from the mean data points of the activation curves (see *Section 3.3.1* and Table 2).

The voltage-dependence of the inactivation of the T-type current was studied using a double pulse protocol; the amplitude of each current elicited by the test pulse was normalized to the maximum current, usually obtained with the conditioning prepulse to -80 mV, and plotted versus the potential of the prepulse, for each myotube (see *Section 3.3.1* and figure 32).

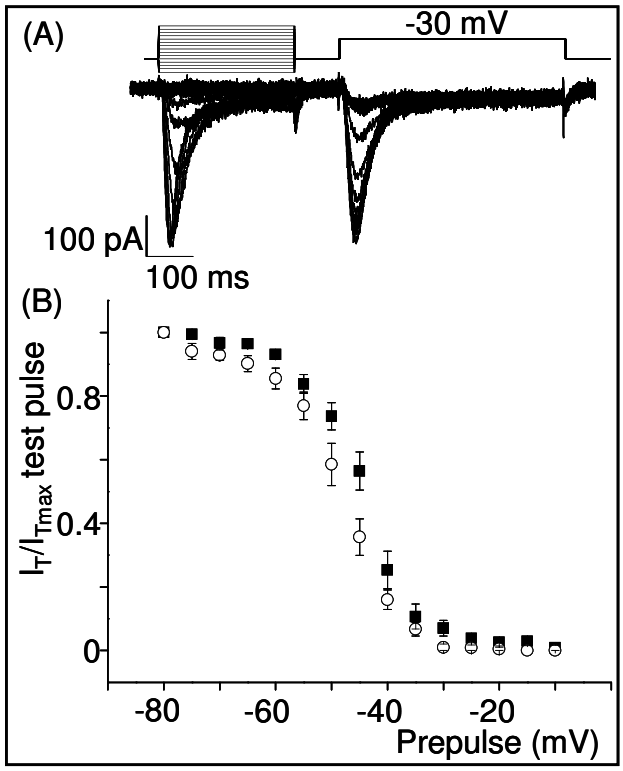

Figure 32: The T-type current (I_T) voltage-dependent inactivation kinetics in human myotubes during the aging process: in (A), sample I_T traces from a double-pulse experiment covering the range of prepulse potentials shown in the protocol; in (B), the averaged normalised relative voltage-dependent inactivation curves (each point is the mean ± *SEM*; ■= young, n=12; ○=old, n=8). The best fitting parameters are summarised in Table 2. Note the statistically significant shift (~4 mV) of the curve towards more negative potentials with aging.

The inactivation curves obtained in young and old myotubes respectively were then averaged, and the results are displayed in figure 32B. The best fitting parameters for $V_{1/2}$ and k, determined from the mean data points of the inactivation curves, are presented in Table 2. Inactivation curve means, obtained

in young and old myotubes, were significantly different (*paired t-test, P=0.0006)*, as was the best fitting parameter for $V_{1/2}$ (*t-test, P=0.0001,* Table 2). The ~4 mV shift of the inactivation curve of the T-type current towards more negative potentials in old myotubes exceeded the remaining voltage drop error, potentially induced by the uncompensated series resistance (see *Section 3.3.1*), so the difference noticed between the T-type current recorded in young and old myotubes can be considered a result of age-related alterations.

T-type Ca^{2+} current	Activation			Inactivation		
	$V_{1/2}$ (mV)	k	*n*	$V_{1/2}$ (mV)	k	*n*
young	-32.14±0.75	5.66±0.55	12	-45.22±0.62	5.62±0.36	10
old	-32.25±0.79	7.04±0.62	8	-49.58±0.60 ***	5.76±0.34	8

Table 2: Kinetic parameters of T-type Ca^{2+} current activation and inactivation in myotubes derived from the differentiation and fusion of satellite cells obtained from young and old human donors (*n*= number of myotubes; data are presented as mean ± *SEM*, *** difference statistically extremely significant, *t-test, P=0.0001*; $V_{1/2}$ is the voltage at which the conductance is half maximal and k describes the steepness of activation of the fitted Boltzmann function).

4.2.3 Age-related changes in L-type Ca^{2+} currents in human myotubes

L-type Ca^{2+} currents (I_L), evoked and recorded in human myotubes as explained in *Section 3.3.1*, are shown in figure 33A. I detected I_L in almost 100% of the young and in about 50% of the old myotubes we recorded from (figure 33B). It is important to note that the majority of these old myotubes did not display voltage-dependent Ca^{2+} currents at all, since they did not display T-type Ca^{2+} currents either (I_T; see previous *Section 4.2.2*). In fact, these two types of Ca^{2+} current were typically detected together in the cells tested, and only in few cases we found either I_L or I_T.

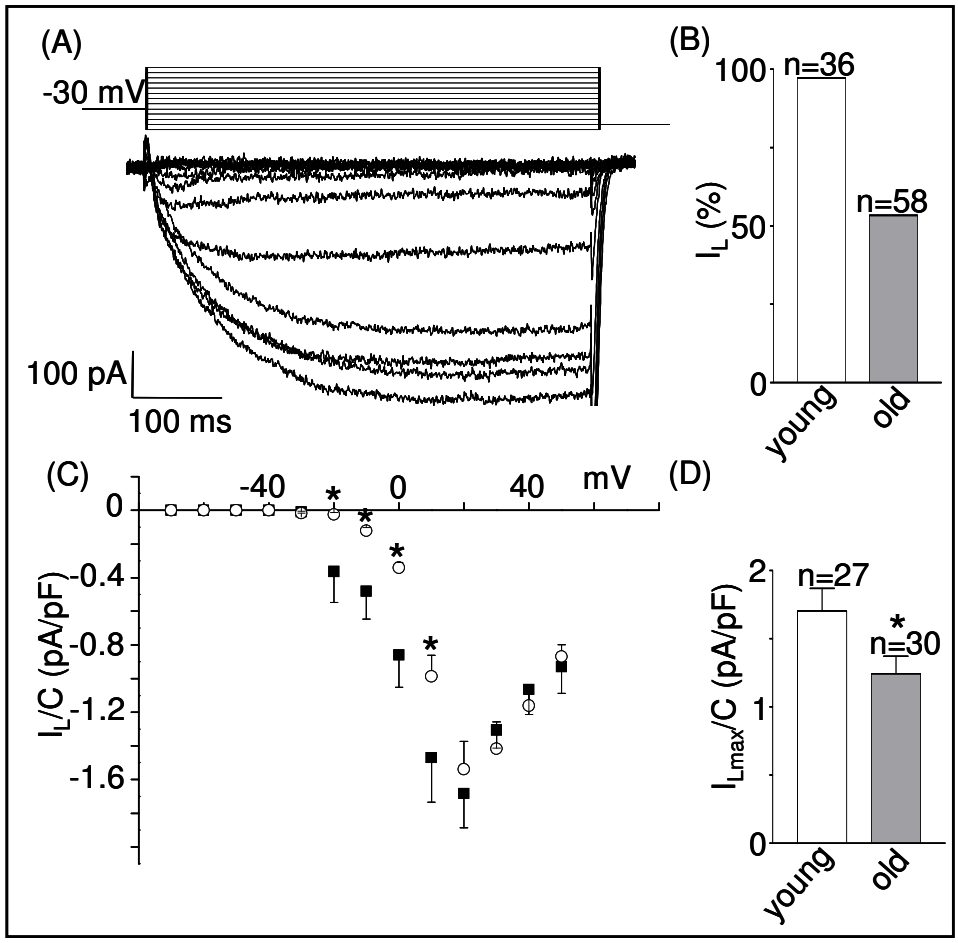

Figure 33: L-type Ca^{2+} current (I_L) occurrence and density in human myotubes during the aging process: (A) shows representative I_L currents recorded in a young human myotube, isolated by applying a 750 ms prepulse to -30 mV. The histogram in (B) shows the percentage of young and old myotubes exhibiting I_L current (n=number of tested myotubes). In (C) the averaged current density-voltage (*(I_L /C)-V*) curves from young and old myotubes (■= young, n=16; ○=old, n=16); each point is the mean ± *SEM*; *= statistically significant difference, paired *t-test, P=0.0051*) and in (D) the histograms of L-type current density during aging, by considering exclusively the maximum peak current value (I_{Lmax}; n=number of tested myotubes, *= difference statistically significant, *t-test, P=0.0326*).

Interestingly, the L-type current density (I_L /C) also decreased significantly in an age-related manner; in fact, both the normalized and averaged (*I_L /C)-V* curves (figure 33C), and the maximum peak current value (I_{Lmax}), generally observed at +20 or +30 mV and normalized to the cell capacitance (figure 33D), significantly differed in young and old myotubes. The normalized and averaged current – voltage relationship (*I_L-V*), and the normalized and averaged activation (*G_L-V)* and inactivation curves were then examined to compare the kinetics of L-type current at different ages (for further details on the protocols used to obtain the L-type current kinetics see *Section 3.3.1* and Luin and Ruzzier, 2007).

In figure 34, two representative recordings of I_L currents are shown, evoked and recorded at different potentials, respectively in a young myotube (figure 34A) and in an old myotube (figure 34B). Besides noting the clear decrease of I_L amplitude in old myotubes (already mentioned above), some additional differences became obvious when comparing the normalized and averaged I_L-V (figure 34C) and G_L-V (figure 34D) activation curves. Indeed, mean values of activation curve data, obtained in young versus old myotubes, were significantly different (*paired t-test, P=0.0188*), as was the best fitting parameter for $V_{1/2}$ (*t-test, P<0.0001)*, provided in Table 3.

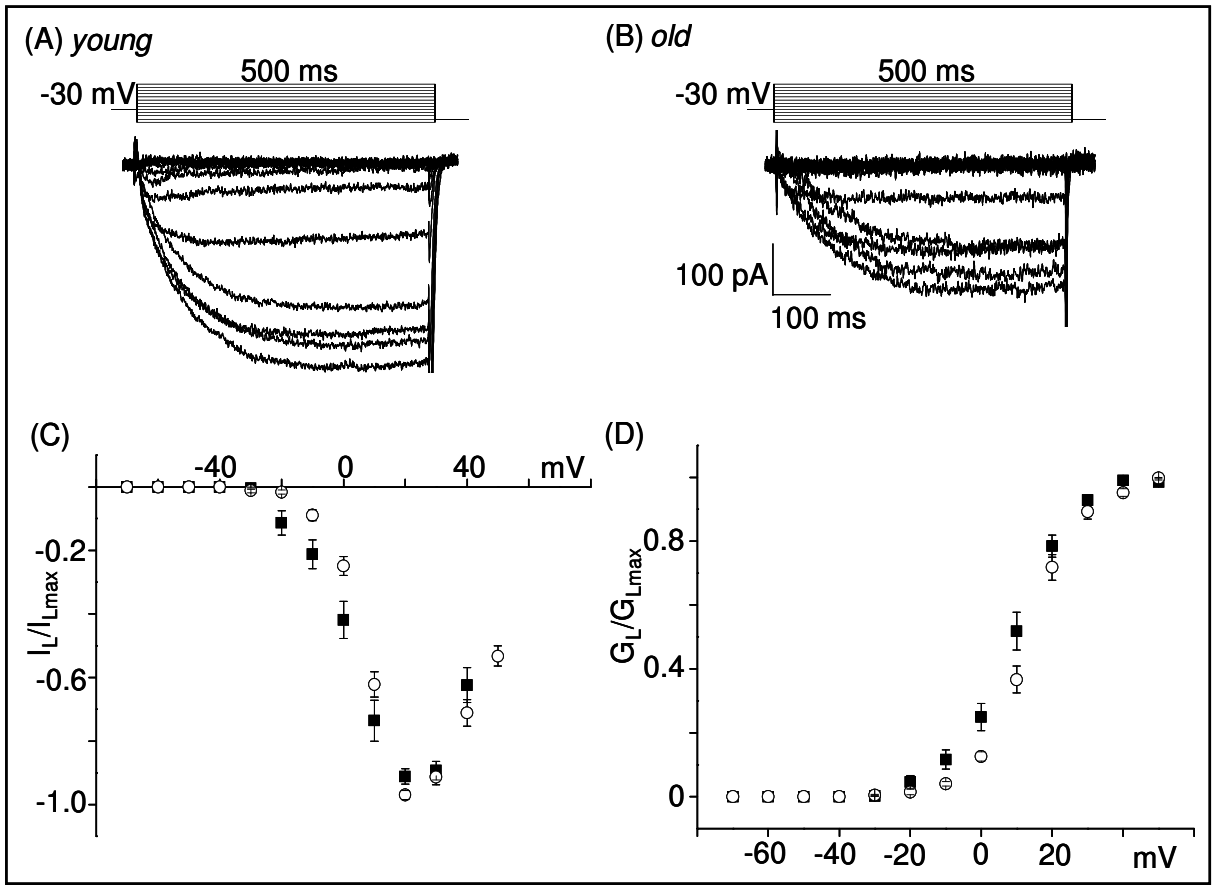

Figure 34: The L-type current (I_L) voltage-dependent activation kinetics in human myotubes during the aging process: (A) and (B) show representative I_L currents recorded respectively in a young and in an old human myotube (same scale, note the clear decrease of I_L amplitude in the exemplificative old myotube); (C) shows the averaged normalised L-type current-voltage (I_L-V) relationships and (D) the activation curves in young and old myotubes (each point is the mean ± *SEM*; ■= young, n=16; ○=old, n=16); the best fitting parameters are summarised in Table 3. Note a significant age-related change in the shape of the I-V and activation curves, especially with test potentials ranging from -20 to +20 mV (see the text for details).

L-type Ca^{2+} current	Activation			Inactivation		
	$V_{1/2}$ (mV)	k	*n*	$V_{1/2}$ (mV)	k	*n*
young	8.73±0.93	7.72±0.49	16	-5.77±0.43	7.30±0.38	5
old	14.47±0.70 ***	7.74±0.45	16	2.38±1.65 **	10.1±1.46	5

Table 3: Kinetic parameters of L-type Ca^{2+} current activation and inactivation in myotubes derived from the differentiation and fusion of satellite cells obtained from young and old donors (*n*= number of myotubes; data are presented as mean ± *SEM*, *** difference statistically extremely significant, *t-test, P<0.0001,* ** difference statistically very significant, *t-test, P=0.0014*; $V_{1/2}$ is the voltage at which the conductance is half maximal and k describes the steepness of activation of the fitted Boltzmann function: see Section 2.2).

Recordings from double-pulse experiments allowed me to study the inactivation kinetics of the I_L current. On comparing the representative I_L traces from young and old myotubes (figure 35A) and the relative normalized and averaged inactivation curves (figure 35B), two different inactivation behaviours could be easily recognised. The first one was peculiar for young myotubes, which usually displayed a complete current inactivation; the second one was typically observed in old myotubes, which showed a greater resistance to inactivation. Data obtained from double-pulse experiments, at the prepulse potential (usually +20 mV) which lead to maximal *prepulse* peak current and maximal *test pulse* current inactivation, were pooled and analysed to obtain the two indexes of inactivation r_{1500} (residual current at 1500 ms) and r_{inact} (degree of maximal voltage-dependent inactivation; see *Section 3.3.1* for details); this analysis indicated that r_{1500} increased during aging in a highly significant way ($r_{1500,young}$[%]=19.4±5.40, *n*=14; $r_{1500,old}$[%]=63.8±3.20, *n*=20; *t-test P<0.0001*), and that r_{inact} was also significantly higher in old myotubes ($r_{inact,old}$[%]=45.0±3.50, *n*=11) than in the majority of young myotubes, where it was close to zero (complete inactivation). In two out of 8 young myotubes however, I found also an incomplete inactivation (data not shown). Moreover, mean values of inactivation curve data obtained in young and old myotubes (figure 35B), were significantly different (*paired t-test, P=0.0077)*, as well as the best fitting parameter for $V_{1/2}$ (*t-test, P=0.0014)* (Table 3).

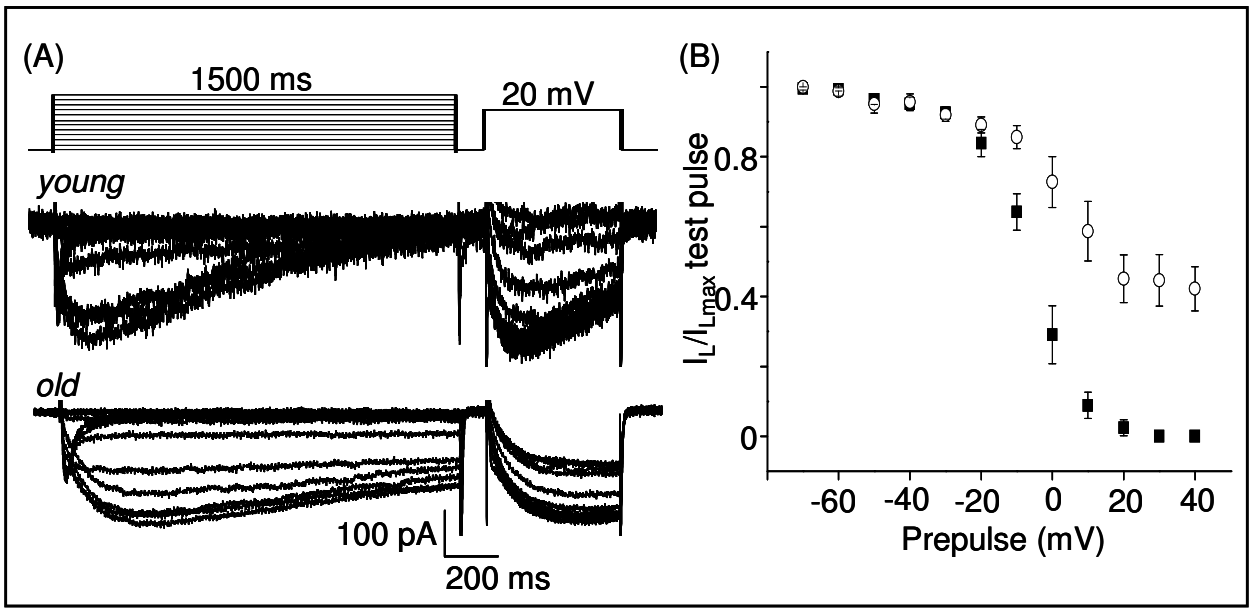

Figure 35: The L-type current (I_L) voltage-dependent inactivation kinetics in human myotubes during the aging process: in (A) sample I_L traces from double-pulse experiments from a young (upper trace) and an old (lower trace) myotube, displaying a different time course and voltage-dependent inactivation; in (B) the averaged normalised relative voltage-dependent inactivation curves (each point is the mean ± *SEM*; ■= young, n=5; ○=old, n=5). The best fitting parameters are summarised in Table 3. Note the upward shift of the curve with aging, which is indicative of a greater resistance to inactivation of the old myotubes (data means are significantly different, *paired t-test, P=0.0077*).

4.2.4 E-C uncoupling in human myotubes during the aging process

In skeletal muscles, L-type Ca^{2+} channels, besides acting as ion-conducting pores, interact mechanically with the ryanodine receptors, and are involved in triggering Ca^{2+} release from the sarcoplasmic reticulum, even in the absence of extracellular Ca^{2+} (excitation-contraction (E-C) coupling mechanism). In order to explore whether the age-related alterations of the L-type Ca^{2+} channels, highlighted by the electrophysiological experiments, had consequences on the excitation-Ca^{2+} release coupling mechanism, I performed videoimaging experiments on 3-6 days differentiated young and old myotubes. To distinguish between *coupled* and *uncoupled* myoubes, the cells were depolarized with high [K^+] (40 mM) in a Ca^{2+}-free solution, applied for 5 s by a gravity-driven perfusion system (see *Section 3.3.2* and figures 36A and B for details). In every experimental field, only multinucleated myotubes were taken into consideration. While E-C coupling was detected in 86 % of young myotubes (*n*=189), only 44% of the old myotubes

(*n*=138) were responsive to the depolarizing stimulus in the absence of extracellular Ca^{2+} (figure 36C).

On the other hand, the $[Ca^{2+}]_i$ transients elicited by depolarization were very similar in *coupled* young and old myotubes: both mean peak values and mean area of the $[Ca^{2+}]_i$ transient, were not significantly different when I compared young (*n*=154) and old (*n*=61) myotubes (figures 36D and E).

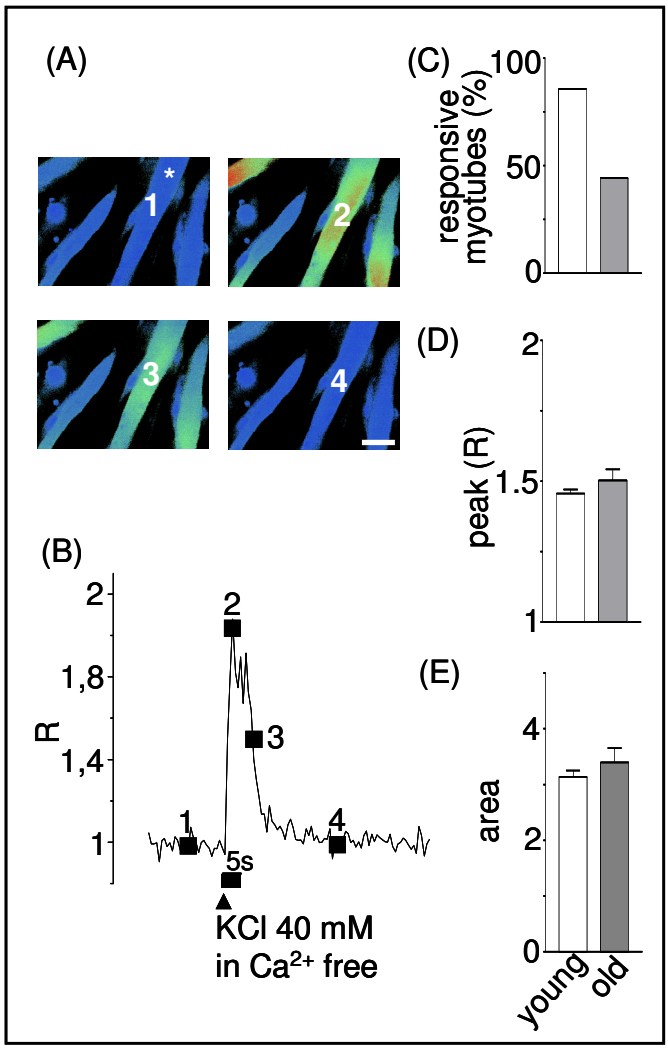

Figure 36: The E-C coupling mechanism in human myotubes during the aging process: in (A) four representative pseudocolor images of the $[Ca^{2+}]_i$ response elicited in one of the myotubes (*) of the optical field (scale bar, 35 µm). In (B) the corresponding temporal plot of the $[Ca^{2+}]_i$ response (the numbers indicate the timing of acquisition of the images shown in (A); the arrow head indicates the beginning and the bar the duration of stimulus application). In (C) the percentage (%) of responsive myotubes among young (white bar, n=189), and old (grey bar, n=138) myotubes; in (D) the averaged peak of $[Ca^{2+}]_i$ transients (R: young, n=154; old, n=61 myotubes), and in (E) the averaged area of $[Ca^{2+}]_i$ transients (young, n=154; old, n=61).

5. Discussion and conclusions

This *Section* has been conceived in particular to briefly summarize and to look for a parallelism between the results obtained with the *in vitro* aging of murine satellite cells model and those related to the physiological process of human skeletal muscle aging *in vivo*, in order to have an overall view of the point at issue. For a critical and detailed discussion specifically on the results got in the two models, please see the discussion of the published results respectively in *Appendix 1* (pag. 83) and in *Appendix 2* (pag. 84).

5.1 Aging in vitro and in vivo

At the beginning of my research I decided to use the *in vitro* aging condition of murine satellite cells as an useful model of the *in vivo* aging of the same cells (see also Decary, 1996); this model allowed me to investigate if the replicative senescence affected their functions. Indeed, cellular senescence was proposed to recapitulate the age-related loss of regenerative capacity of cells *in vivo* (in Campisi and d'Adda di Fagagna, 2007). However, the relationship between cell aging *in vivo* and *in vitro* is still matter of debate (reviewed in Rubin, 1997), even if there are several pieces of evidence showing that senescent cells may persist and accumulate with age *in vivo* and that replicative senescence contributes to aging (Dimri et al, 1995, Campisi, 2001).

Interestingly, the results show a clear parallelism between aging *in vitro* and *in vivo* of satellite cells, since both the ability to fuse and the calcium homeostasis are proved to change in both models (see next *Sections 5.2* and *5.3*).

It has still to be clarified if the β-galactosidase activity at pH 6.0 is a possible biomarker of senescence *in vitro* and *in vivo* or, more probably, a delusion. In the case of i28 satellite cells aged *in vitro*, no significant difference has been noted if compared with cells at early passages (see *Section 4.1.5*). On the other hand, considering human cells the results obtained are even more unsatisfying; in fact, the staining seems to be non-specific, and unrelated to age (see *Section 4.2.1*). As stated by several authors (see for example Coates, 2002; Cristofalo, 2005; Yang and Hu, 2005), the β-galactosidase activity at pH 6.0 could be a reliable biomarker of aging, but only after determining the real mechanisms underlying its eventual increase during aging in culture and/or *in vivo*. At the same time, it would be

necessary to control or exclude all the other possible confounding factors, that could invalidate the assay.

One of the major goal of the last years research on aging has been to clarify the precise relationship between the process of organism aging and aging of cells, and to find out specific and universal biomarkers of aging. Unfortunately, these two issues seem to be still far to be solved.

5.2 The differentiation and fusion potency in aging skeletal muscle

Both the results obtained using the model of *in vitro* aging of murine satellite cells (see *Section 4.1.2*) and that obtained observing the myotubes deriving from the differentiation of human satellite cells from different age donors (see *Section 4.2.1*) confirmed that there is an age-related decrease in the quality and in the quantity of fusion, as already known from previous works (see Renault et al., 2000; Lorenzon et al., 2004). In general, it could be state that senescent satellite cells fuse more slowly and less efficiently, leading to less myotubes, which are also smaller and thinner. Being the regenerative potential of skeletal muscle determined at least in part by satellite cell differentiation, what I observed may be one of the causes of the age-related decline in muscle mass and force (see *Section1.2*).

5.3 Calcium currents and homeostasis

- T-type Ca^{2+} currents: The data reported on murine myotube cells aged *in vitro* (see *Section 4.1.3*) and on old human myotubes (see *Section 4.2.2*) are fully in accordance; in fact, in both models, I have shown for the first time that the occurrence of T-type currents significantly decreased with aging, without any change in the current density. Moreover, in the human model, a significant shift in the inactivation curve towards more negative potentials with aging was revealed, with a consequent influence on the steady-state "window" Ca^{2+} current through T-type channels.

These results on T-type Ca^{2+} currents demonstrate that, extensively, less Ca^{2+} would be available via T-type channels in the old myotubes. It is important to consider that an increase of intracellular Ca^{2+} concentration may be necessary for fusion between myoblasts and between myoblasts and myotubes (see *Section 1.3*), and that one of the sources of this Ca^{2+} would be the entry via T-type Ca^{2+} channels. To strengthen this hypothesis, I have also shown that in the murine

model, the inhibition of T-type current by Ni^{+} suppressed i28 myoblast fusion, as also shown previously for human cells in other works (see Bjielenga et al., 2000).
Thus, overall, a correlation between defective T-type Ca^{2+} channels and the senescent satellite cells feature of fusing more slowly and less efficiently can be proposed.
- L-type Ca^{2+} currents and *E-C coupling*: Also in this case, the results obtained in the model of *in vitro* aging are in accordance with the results obtained with human physiologically aged satellite cells. Indeed, I demonstrated for the first time that the density of L-type currents in myotubes derived from the differentiation and fusion of both *in vitro* aged murine satellite cells (see *Section 4.1.3-4.1.4*) and of *in vivo* aged human satellite cells (see *Section 4.2.3*) were significantly reduced, compared with those derived from young satellite cells. Moreover, in the murine model, the L-type channels seemed to be expressed later during the differentiation time, while in the human model the occurrence clearly decreased from 100% in young myotubes to about 50% in old myotubes. So, less Ca^{2+} might be available for differentiation and fusion of old myotubes, even when myoblasts switch to this alternative source of Ca^{2+} influx. What seems to be very relevant too, is the greater resistance to inactivation shown by L-type current in old myotubes in both models. This could be a sort of compensatory mechanism to hinder the age-related reduction of L-type current density and the lower availability of intracellular Ca^{2+}, indispensable for skeletal muscle contraction.
The illustrated electrophysiological results demonstrated an age-related decrease of the activity of L-type channels; moreover, the videoimaging experiments carried out on human myotubes showed a clear age-related decrease in the occurrence of the E-C coupling. These results strengthen even more the possibility that the age-related absence of the E-C coupling mechanism could be due to the reduction of L-type channel activity.
Altogether, my results on L-type channels fit with the hypothesis that alteration of the mechanisms controlling different components of the excitation-contraction apparatus could be one of the causes of the age-related decline in skeletal muscle strength (among others, see also Delbono et al., 1995; Renganathan et al., 1997; Lorenzon et al., 2004; Payne et al., 2004).

5.4 Conclusions and future developments

What is possible to read between the lines of the just briefly summarized results, is a last possible and questionable parallelism between the two species of mammals I dealt with, the mouse and the human ones. In fact, every time I have compared the models of aging *in vitro* and *in vivo*, I have also inevitably compared these two species. So, from the results obtained, it may be assumed that at least some causes and aspects of aging would be similar in the two species, as already shown from genetic studies (see Welle, 2001).

This can be consolatory when thinking about the real difficulty to obtain human cells, to maintain them in culture, and to do on them electrophysiological experiments, if compared with the murine ones. Of course, it would be better to work on human cells to really understand the physiological process of skeletal muscle aging, but I think that future experiments carried on satellite cells derived from young and old mice would be helpful, also by considering the experimental difficulties of working on human cells.

The feasible experiments would have been conceived to explore the molecular processes at the basis of the age-related changes in the voltage-dependent L- and T-type Ca^{2+} currents, as for example the possible alterations of the different channel subunits expression, possibly due to aging-associated changes in genes transcription and protein expression, or modified post-translational processing.

In conclusion, I reckon that understanding the molecular basis of age-related physiological changes requires a multidisciplinary experimental approach and that the aging of skeletal muscle should be studied using an extensive range of chemical, biochemical, biomolecular, structural and physiological techniques.

Meanwhile, with the research that has been going ahead with my Ph. D. project, a further strong evidence has been given that in humans, as in other mammals, the satellite cells and the regulation of Ca^{2+} homeostasis have a decisive role in the physiological process of skeletal muscle aging.

6. References

1. C.A. Ahern, P. Powers, G.H. Biddlecome et al., Modulation of L-type Ca^{2+} release by the gamma1 subunit of the dihydropyridine receptor of skeletal muscle, BMC Physiol. 1 (2001) 8.
2. J.E. Anderson, The satellite cell as a companion in skeletal muscle plasticity: currency, conveyance, clue, connector and colander, J. Exper. Biol. 209 (2006) 2276-2292.
3. S. Arnadeu, N. Holzer, S. Kőnig, C.R. Bader, L. Bernheim, Calcium sources used by post-natal human myoblasts during initial differentiation, J. Cell. Physiol. 208 (2006) 435-445.
4. M.J. Barclay, A. Morgan, R.D. Burgoyne, Calcium-dependent regulation of exocytosis, Cell Calcium 38 (2005) 343-353.
5. K.G. Beam, C.M. Knudson, Calcium currents in embryonic and neonatal mammalian skeletal muscle, J. Gen. Physiol. 91 (1988) 781-798.
6. S. Beccafico, C. Puglielli, T. Pietrangelo, R. Bellomo, G. Fanò, S. Fulle, Age-dependent effects on functional aspects in human satellite cells, Ann. N. Y. Acad. Sci. 1100 (2007) 345-352.
7. M.W. Berchtold, H. Brinkmeier, M. Müntener, Calcium ion in skeletal muscle: its crucial role for muscle function, plasticity and disease, Physiol. Rev. 80 (2000) 1215-1265.
8. L. Bernheim, C.R. Bader, Human myoblast differentiation: Ca^{2+} channels are activated by K^+ channels, News Physiol. Sci. 17 (2002) 22-26.
9. M.J. Berridge, M.D. Bootman, H.L. Roderick, Calcium signalling: dynamics, homeostasis and remodelling, Nat. Rev. Mol. Cell Biol. 4 (2003) 517-529.
10. C. Berthier, A. Monteil, P. Lory, C. Strube, Alpha(1H) mRNA in single skeletal muscle fibers accounts for T-type calcium current transient expression during fetal development in mice, J. Physiol. 539 (2002) 681-691.
11. M. Beurg, M. Sukhareva, C.A. Ahern et al., Differential regulation of skeletal muscle L-type Ca2+ current and excitation-contraction coupling by the dihydropyridine receptor beta subunit, Biophys. J. 76 (1999) 1744-1756.

12. I. Bidaud, A. Monteil, J. Nargeot, P. Lory, Properties and role of voltage dependent calcium channels during mouse skeletal muscle differentiation, J. Muscle Res. Cell. Motil. 27 (2006) 75-81.
13. P. Bijlenga, J. Liu, E. Espinos, C. Haenggeli, J. Fischer-Lougheed, C.R. Bader, L. Bernheim, T-type α1H Ca^{2+} channels are involved in Ca^{2+} signalling during terminal differentiation (fusion) of human myoblasts, Proc. Natl. Acad. Sci. U S A 97 (2000) 7627-7632.
14. H.M. Blau, C. Webster, G.K. Pavlath, Defective myoblasts identified in Duchenne muscular dystrophy, Proc. Natl. Acad. Sci. USA 80 (1983) 4856-4860.
15. B.A. Block, T. Imagawa, K.P. Campbell, C. Franzini-Armstrong, Structural evidence for direct interaction between the molecular components of the transverse tubule/sarcoplasmic reticulum junction in skeletal muscle, J. Cell Biol. 107 (1988) 2587-2600.
16. S. Boncompagni, L. d'Amelio, S. Fulle, G. Fanò, F. Protasi, Progressive disorganization of the excitation-contraction coupling apparatus in aging human skeletal muscle as revealed by electron microscopy: a possible role in the decline of muscle performance, J. Gerontol. A Biol. Sci. Med. Sci. 61 (2006) 995-1008.
17. N.L. Brice, N.S. Berrow, V. Campbell et al., Importance of the different beta-subunits in the membrane expression of the alpha1A and alpha2 calcium channel subunits: studies using a depolarization-sensitive alpha1A antibody, Eur. J. Neurosci. 9 (1997) 749-759.
18. S.V. Brooks, J.A. Faulkner, Isometric, shortening, and lengthening contractions of muscle fiber segments from adults and old mice, Am. J. Physiol. 267 (1994) C507-513.
19. J.M. Caffrey, A.M. Brown, M.D. Schneider, Ca^{2+} e Na^{+} currents in developing skeletal myoblasts are expressed in a sequential program: reversible suppression by transforming growth factor beta-1, an inhibitor of the myogenic pathway, J. Neurosc. 9 (1989) 3443-3453.
20. J. Campisi, From cells to organisms: Can we learn about aging from cells in culture?, Exper. Gerontol. 36 (2001) 607-618.
21. J. Campisi, F. d'Adda di Fagagna, Cellular senescence: when bad things happen to good cells, Nat. Rev. Mol. Cell. Biol. 8 (2007) 729-740.

22. E. Carmeli, R. Coleman, A.Z. Reznick, The biochemistry of aging muscle, Exper. Gerontol. 37 (2002) 477-489.
23. R.M. Case, D. Eisner, A. Gurney, O.Jones, S. Muallem, A. Verkhratsky, Evolution of calcium homeostasis: From birth of the first cell to an amnipresent signalling system, Cell Calcium 42 (2007) 345-350.
24. W.A. Catterall, Structure and function of voltage-gated sodium and calcium channels, Curr. Opin. Neurobiol. 1 (1991) 5-13.
25. W.A. Catterall, Structure and regulation of voltage-gated Ca^{2+} channels, Annu. Rev. Cell. Dev. Biol. 16 (2000) 521-545.
26. W.A. Catterall, E. Perez Reyes, T.P. Snutch, J. Striessnig, International Union of pharmacology. XLVIII. Nomenclature and structure-function relationships of voltage-gated calcium channels, Pharmacol. Rev. 57 (2005) 411-425.
27. S. Chakraborti, S. Das, P. Kar et al., Calcium signaling phenomena in heart diseases: a perspective, Mol. Cell. Biochem. 298 (2007) 1-40.
28. W. Cheng, X. Altafaj, M. Ronjat, R. Coronado, Interaction between the dihydropyridine receptor Ca^{2+} channel β-subunit and ryanodine receptor type 1 strenghenes excitation-contraction coupling, Proc. Natl. Acad. Sci. 102 (2005) 19225-19230.
29. P.J. Coates, Markers of senescence?, J. Pathol. 196 (2002) 371-373.
30. C. Cognard, B. Constantin, M. Rivet-Bastide, N. Imbert, C. Besse, G. Raymond, Appearance ed evolution of calcium currents and contraction during the early post-fusional stages of rat skeletal muscle cells developing in primary culture, Development 117 (1993) 1153-1161.
31. I.M. Conboy, T.A. Rando, Aging, stem cells and tisuue regeneration, Cell Cycle 4 (2005) 407-410.
32. E.H. Chen, E. Grote, W. Mohler, A. Vignery, Cell-cell fusion, FEBS Lett.581 (2007) 2181-2193.
33. B. Constantin, C. Cognard, G. Raymond, Myoblast fusion requires cytosolic calcium elevation but not activation of voltage-dependent calcium channels, Cell Calcium 19 (1996) 365-374.
34. D.E. Crews, Senescence, aging and disease, J. Physiol. Antropol. 26 (2007) 365-372.

35. V.J. Cristofalo, SA β Gal staining: Biomarker or delusion?, Exper. Gerontol. 40 (2005) 836-838.
36. E. Dargelos, S. Poussard, C. Brulé, L. Daury, P. Cottin, Calcium-dependent proteolytic system and muscle dysfunctions: A possible role of calpains in sarcopenia, Biochimie (2007), *Epub ahead of print.*
37. S. Decary, V. Mouly, C. Ben Hamida, A. Sautet, J.P. Barbet, G.S. Butler-Browne, Replicative potential and telomere length in human skeletal muscle: implications for satellite cell-mediated gene therapy, Hum. Gene Ther. 8 (1997) 1429-1438.
38. S. Decary, V. Mouly, G.S. Butler-Browne, Telomere length as a tool to monitor satellite cell amplification for cell-mediated gene therapy, Hum. Gene Ther. 7 (1996) 1347-1350.
39. O. Delbono, Molecular mechanisms and therapeutics of the deficit in specific force in aging skeletal muscle, Biogerontology 3 (2002) 265-270.
40. O. Delbono, K.S. O' Rourke, W.H. Ettinger, Excitation-calcium release uncoupling in aged single human skeletal muscle fibers, J. Membr. Biol. 148 (1995) 211-222.
41. O. Delbono, M. Renganathan, M.L. Messi, Regulation of mouse skeletal muscle L-type Ca^{2+} channel by activation of the insulin-like growth factor-1 receptor, J. Neurosci. 17 (1997) 6918-6928.
42. J. Dhawan, T.A. Rando, Stem cells in postnatal myogenesis: molecular mechanisms of satellite cell quiescence, activation and replenishment, Trends Cell. Biol. 15 (2005) 666-673.
43. A. Di Iorio, M. Abate, D. Di Renzo et al., Sarcopenia: age-related skeletal muscle changes from determinants to physical disability, Int. J. Immunopathol. Pharmacol. 19 (2006) 703-719.
44. G.P. Dimri, X. Lee, G. Basile et al., A biomarker that identifies senescent human cells in culture and in aging skin in vivo, Proc. Natl. Acad. Sci. USA 92 (1995) 9363-9367.
45. T.J. Doherty, Invited review: aging and sarcopenia, J. Appl. Physiol. 95 (2003) 1717-1727.
46. A.C. Dolphin, A short history of voltage-gated calcium channels, Br. J. Pharmacol. 147 (2006) S56-S62.

47. A.F. Dulhunty, C.S. Haarmann, D. Green, D.R. Laver, P.G. Board, M.G. Casarotto, Interactions between dihydropyridine receptors and ryanodine receptors in striated muscle, Prog. Biophys. Mol. Biol. 79 (2002) 45-75.
48. E.E. Dupont-Versteegden, Apoptosis in muscle atrophy: Relevance to sarcopenia, Exper. Gerontol. 40 (2005) 473-481.
49. C. Dutta, E.C. Hadley, J. Lexell, Sarcopenia and physical performance in old age:overview, Muscle Nerve 5 (1997) S5-9.
50. E. Edstrőm, M. Altun, E. Bergman, Factors contributingto neuromuscolar impairment and sarcopenia during aging, Physiol. Behav. 92 (2007) 129-135.
51. M. Endo, Calcium ion as a second messenger with special reference to excitation-contraction coupling, J. Pharmacol. Sci. 100 (2006) 519-524.
52. A. Entwistle, R.J. Zalin, S. Bevan, A.E. Warner, The control of chick myoblasts fusion by ion channels operated by prostaglandins and acetylcholine, J. Cell. Biol. 106 (1988) 1693-1702.
53. W.J. Evans, Protein nutrition, exercise and aging, J. Am. Coll. Nutr. 23 (2004) 601S–9S.
54. P. Fatt, B Katz, The electrical properties of crustacean muscle fibres, J. Physiol. 120 (1953) 171-204.
55. R.D. Fields, P.R. Lee, J.E. Cohen, Temporal integration of intracellular Ca^{2+} signalling networks in regulating gene expression by action potentials, Cell Calcium 37 (2005) 433-442.
56. C. Franzini-Armstrong, Studies of the triad, J. Cell. Biol. 47 (1970) 488-499.
57. C. Franzini-Armstrong, The sarcoplasmatic reticulum and the control of muscle contraction, FASEB J. 13 (1999) S266-270.
58. D. Freise, B. Held, U. Wissenbach et al., Absence of the γ subunit of the skeletal muscle dihydropyridine receptor increases L-type Ca2+ currents and alters channel inactivation properties, J. Biol. Chem. 275 (2000) 14476-14481.
59. S. Fucile, Ca^{2+} permeability of nicotinic acetylcholine receptors, Cell Calcium 35 (2004) 1-8.
60. J. Garcia, K.G. Beam, Measurement of calcium transients and slow calcium current in myotubes, J. Gen. Physiol. 103 (1994) 107-123.

61. K. Goldring, T. Partridge, D. Watt, Muscle stem cells, J. Pathol. 197 (2002) 457-467.
62. M. Grabner, R.T. Dirksen, N. Suda, K.G. Beam, The II-III loop of skeletal muscle Dihydropyridine receptor is responsible for the bi-directional coupling with the Ryanodine receptor, J. Biol. Chem. 274 (1999) 21913-21919.
63. F. Grassi, S. Fucile, F. Eusebi, Ca2+ signalling pathways activated by acetylcholine in mouse C2C12 myotubes, Pflugers Arch. 428 (1994) 340-345.
64. L.J.S. Greenlund, K.S. Nair, Sarcopenia-consequences, mechanisms, and potential therapies, Mech. Aging Dev. 124 (2003) 287-299.
65. J. Gros, M. Manceau, V. Thomé, C. Marcelle, A common somitic origin for embryonic muscle progenitors and satellite cells, Nature 435 (2005) 954-958.
66. E. Gussoni, Y. Soneoka, C.D. Strickland, E.A. Buzney, M.K. Khan, A.F. Flint, L.M. Kunkel, R.C. Mulligan, Dystrophin expression in the mdx mouse restored by stem cell transplantation, Nature 401 (1999) 390-394.
67. G. Hajnoczky, G. Csordas, S. Das, C. Garcia-Peres, M Saotome S.S. Roy, M. Yi, Mitochondrial calcium signalling and cell death: Approaches for assessing the role of mitochondrial Ca^{2+} uptake in apoptosis, Cell Calcium 40 (2006) 553-560.
68. T.J. Hawke, D.J. Garry, Myogenic satellite cells: physiology to molecular biology, J. Appl. Physiol. 91 (2001) 534-551.
69. R.T. Hepple, Dividing to Keep Muscle Together: The Role of Satellite Cells in Aging Skeletal Muscle. Sci. Aging Knowl. Environ. 3 (2006) pe3.
70. R.S. Hikida, s. Walsh, N. Barylski, G. Campos, F.C. Hagerman, R.S. Staron, Is hypertrophy limited in elderly muscle fibers? A comparison of elderly and young strenght-trained men, Basic. Appl. Myol. 8 (1998) 419-427.
71. A. Ho, W. Wagner, U. Mahlknecht, Stem cells and ageing. The potential of stem cells to overcome age-related deteriorations of the body in regenerative medicine, EMBO Rep. 6 (2005) S35-S38.

72. M. Iino, T. Yamazawa, Y. Miyashita, M. Endo, H. Kasai, Critical intracellular Ca^{2+} concentration for all-or-none Ca^{2+} spiking in single smooth muscle cells, EMBO J. 12 (1993) 5287-5291.
73. A. Irintchev, M. Langer, M. Zweyer, R. Theisen, A. Wernig, Functional improvement of damaged adult mouse muscle by implantation of primary myoblasts, J. Physiol. 500 (1997) 775-785.
74. K.A. Jackson, T. Mi, M.A. Goodell, Hematopoietic potential of stem cells isolated from murine skeletal muscle, Proc. Natl. Acad. Sci. USA 96 (1999) 14482-14486.
75. K. Jurkat- Rott, F. Lehmann-Horn, Muscle channelopathies and critical points in functional and genetic studies, J. Clin. Invest. 115 (2005) 2000-2009.
76. F. Kadi, N. Charifi, C. Denis, J. Lexell, Satellite cells and myonuclei in young and eldely women and men, Muscle Nerve 29 (2004) 120-127.
77. B. Katz, R. Miledi, The effect of calcium on acetylcholine release from motor nerve terminals, Proc. R Soc. Lond. B: Biol. Sci. 161 (1965) 496-503.
78. S.J. Kaufman, R.F. Foster, Replicating myoblasts express a muscle-specific phenotype, Proc. Natl. Acad. Sci. USA 85 (1988) 9606-9610.
79. R.M. Krause, M. Hamann, C.R. Bader, J.-H. Liu, A. Baroffio, L. Bernheim, Activation of nicotinic acetylcholine receptors increases the rate of fusion of cultured human myoblasts, J. Physiol. 489 (1995) 779-790.
80. L. Larsson, B. Ramamurthy, Aging-related changes in skeletal muscle – Mechanism and interventions, Drugs and Aging 17 (2000) 303-316.
81. P. Linsdell, W.J. Moody, Electrical activity and calcium influx regulate ion channel development in embryonic Xenopus skeletal muscle, J. Neurosci. 15 (1995) 4507-4514.
82. J. Liu, S. König, M. Michel, S. Arnadudeau, J. Fischer-Lougheed, C.R. Bader, L. Bernheim, Acceleration of human myoblast fusion by depolarization: graded Ca^{2+} signals involved, Development 130 (2003) 3437-2446.
83. P. Lorenzon, E . Bandi, F. de Guarrini et al., Aging affects the differentiation potential of human myoblasts, Exper. Gerontol. 39 (2004) 1545-1554.

84. T.J. Marcell, Sarcopenia:causes, consequences, and preventions, J. Gerontol. 58 (2003) 911-916.
85. A.N. Martonosi, S. Pikula, The network of calcium regulation in muscle, Acta Biochim. Pol. 50 (2003) 1-30.
86. G.M. Martin, Keynote lecture: An update on the what, why and how questions of ageing, Exper. Gerontol. 41 (2006) 460-463.
87. A. Mauro, Satellite cell of skeletal muscle fibers, J. Biophys. Biochem. Cytol. 9 (1961) 493-495.
88. S. Machida, E.E. Spangenburg, F.W. Booth, Primary rat muscle progenitor cells have decreased proliferation and myotube formation during passages, Cell Prolif. 37 (2004) 267-277.
89. T.F. McDonald, S. Pelzer, W. Trautwein, D.J. Pelzer, Regulation and modulation of calcium channels in cardiac, skeletal and smooth muscle cells, Physiol. Rev. 74 (1994) 365-507.
90. J.E. Morgan, T.A. Partridge, Muscle satellite cells, Int. J. Biochem. Cell. Biol. 35 (2003) 1151-1156.
91. V. Mouly, A. Aamiri, S. Perie et al., Myoblast transfer therapy: is there any light at the end of the tunnel?, Acta Myol. 24 (2005) 128-133.
92. A. Musarò, N. Rosenthal, Transgenic mouse models of muscle aging, Exper. Gerontol. 34 (1999) 17-156.
93. T. Nabhani, T. Shah, J. Garcia, Skeletal muscle cells express different isoforms of the calcium channel alpha2/delta subunit. Cell. Biochem. Biophys. 42 (2005) 13-20.
94. J. Nakai, R.T. Dirksen , H.T. Nguyen , I.N. Pessah , K.G. Beam , P.D. Allen, Enhanced dihydropyridine receptor channel activity in the presence of ryanodine receptor, Nature 380 (1996) 72-75.
95. J. Nakai , N. Sekiguchi , T.A. Rando , P.D. Allen , K.G. Beam, Two regions of the ryanodine receptor involved in coupling with L-type Ca2+ channels, J. Biol. Chem. 273 (1998) 13403-13406.
96. G.J. Obermair, G. Kugler, S. Baumgartner, P. Tuluc, M. Grabner, B.E. Flucher, The Ca^{2+} channel $\alpha_2\delta$-1 subunit determines Ca^{2+} current kinetics in skeletal muscle but not targeting of α_{1S} or excitation-contraction coupling, J. Biol. Chem. 280 (2005) 2229-2237.

97. A.M. Payne, Z. Zheng, E. Gonzàlez, Z. Wang, M.L. Messi, O. Delbono, External Ca^{2+}-dependent excitation-contraction coupling in a population of ageing mouse skeletal muscle fibres, J. Physiol. 560 (2004) 137-155.
98. G.K. Pavlath, V. Horsley, Cell fusion in skeletal muscle Central rol of NFATC2 in regulating muscle cell size, Cell Cycle 2 (2003) 420-423.
99. E. Perez-Reyes, Molecular physiology of low-voltage-activated T-type calcium channels, Physiol. Rev. 83 (2003) 117-161.
100. E. Perez-Reyes, Paradoxical role of T-type calcium channels in coronary smooth muscle, Mol. Interv. 4 (2004) 16-18.
101. E. Perez-Reyes, Molecular characterization of T-type calcium channels, Cell Calcium 40 (2006) 89-96.
102. K.S. Nair, Aging muscle, Am. J. Clin. Nutr. 81 (2005) 953-963.
103. A. Pisaniello, C. Serra, D. Rossi et al., The block of ryanodine receptors selectively inhibits fetal myoblast differentiation, J. Cell Sci. 116 (2003) 1589-1597.
104. D.R. Plant, G. Lynch, Excitation-contraction coupling and sarcoplasmatic reticulum function in mechanically skinned fibres from fast skeletal muscles of aged mice, J. Physiol. 543 (2002) 169-176.
105. G.A. Porter, R.F. Makuck, S.A. Rivkees, Reduction in intracellular calcium levels inhibits myoblast differentiation, J. Biol. Chem. 277 (2002) 28942-28947.
106. E. Prochniewicz, L.V. Thompson, D.D. Thomas, Age-related decline in actomyosin structure and function, Exper. Gerontol. 42 (2007) 931-938.
107. R.J. Przybylski, V. Szigeti, S. Davidheiser, A.C. Kirby, Calcium regulation of skeletal myogenesis. II. Extracellular and cell surface effects, Cell Calcium 15 (1994) 132-142.
108. M. Puceat, M. Jaconi, Ca^{2+} signalling in cardiogenesis, Cell Calcium 38 (2005) 383-389.
109. V. Renault, G. Piron-Hamelin, C. Forestier et al., Skeletal muscle regeneration and the mitotic clock, Exper. Gerontol. 35 (2000) 711-719.
110. V. Renault, E. Rolland, L. Thornell, V. Mouly, G. Butler-Browne, Distribution of satellite cells in the human vastus lateralis muscle during aging, Exper. Gerontol. 37 (2002) 1511-1512.

111. M. Renganathan, W.E. Sonntag, O. Delbono, L-type Ca2+ channel-insulin-like growth factor-1 receptor signaling impairment in aging rat skeletal muscle, Biochem. Biophys. Res. Commun. 235 (1997) 784-789.
112. E. Rios, G. Pizarro, Voltage sensor of excitation-contraction coupling in skeletal muscle, Physiol. Rev. 71 (1991) 849-908.
113. I.H. Rosenberg, Sarcopenia: Origins and Clinical Relevance, J. Nutr. 127 (1997) 990S.
114. H. Rubin, Cell aging in vivo and in vitro, Mech. Aging Dev. 98 (1997) 1-35.
115. S.M. Roth, G.F. Martel F.M. Ivey et al., Skeletal muscle satellite cell populations in healthy young and older men and women, Anat. Rec. 260 (2000) 351-358.
116. S. Sajko, L. Kubinova, E. Cvetko, M. Kreft, A. Wernig, I. Erzen, Frequency of M-caderin-stained satellite cells declines in human muscles during aging, J. Histochem. Cytochem. 52 (2004) 179-185.
117. L.A. Schaap, S.M.F. Pluijm, D.J.H. Deeg, m. Visser, Inlammatory markers and loss of muscle mass (sarcopenia) and strenght, Am. J. Med. 119 (2006) 526.e9-17.
118. P. Seale, M.A. Rudnicki, A new look at the origin, function and 'stem-cell' status of muscle satellite cells, Dev. Biol. 218 (2000) 115-124.
119. S. Seigneurin-Venin, E. Parrish, I. Marty et al., Involvement of the dihydropyridine receptor and internal Ca2+ stores in myoblast fusion, Exp. Cell. Res. 223 (1996) 301-307.
120. M. Serrano, M.A. Blasco, Putting the stress on senescence, Curr. Opin. Cell Biol. 13 (2001) 748-753.
121. R. Shafer, U. Knauf, M. Zweyer et al., Age dependence of the human skeletal muscle stem cell in forming muscle tissue, Artif. Organs 30 (2006) 130-140.
122. A. Shainberg, G. Yagil, D. Yaffe, Control of myogenesis in vitro by Ca concentration in nutritional medium, Exp. Cell. Res. 58 (1969) 163-167.
123. G. Shefer, D.P. Van de Mark, J.B. Richardson, Z. Yablonka-Reuveni, Satellite-cell pool size does matter: Defining the myogenic potency of aging skeletal muscle, Dev. Biol. 294 (2006) 50-66.

124. R. Shirokov, G. Ferreira, J. Yi, E. Rios, Inactivation of gating currents of L-type calcium channels. Specific role of the alpha 2 delta subunit, J. Gen. Physiol. 111 (1998) 807-823.
125. A.M. Solomon, P.M.G. Bouloux, Modifying muscle mass- the endocrine perspective, J. Endocrinol. 191 (2006) 349-360.
126. C. Strube, Y. Tourneur, C. Ojeda, Functional expression of the L-type calcium channel in mice skeletal muscle during prenatal myogenesis, Biophysic. J. 78 (2000) 1282-1292.
127. K. Talavera, B. Nilius, Biophysics and structure-function relationship of T-type Ca^{2+} channels, Cell Calcium 40 (2006) 97-114.
128. M.V. Taylor, Muscle differentiation: signalling cell fusion, Curr. Biol. 13 (2003) R964-R966.
129. L.E. Thornell, M. Lindstroem, V. Renault, V. Mouly, G.S. Butler-Browne, Satellite cells and training in the elderly, Scand. J. Med. Sci. Sports 13 (2003) 48-55.
130. D. Ursu, R.P. Schuhmeier, M. Freichel, V. Flockererzi, W. Melzer, Altered inactivation of Ca^{2+} current and Ca^{2+} release in mouse muscle fibers deficient in the DHP receptor γ_1 subunit, J. Gen. Physiol. 124 (2004) 605-618.
131. A.A. Vandervoort, Aging of the human neuromuscular system, Muscle Nerve 25 (2002) 17-25.
132. Z. Wang, M.L. Messi, O. Delbono, L-type Ca^{2+} channel charge movement and intracellular Ca^{2+} in skeletal muscle fibers from aging mice, Biophys. J. 78 (2000) 1947-1954.
133. B.T. Weinert & P.S. Timiras, *Physiology of Aging* Invited Review: theories of aging, J. Appl. Physiol. 95 (2003) 1706-1716.
134. N. Weisleder, M. Brotto, S. Komazaki et al., Muscle aging is associated with compromised Ca^{2+} spark signaling and segregated intracellular Ca^{2+} release, J. Cell. Biol. 174 (2006) 639-645.
135. S. Welle, A. Brooks, C.A. Thornton, Senescence-related changes in gene expression in muscle: similarities and differences between mice and men, Physiol. Genomics. 5 (2001) 67-73.
136. A. Wernig, R. Schafer, U. Knauf et al., On the regenerative capacity of human skeletal muscle, Artif. Organs 29 (2005) 192-198.

137. A. Wernig, M. Zweyer, A. Irintchev, Function of skeletal muscle tissue formed after myoblast transplantation into irradiated mouse muscle, J. Physiol. 522 (2000) 333-345.
138. N. Yang, M. Hu, The limitations and validities of senescence associated-β-galactosidase activity as an aging marker for human foreskin fibroblast Hs68 cells, Exper. Gerontol. 40 (2005) 813-819.
139. P.S. Zammit, J.P. Golding, Y. Nagata, V. Hudon, T.A. Partridge, J.R. Beauchamp, Muscle satellite cells adopt divergent fates: a mechanism for self-renewal?, J. Cell Biol. 166 (2004) 347-357.

7. Published results

7.1 Appendix 1

- ***E. Luin, F. Ruzzier "The role of L- and T-type Ca2+ currents during the in vitro aging of murine myogenic (i28) cells in culture" Cell Calcium 41 (2007) 479-489.***

The role of L- and T-type Ca^{2+} currents during the *in vitro* aging of murine myogenic (i28) cells in culture

Elisa Luin* and Fabio Ruzzier

Department of Physiology and Pathology and Centre for Neuroscience B.R.A.I.N., University of Trieste, Via A. Fleming 22, I-34127 Trieste, Italy

* **Corresponding Author**: Department of Physiology and Pathology, University of Trieste, Via A. Fleming 22, I-34127 Trieste, Italy
Tel: +39-040-5587182; FAX + 39-040-567862; e-mail: elisaluin@dfp.units.it

Summary
The age-related decline in skeletal muscle strength could, in part, result from alterations in the mechanism of excitation-contraction coupling, responsible for muscle contraction. In the present work, we used the *in vitro* aging of murine myogenic (i28) cells as a model, to investigate whether the inefficiency of aged satellite cells to generate functional skeletal muscle fibres could be partly due to defective voltage-dependent Ca^{2+} currents. The whole-cell patch clamp technique was employed to measure L- and T-type Ca^{2+}currents in myotubes derived from the differentiation and fusion of these cells reaching replicative senescence. Our data showed that the expression and the amplitude of these currents decreased significantly during *in vitro* aging. Moreover, the analysis of the L-type current evoked in *young* and *old* cells by positive voltage steps, revealed no differences in the kinetics of activation, but significant alterations in the rate of inactivation. These effects of *in vitro* aging on voltage-dependent Ca^{2+} currents could also be related to their inability to fuse into myotubes. Taken together, our data support the hypothesis that age-related effects on voltage-dependent L-type and T-type currents could be one of the causes of the failure of satellite cells to efficiently counteract the impairment in muscle force.

1. Introduction

During the aging process, mammalian skeletal muscle undergoes significant changes that have been investigated by several groups in recent years (for review see [1-5]). Indeed, the mechanism underlying impaired motor performance in old age involves the central and peripheral nervous system and the muscle tissue itself. However, it is not still clear how nerve and muscles reciprocally influence gene expression, cellular mechanisms and age-related neurodegeneration [3]. In skeletal muscle, the age-related decline in force is a complex phenomenon linked to sarcopenia, an involuntary loss of muscle mass and strength [6]. One of the main causes of sarcopenia is the reduction of the pool of muscle satellite cells, the most specific myogenic cells available postnatally for skeletal muscle growth and repair (reviewed in [7-9]). Exhaustion of their proliferative ability in aged muscle, could thus be a consequence of the continuous demand on their activity for muscle tissue regeneration [10].

The deficit in specific contractile force (*i.e.* force normalised to muscle cross-sectional area) could not however, be explained by muscle atrophy [11]. Thus, other possible concomitant causes have been suggested, like changes of the sarcolemmal excitability [12,13], and alterations of the mechanisms controlling Ca^{2+} handling [14,15], also altered in the aging process of other tissues (see for example [16]). In skeletal muscle, it is particularly important to consider alterations in the mechanism of excitation-contraction coupling (EC coupling), responsible for contraction [14,15]. The structural substratum for normal EC coupling is the mechanical interaction between the dihydropyridine-sensitive voltage-dependent L-type Ca^{2+} channels (dihydropyridine receptors: DHPRs), organized in tetrads at the sarcolemma T- tubules, and the ryanodine-sensitive Ca^{2+} channels (ryanodine receptors: RyR1s) located in the sarcoplasmic reticulum membranes ([17]; reviewed in [18]). Recently, it was shown that both mouse and human aged skeletal muscle fibres exhibit alterations in DHPR and RyR1 expression, which could lead to so-called EC uncoupling [14,15,19,20]. Moreover, in the elderly, muscle fibers derived from the proliferation and differentiation of *in vivo* aged satellite cells could also be characterized by EC uncoupling; thus, sarcopenia could be due, at least in part, to a reduced efficiency of aged satellite cells to generate functional skeletal muscle fibres [21].
The deficit in contractile force could also be a consequence of changes in sarcolemmal excitability. It has already been observed that a reduction in skeletal muscle Cl^- conductance occurs in aged rats [12], and a modification of K^+ channel activity is seen in old rats and humans [13,22,23]. Interestingly, an increase in Na^+ current density has been reported in old rats [24], but not in old mice [25]. Changes in muscle Na^+ channel expression or behaviour would be of great importance in the age-related impairment in muscle force, since voltage-gated Na^+ channels are responsible for the generation and propagation of the action potential in skeletal muscle fibres. The above alterations in sarcolemmal excitability could also involve changes in the properties of voltage-gated Ca^{2+} channels [26] that play an essential physiological role, not only in the function of normal adult skeletal muscle, but also in the process of myogenesis [27]. The DHPR, besides acting as a voltage-sensor to trigger the contractile machinery for EC coupling, produces a slow high voltage- activated (HVA) Ca^{2+} current identified as L-type (I_L). On the

other hand, during myogenesis, also a low voltage-activated (LVA) Ca^{2+} current was identified as a transiently expressed T-type current (I_T), which most likely mediates the influx of Ca^{2+} strictly required for fusion between myoblasts or between myoblasts and myotubes [28,30]. Since it was shown [10] that senescent satellite cells fused more slowly and less efficiently, a possible role could also be suggested for a defective T-type channel.

A useful model of *in vivo* aging of satellite cells is the aging of the same cells *in vitro* under culture conditions [31]; this model would allow us to investigate if the replicative senescence affects their regenerating ability. The main goals of the present study were therefore *(1)* to reproduce the physiological muscle aging process that occurs *in vivo*, by maintaining mouse myogenic cells in culture until the stage of replicative senescence, determined by examining the effect of *in vitro* aging on their ability to differentiate and fuse into myotubes, and *(2)* to analyse the properties of L-and T-type Ca^{2+} currents in myogenic cells during *in vitro* aging, focusing in particular on the activation and inactivation kinetics of the L-type current, in order to study their possible involvement in age-associated alteration in Ca^{2+}homeostasis. To this end, the whole-cell patch clamp recording technique was employed to measure Ca^{2+} currents in myotubes derived from the differentiation and fusion of satellite cells reaching proliferative senescence.

2. Materials and methods

2.1 Cell culture

All the experiments were performed on myotubes derived from the *in vitro* differentiation and fusion of expanded primary mouse myoblasts (called i28), kindly supplied to us by Dr A. Wernig, Department of Physiology and Medical Policlinic, University of Bonn, Germany (see [32]). Myogenic cells could be maintained as exponentially-growing myoblasts in the presence of HAM'S F-10 growth medium (GM) plus 20% fetal calf serum (FCS), L-glutamine (2 mM), penicillin (100 units/ml), and streptomycin (100 µg/ml). The myoblasts were plated at a density of about 35000 cells in 90 mm Petri dishes. To induce cell differentiation and fusion, mononucleated myoblasts were plated at a density of 70000 cells in 35 mm matrigel -coated Petri dishes (matrigel kindly given to us by Drs A. Albini and D. Noonan, CBA, Genova) and 1 day after plating, the growth medium was replaced with a differentiation medium (DM) consisting of DMEM supplemented with 2% horse serum and L-glutamine, penicillin and streptomycin as above. The differentiation medium was renewed every three days to avoid loss of nutrients and growth factors. Cultures were maintained at 37°C in a humid air atmosphere containing 5% CO_2.

2.2 Cell senescence

The proliferative capacity of myoblasts was evalueted by counting the number of cells in culture at seeding and at harvesting. At each cell passage, the mean population doubling was calculated using the formula:
$MPD=[\log (N_h/N_s)]/\log 2$
where N_h is the harvest cell number and N_s the seeded cell number per Petri dish. The number of total divisions reached by the cell culture was derived from the sum of MPD calculated at each passage. The state of 'replicative senescence' (about 90 divisions) was determined by examining the effect of *in vitro* aging on the morphology of the plated myoblasts and the failure of such cells to differentiate, align and start to merge into multinucleated myotubes within 4 days in differentiation medium, renewed every two days of culture.

2.3 Differentiation index

At different population doublings, the efficiency of differentiation of i28 cultures was quantified by counting the percentage of myotubes and the mean number of nuclei per myotube. Nuclei were revealed under fluorescence microscopy by DAPI (4,6-diamino-2-phenylindole) staining; the cells plated on matrigel-coated coverslips were first fixed at room temperature in freshly prepared 3.7% paraformaldehyde in PBS for 15 min, permeabilized by a 5 min incubation in 100% methanol and then stained for 10 min with DAPI (10 µM in PBS). The fluorescence images of the cells rinsed in normal external solution (NES) were compared to the corresponding bright-field images in order to identify the multinucleated myotubes. In particular, 10 randomly chosen optical fields per coverslip were analysed. Fluorescence and bright-field images were collected by a CCD camera (SensiCam; PCO Computer Optics, Kelheim, Germany) connected to an inverted

microscope (Zeiss Axiovert 100) and the analog output was digitized and integrated in real time by an image processor; image acquisition was made using specific software (Imaging Workbench 2.2.1.55; Axon Instruments, Foster City, CA).

2.4 Electrophysiological recordings

Myotubes with a compact shape, a smooth cell membrane appearance, without branches and not too large were selected for the experiments. Calcium currents were recorded at room temperature (20-24 ℃) by means of the whole-cell configuration of the patch-clamp technique using an Axopatch 200B amplifier (Axon Instruments). Patch pipettes were fabricated from borosilicate glass and fire-polished to a final tip resistance of 5-7 MΩ when filled with internal solution (see below). Data acquisition and command voltage pulse generation were performed with a Digidata 1320 interface controlled by pCLAMP 8 software (Axon Instruments). Currents were filtered at 1 kHz and sampled at 5 kHz. The analog circuitry of the amplifier was used to reduce the capacitive transients as much as possible and to compensate the series resistance close to the point of amplifier oscillation. For subtraction of remaining linear leak and capacity, a standard P/4 protocol (leak holding potential –90 mV) was used in all measurements. Cell membrane capacitance (C_m) was determined by integration of the capacity transient elicited in response to a 10 mV hyperpolarizing pulse from a holding potential of –60 mV and was also used to calculate the calcium current density of each cell. The time constant for charging membrane capacity of each cell was calculated by fitting the capacity transient by a single exponential function.
The average effective membrane capacitance (C_m) for all experiments was 108.4 ± 6.6 pF (n=109), the average series resistance (R_s) after compensation was 8.89 ± 0.30 MΩ (n=109) and the average time constant for charging the membrane capacity (calculated from $\tau=C_m*R_s$) was 1.89 ± 0.11 ms (n=109); the average voltage error (V_e) due to uncompensated series resistance (from $V_e=R_s*I_{Ca,max}$) was 5.10 ± 0.37 mV for L-type currents (n=100) and 1.62 ± 0.24 mV for T-type currents (n=27). Calcium currents were activated from a holding potential of –60 mV, after a 750 ms hyperpolarizing stimulus (-90 mV) to remove inactivation. 500 ms test pulses were applied in 10 mV increments, ranging from –70 to +40 mV; in this way, it was possible to activate both L- and T-type Ca^{2+} currents. L-type currents were isolated by using a 750 ms depolarizing (-30 mV) conditioning prepulse, that inactivated the T-type currents; in a few cases, only T-type currents were elicited, by blocking L-type currents with the specific L-channel blocker verapamil (20 μM) applied by a gravity-driven perfusion system. To determine current-voltage (I-V) relationships, the peak L-type Ca^{2+} current was measured as a function of test potential. Data were transformed to a conductance-voltage [G-V] curve using the following equation:

$$G(V) = I(V)/(V-E_{rev}),$$

where E_{rev} is the reversal potential for the L-type Ca^{2+} current estimated by linear extrapolation of the I-V curve. For comparison of the activation kinetics of the L-type Ca^{2+} current in groups of cells of different age, the [G-V] curves of each group were normalised to the maximum conductance value (Gmax), averaged and then fitted with the Boltzmann function

$$G(V)/Gmax = 1/(1+\exp[-(V-V_{1/2})/k])$$

where $V_{1/2}$ is the voltage at which the conductance is half maximal and k describes the steepness of activation. To measure L-type current inactivation, cells were held at –60 mV, then stepped using a series of 1500 ms depolarizing voltages from –70 to +40 mV in 10 mV increments (prepulses) to promote inactivation, then stepped to –60 mV for 100 ms to close non-inactivated channels, then stepped for 500 ms to the test potential of +10 mV and finally turned back to –60 mV to permit recovery from inactivation. To determine voltage-dependent inactivation, the peak L-type Ca^{2+} current was normalised to the maximal current (I_{max}, generally observed with the prepulse at –70 mV) and measured as a function of prepulse potential. To compare differently aged cell groups, the inactivation curves within each group were averaged and then fitted with the Boltzmann equation

$I(V)/Imax = 1/(1+\exp[(V-V_{1/2})/k])$

with $V_{1/2}$ being the voltage of half-inactivation and k a measure for the steepness.

2.5 Recording solutions and chemicals:

To record Ca^{2+} currents alone, in the absence of Na^+ and K^+ currents, the bath solution contained (in mM): 135 TEA-Cl, 2.5 $CaCl_2$, 0.8 $MgCl_2$, 5.6 glucose and 10 Hepes (pH adjusted to7.4 with TEA-OH). The pipette solution contained (in mM): 130 CsCl, 0.005 $CaCl_2$, 1 $MgCl_2$, 5.6 glucose, 10 Hepes, 1 EGTA and 2 ATP (pH adjusted to 7.2 with TEA-OH). Fetal calf serum was purchased from Mascia Brunelli (Milano, Italy) and horse serum from ICN Biomedicals (Costa Mesa, CA, USA). All the other chemicals, unless otherwise stated, were from Sigma (St Louis, MO, USA).

2.6 Data acquisition and statistical analysis

For data acquisition and analysis, the pCLAMP software package (v. 8.0, Axon Instruments) and Origin 5 (Microcal Software, Northampton, MA) softwares were used. All data, when possible, are presented as mean ± SEM. Differences between data group means were evaluated by Student's t-test and a *P* value <0.05 was considered statistically significant.

3. Results

3.1 Differentiation and fusion in myotubes of i28 cells during in vitro aging

Myogenic i28 cells were maintained as exponentially growing myoblasts in a growth medium (GM) until the state of 'replicative senescence' (about 90 cell divisions). The differentiation and fusion capacity of two different classes of cells, *young* and *old*, with less than 30 and more than 50 divisions respectively, were taken into consideration (figure 1A). Myotubes at three and six days in differentiation medium (DM) were analysed for each group. By revealing the nuclei by DAPI (see Materials and methods and figure 1B), we found that both

young and *old* myoblasts during their time in DM increased in dimension and in differentiation, judged by the increase in the nuclei per myotube ratio (figure 1D). Nevertheless, during the *in vitro* aging, the differentiation and fusion appeared defective. Both at three and six days in DM, we observed a drastic loss of multinucleated cells (figure 1C) and in the number of nuclei (figure 1D). Moreover, the myotubes originating from *old* satellite cells, approaching the stage of cellular senescence, appeared smaller and thinner, in comparison to *younger* cells at the same day in DM. Small myotubes originating from *old* satellite cells rarely had branches, contrary to what was observed in myotubes derived from *young* cells. However, we did not perform any methodical quantification of the branching, since the myotubes with branches were difficult to space- and voltage- clamp and so were rejected for patch-clamp experiments.

3.2 The expression and density of L- and T-type currents during in vitro aging

L-type and T-type currents were evoked in myotubes using an activation protocol with 500 ms test pulses in 10 mV increments ranging from -70 to +40 mV (see Materials and methods) (figure 2A). In general, L-type Ca^{2+} currents were detected in almost 100% of myotubes, but the occurrence decreased to 75% (n=29) in three-day differentiated myotubes originating from the fusion of *old* cells (more than 50 divisions). However, it seemed that there was an age-related delay in maturation; in fact, if we took into consideration the six-day differentiated myotubes derived from *old* cells, I_L was again present in almost all cells (figure 2A, right panel). On the other hand, at 3 and 6 days in DM, T-type Ca^{2+} currents were expressed only in 11 and 56 % respectively of myotubes originated from *young* cells, and the presence clearly decreased to 7 and 9 % in myotubes derived from *old* cells (figure 2A, right panel). Moreover, none of the cells tested displayed only I_T, which is probably never expressed before I_L.

In all the cells, the densities of L-type and T-type Ca^{2+} currents were calculated taking into account the maximum peak current value (I_{max}), generally observed at 0 or +10 mV for L-type and at –30 mV for T-type current (figure 2A, left panel), normalised to the effective cell capacitance. As shown in figure 2B, the L-type current density significantly decreased during the *in vitro* aging of i28 cells. Moreover, a decreasing trend of T-type current density was also evident, even if the reduction was not statistically significant. Here and later, three- and six-day differentiated cells were grouped together because of no significant differences in L-type and T-type current density and kinetics (see below) taking into consideration different days in the differentiation medium.

3.3 L-type current kinetics during in vitro aging

To further investigate the properties of the slow L-type Ca^{2+} current (isolated from T-type as described in Materials and methods; compare figure 3A and 3B) in myotubes derived from i28 cells at different stages of replicative senescence, we studied the activation and inactivation kinetics. The I-V relationship, determined by measuring the peak L-type Ca^{2+} current as a function of test potential (see figure 3B) was examined, and no significant differences were found when comparing the

normalized and averaged I-V curves from cells of different age (figure 3C). Also, the best fitting parameters for $V_{1/2}$ and k, determined from the mean data points of the activation and inactivation curves (see Materials and methods) showed no significant differences (taking also into account the voltage error due to series resistance) comparing myotubes derived from *young* cells and those derived from *old* ones (see figure 3D and Table 1).

Interestingly, alterations in the kinetics of inactivation of L-type Ca^{2+} currents could be observed in aged satellite cells.

To measure I_L inactivation, the current was evoked with two depolarizing voltage steps from the holding potential (-60 mV) in double-pulse experiments; the first pulse (*prepulse*) ranged from -70 to +40 mV and the second (*test pulse*), given after a 100 ms interpulse interval, was held at +10 mV (see Materials and methods and figure 4A). The greater resistance to inactivation of *old* cells was evident by comparing the *young* and *old* voltage-dependent inactivation curves (figure 4B). In fact, when comparing myotubes derived from *young* and *old* cells, at least two different inactivation behaviours were observed for L-type current, as illustrated in figure 5. The first one was peculiar for myotubes derived from *young* cells, which usually displayed a rapid phase of inactivation followed by a slower phase; the second one was typically observed in myotubes derived from *old* cells, which showed a very slow decay of the current. In both cases, the time course of inactivation, during the 1500 ms depolarization to 0 mV, could usually be well fitted by a single exponential component (figure 5A); statistical analysis of the data (figure 5B) indicated a significantly different mean for the time constant of inactivation (ζ_i) found in myotubes derived from the fusion of *young* cells ($\zeta_{i,mean}$= 0.89±0.13 s, n=7) and *old* cells ($\zeta_{i,mean}$= 2.47±0.30 s, n=13). In some cases however, a double exponential time course was observed in myotubes derived from *young* cells (n=4, data not shown).

Moreover, recordings from double-pulse experiments, at the prepulse potential (usually 0 or +10 mV) which lead to maximal *prepulse* peak current and maximal *test pulse* current inactivation, were pooled and analysed to obtain other two indexes of inactivation: 1) the rate of the Ca^{2+} current inactivation (r_{1500}, or residual current at 1500 ms), expressed as the percent current reduction at the end of the *prepulse* (I_{1500}) compared to the peak *prepulse* current (I_{peak})

r_{1500} [%]=(I_{1500}/ I_{peak})*100

and 2) the degree of maximal voltage-dependent inactivation (called r_{inact}), determined as the ratio of the *test* current (at 0 or 10 mV) and the highest current measured during the set of test pulses (I_{max})

r_{inact}[%]=($I_{(0\text{-}10mV)}$/ I_{max})*100.

In accordance with the results obtained for ζ_i, data analysis, this further analysis indicated that r_{1500} increased during aging in a significant way. On the other hand, r_{inact} was also significantly higher in *old* cells (see figure 6). The correlation between these two indexes of inactivation was highly significant (ρ=0.89; P<0.001).

4. Discussion

Sarcopenia is the most evident phenomenon of skeletal muscle aging, and now it appears of great importance to understand the basic cellular mechanisms underlying muscle function impairment in the elderly. Our first goal was to study the natural muscle aging process that occurs *in vivo*, by trying to reproduce it in a simpler model of muscle aging *in vitro*. To that end, we chose to work with muscle satellite cells, which are the best known myogenic cells available postnatally, that are able to differentiate and fuse into myotubes under the right conditions, and are one of the most creditable key factors in the process of muscle aging. By maintaining murine i28 satellite cells in culture for several passages, it was possible to observe the gradual changes in morphology and shape of myotubes derived from myoblasts approaching the so-called 'replicative senescence'. We showed that at later passages, i28 cells were not able to fuse as efficiently as in earlier passages; in fact, both the multinucleated cells present in culture and the number of nuclei per myotube decreased significantly. The accumulation of cell generations *in vitro* inevitably entails, among other things, DNA damage, telomere dysfunction, a different pattern of gene expression, various types of stresses (particularly oxidative stress), and epigenetic changes [33-35], that could lead to the altered phenotype displayed. The negative changes that occur during *in vitro* senescence have been seen to characterise also *in vivo* aged mammalian skeletal muscle ([2,6]; for review see [1,4,5]). Even if the relationship between cell aging *in vivo* and *in vitro* is still matter of debate (reviewed in [36]), there are several pieces of evidence showing that senescent cells may persist and accumulate with age *in vivo* and that replicative senescence contributes to aging [37,38]. In the skeletal muscle context, satellite cells are of particular importance, because the regenerative potential of these muscles is determined at least in part by the proliferative potential of their myogenic satellite cells [39] and the muscle mass, endurance and force, seem to be related to satellite cell differentiation [40]. Indeed, sarcopenia could be related to the already shown age-related decrement of the proliferative capacity of these cells [10,41-44].

Our present results in the i28 murine model have confirmed what has been shown for human satellite cells isolated from donors of different ages and aged *in vitro* [10,21]: there was an age-related decrease in the quality of myoblast fusion, since the myotubes derived from *old* cells in culture were smaller and thinner, and an age-related decrease in the quantity of the fusion was also evident from the reduction of the number of myotubes formed in culture and in the number of their nuclei. Recently, it was hypothesized that voltage-gated T-type Ca^{2+} channels were involved in some muscle developmental processes and were specifically required for myoblast fusion [28-30,45]. The expression of the α1H subunit of the T-type channel in skeletal muscle has been found only during myogenesis in embryonic and newborn muscle and disappears at three weeks of age ([45]; also reviewed in [46]) and it was shown that the inhibition of T-type current by the T-channel blockers amiloride or Ni^{+} suppressed human myoblast fusion [28,29]. Since *young* i28 satellite cells could proliferate well as myoblasts, and differentiate and fuse in myotubes when activated, and this ability was lacking when aged *in vitro*, we hypothesized that senescent satellite cells could exhibit a defective T-type Ca^{2+} channel. We tested this hypothesis by monitoring T-type current expression in myotubes derived from the fusion of i28 satellite cells at different stages of replicative senescence, and we found that the occurrence of myotubes in which this current was detected evidently decreased during *in vitro* aging by so

much, that only four out of 52 myotubes derived from *old* cells tested showed T-type currents. As illustrated in Results, the T-type current density also showed an age-related decreasing trend, even if the reduction was not statistically significant (probably because of the small number of data collected, due to the moderate expression of T-type currents at every stage of the culture). Indeed, fusion-competent myoblasts were found to show an increase of intracellular Ca^{2+} concentration, necessary for fusion between myoblasts or between myoblasts and myotubes [47], but the source of this Ca^{2+} and its mode of mobilization are still the object of discussion [28,30,48,49]. In preliminary experiments, we have seen that in our murine model, the inhibition of T-type current by Ni^{+} (50 μM) suppressed i28 myoblast fusion (data not shown), supporting the idea that *young* cells fuse better because they have higher T-type current density. Since the fusion was not sensitive to the specific L-type current blocker verapamil (20 μM; data not shown), we suggest that this type of current is not the principal source of Ca^{2+} required for fusion [see also 50].

Together with the age-related loss of muscle mass, attributed to the decreasing number and size of muscle fibres and to the inability of satellite cells to proliferate well, differentiate and fuse, the other peculiar aspect of aged skeletal muscle is the decline of muscle contractile force (for a review see [51]). In fact, it seems that the age-related impairment in force could be explained only partially by the loss in mass [11], so other age-associated deficits in the mechanisms underlying the decline in muscle force have been investigated, with particular interest in possible alterations of sarcolemmal excitability and in the mechanisms controlling Ca^{2+} handling. We focussed our attention on one of the key molecules involved in Ca^{2+} homeostasis and skeletal muscle contractility: the dihydropyridine receptor (DHPR), which carries the L-type Ca^{2+}current. In this study, we demonstrated for the first time, that the density of L-type currents in myotubes derived from the differentiation and fusion of *in vitro* aged satellite cells were significantly reduced, compared with those derived from *young* satellite cells; moreover, in myotubes derived from *old* cells, the L-type channels seemed to be expressed later during the differentiation time. Our results, obtained in this model of *in vitro* aging, are in accordance with other recent results obtained in mouse and human physiologically aged skeletal muscle fibres (*in vivo* aging). Indeed, from 1995, Delbono and colleagues have been showing the contribution of alterations in excitation- Ca^{2+} release coupling to age-related mammalian muscle decline. In particular, a significant reduction of maximum L-type Ca^{2+} channel charge movement (Qmax), of L-type current density, and of peak intracellular Ca^{2+} evoked by sarcolemmal depolarization were found in muscle fibres of old human subjects and of old rodents [14,15,19,20,26]. Moreover, a slower depolarization-induced force response for EDL muscle skinned fibres from old compared with young mice was shown, indicating some level of DHPR-RyR uncoupling [52]. Recently it was also shown that the *in vitro* aging of satellite cells isolated from a human *young* donor slowed down the establishment of the EC coupling mechanism and the appearance of functional RyR and DHPR channels, similar to what has been shown for cells isolated from an old donor, thus suggesting a functional parallelism between *in vitro* and *in vivo* aging [21].

A putative mechanism for explaining the observed lower density of I_L currents in myotubes derived from *old* cells could be the possible age-related lack of the

interaction between DHPR and RyR1 (reviewed in [3]); in fact, it has been suggested that, besides the orthograde signal whereby DHPR signals RYR1 to open (EC coupling mechanism), there is a retrograde signal, by which RYR1 enhances its function [53-56]. Moreover, experiments on mice homozygous for a disrupted RyR1 gene (termed "dyspedic mice") proved that RyR1 promotes the activity of skeletal L-channels, influencing their expression level, kinetics and conductance [57]. We wanted to further investigate other possible dysfunctions of the L-type Ca^{2+} channel which could occur during *in vitro* aging, by analysing the activation and inactivation kinetics of the L-type current. Firstly, we showed that aging *in vitro* did not affect the I-V relationship and the best fitting parameters for $V_{1/2}$ (voltage of half-activation or half-inactivation) and k (steepness factor), determined from mean data points of the activation and inactivation curves. Interestingly, an *ex vivo* study on fibres of young and old mice also showed no age-related shift in the voltage-dependence of L-type Ca^{2+}current [20], which is consistent with our data obtained during *in vitro* aging.

A deeper analysis of the inactivation kinetics, pointed out some differences between L-type currents (I_L) expressed in myotubes derived from *young* cells and in myotubes derived from *old* cells. Firstly, the two different L-channel (DHPR) inactivation behaviours, observed by comparing the L-type currents in myotubes derived from *young* and *old* cells, were well reflected by the significantly different value of the analysed time constant of inactivation (ζ_i). Interestingly, two different behaviours for the L-type channel displayed by its kinetics of inactivation have already been found in rat myoballs [58] and in rabbit T-tube microsomes fused in planar lipid bilayers [59], and it has already been hypothesized [58] that the two different inactivation behaviours (shown by means of 81±25 ms and 1.32±0.39 s for the fast and the slow time constant respectively) could reflect either the presence of two different subtypes of DHPR or two different modes of expression of the same subunit. Indeed, age-related changes in expression patterns of L-type channel subunits or regulatory proteins could be an important factor leading to a different inactivation behaviour (see below). In our model, it was further proved that myotubes derived from *young* cells were more susceptible to inactivation, since both the rate of Ca^{2+} current inactivation, (expressed as percent relative current reduction at the end of the prepulse of the protocol of inactivation (r_{1500})), and the fraction of test I_L that resisted inactivation by a prepulse (I/I_{max}), were smaller than in myotubes derived from *old* cells. We can presume that the mechanism of inactivation of this current is mainly voltage-dependent, and that a change of this mechanism is possibly age-related. In fact, it was already shown in a variety of skeletal muscle preparations that in skeletal muscle cells, Ca^{2+} channels inactivate in a voltage-dependent manner through a mechanism that does not require Ca^{2+} entry from the extracellular compartment (see for example [58-60]), and in particular, it was recently demonstrated that there is no extracellular Ca^{2+} dependence of I_L inactivation in fibres of both young or old murine skeletal muscle [20].

We cannot presently exclude an inactivation mechanism dependent on intracellular Ca^{2+}, released from the sarcoplasmatic reticulum into the cytoplasm upon depolarization by the EC coupling mechanism. Even if in frog muscle fibres this inactivation mechanism was ruled out [60], a motif in the carboxyl-terminus that permits the binding of Ca^{2+} (and thus Ca^{2+}-dependent inactivation), is to a

certain degree conserved in all L-type Ca^{2+} channel α1-subunits (reviewed in [61]; see also [62]); in particular, the amino acids 1393-1527 of the same terminus of the skeletal muscle α1-subunit binds Ca^{2+} and Ca^{2+}-binding proteins, like calmodulin [55]. If this Ca^{2+} release hypothesis proves at least in part to be correct, the lower susceptibility to inactivation of I_L currents in myotubes derived from *old* cells could be explained by the lower availability of intracellular Ca^{2+}, due to the age-related EC uncoupling mode (for a review see [51]). On the other hand, the age-related lower susceptibility to inactivation of I_L currents could be seen as a sort of compensatory mechanism to hinder the reduction of L-type current density and the lower availability of intracellular Ca^{2+}, indispensable for skeletal muscle contraction. In fact, our results suggest that in myotubes derived from *old* cells the L-type current is not only less sensitive to inactivation, but also less expressed and has a smaller amplitude when compared with myotubes derived from *young* cells. These differences could arise from age-related alterations of the channel principal subunit (α1) function, due to senescence-associated changes in genes transcription and protein expression or modified post-translational processing [1,32,63], and also from alterations in the expression and functionality of the accessory subunits. In particular it was recently shown that specific isoforms of α2-δ subunit [64,65] and of γ subunit [66,67] are particularly important in the modulation of the inactivation kinetics and that the β subunit is very important for the sarcolemmal expression of the α subunit [68] and for regulation of the EC coupling mechanism [69].

In conclusion, our data support the idea that important age-related alterations in Ca^{2+} channel properties occurred in muscle satellite cells *in vitro*, leading to the hypothesis that aging effects on voltage-dependent L- and T-type currents could be one of the causes of the inability of such cells to efficiently counteract age-related impairment in muscle force. However, a clear cause-and-effect relationship at a molecular level has yet to be established, and other molecular and electrophysiological studies are needed to explain the complex process of skeletal muscle aging *in vitro* and *in vivo*.

Aknowledgments

We wish to thank Dr. Anton Wernig (University of Bonn) for the generous supply of i28 cells, Drs Daniela Pietrobon (University of Padova) and Fabio Francini (University of Firenze) for their helpful suggestions and Dr Andy Constanti (School of Pharmacy, University of London) for valuable comments and final revision. This work was supported by grants from the University of Trieste, MIUR-Italy (PRIN and FIRB projects) and Regione Friuli-Venezia Giulia to F.R.

References

[1] L. Larsson, B. Ramamurthy, Aging-related changes in skeletal muscle – Mechanism and interventions, Drugs Aging. 17 (2000) 303-316.
[2] A.E. Barani, A. Curieux, O. Sabido, D. Freyssenet, Age-related changes in the mitotic and metabolic characteristics of muscle-derived cells, J. Appl. Physiol. 95 (2003) 2089-2098.
[3] O. Delbono, Neural control of aging skeletal muscle, Aging Cell 2 (2003) 21-29.
[4] T.J. Doherty, Invited review: aging and sarcopenia, J. Appl. Physiol. 95 (2003) 1717-1727.
[5] L.J.S. Greenlund, K.S. Nair, Sarcopenia-consequences, mechanisms, and potential therapies, Mech. Aging Dev. 124 (2003) 287-299.
[6] L. Larsson, T. Ansved, Effects of ageing on the motor unit, Prog. Neurobiol. 45 (1995) 397-458.
[7] P. Seale, M.A. Rudnicki, A new look at the origin, function and 'stem-cell' status of muscle satellite cells, Dev. Biol. 218 (2000) 115-124.
[8] T.J. Hawke, D.J. Garry, Myogenic satellite cells: physiology to molecular biology, J. Appl. Physiol. 91 (2001) 534-551.
[9] E. Negroni, G.S. Butler-Browne, V. Mouly, Myogenic stem cells: regeneration and cell therapy in human skeletal muscle, Pathol. Biol. 54 (2006) 100-108.
[10] V. Renault, G. Piron-Hamelin, C. Forestier et al., Skeletal muscle regeneration and the mitotic clock, Exp. Gerontol. 35 (2000) 711-719.
[11] S.V. Brooks, J.A. Faulkner, Isometric, shortening, and lengthening contractions of muscle fiber segments from adults and old mice, Am. J. Physiol. 267 (1994) C507-513.
[12] A. De Luca, D. Tricarico, S. Pierno, D. Conte Camerino, Aging and chloride channel regulation in rat fast-twitch muscle fibres, Pflugers Arch. 427 (1994) 80-85.
[13] D. Tricarico, R. Petruzzi, D. Conte Camerino, Changes of the biophysical properties of calcium-activated potassium channels of rat skeletal muscle fibres during aging, Pflugers Arch. 434 (1997) 822-829.
[14] O. Delbono, K.S. O' Rourke, W.H. Ettinger, Excitation-calcium release uncoupling in aged single human skeletal muscle fibers, J. Membr. Biol. 148 (1995) 211-222.
[15] Z. Wang, M.L. Messi, O. Delbono, L-type Ca^{2+} channel charge movement and intracellular Ca^{2+} in skeletal muscle fibers from aging mice, Biophys. J. 78 (2000) 1947-1954.
[16] E.C. Toescu, A. Verkhratsky, P.W. Landfield, Ca2+ regulation and gene expression in normal brain aging, Trends Neurosci. 27 (2004) 614-620.
[17] B.A. Block, T. Imagawa, K.P. Campbell, C. Franzini-Armstrong, Structural evidence for direct interaction between the molecular components of the transverse tubule/sarcoplasmic reticulum junction in skeletal muscle, J. Cell Biol. 107 (1988) 2587-2600.
[18] E. Rios, G. Pizarro, Voltage sensor of excitation-contraction coupling in skeletal muscle, Physiol. Rev. 71 (1991) 849-908.
[19] O. Delbono, M. Renganathan, M.L. Messi, Regulation of mouse skeletal muscle L-type Ca^{2+} channel by activation of the insulin-like growth factor-1 receptor, J. Neurosci. 17 (1997) 6918-6928.

[20] A.M. Payne, Z. Zheng, E. Gonzàlez, Z. Wang, M.L. Messi, O. Delbono, External Ca^{2+}-dependent excitation-contraction coupling in a population of ageing mouse skeletal muscle fibres, J. Physiol. 560.1 (2004) 137-155.

[21] P. Lorenzon, E . Bandi, F. de Guarrini et al., Aging affects the differentiation potential of human myoblasts, Exp. Gerontol. 39 (2004) 1545-1554.
[22] D. Tricarico, D. Conte Camerino, ATP-sensitive K+ channels of skeletal muscle fibers from young adult and aged rats: possible involvement of thiol-dependent redox mechanisms in the age-related modifications of their biophysical and pharmacological properties, Mol. Pharmacol. 46 (1994) 754-761.
[23] E. Nurowska, B. Dworakowska, M. Kloch, M. Sobol, K. Dolowky, A. Wernig, F. Ruzzier, Potassium currents in human myogenic cells from donors of different ages. Exp. Gerontol. 41 (2006) 635-640.
[24] J. Desaphy, A. De Luca, P. Imbrici, D. Conte Camerino, Modification by ageing of the tetrodotoxin-sensitive sodium channels in rat skeletal muscle fibres, Biochim. Biophys. Acta 1373 (1998) 37-46.

[25] Z.M. Wang , Z. Zheng , M.L. Messi, O. Delbono, Extension and magnitude of denervation in skeletal muscle from ageing mice, J. Physiol**.** 565 (2005) 757-64.

[26] M. Renganathan, W.E. Sonntag, O. Delbono, L-type Ca2+ channel-insulin-like growth factor-1 receptor signaling impairment in aging rat skeletal muscle, Biochem. Biophys. Res. Commun. 235 (1997) 784-789.

[27] C. Cognard, B. Constantin, M. Rivet-Bastide, N. Imbert, C. Besse, G. Raymond, Appearance ed evolution of calcium currents and contraction during the early post-fusional stages of rat skeletal muscle cells developing in primary culture, Development 117 (1993) 1153-1161.
[28] P. Bijlenga, J. Liu, E. Espinos, C. Haenggeli, J. Fischer-Lougheed, C.R. Bader, L. Bernheim, T-type α1H Ca^{2+} channels are involved in Ca^{2+} signalling during terminal differentiation (fusion) of human myoblasts, Proc. Natl. Acad. Sci. U S A 97 (2000) 7627-7632.
[29] L. Bernheim, C.R. Bader, Human myoblast differentiation: Ca^{2+} channels are activated by K^+ channels, News Physiol. Sci. 17 (2002) 22-26.
[30] J. Liu, S. König, M. Michel, S. Arnadudeau, J. Fischer-Lougheed, C.R. Bader, L. Bernheim, Acceleration of human myoblast fusion by depolarization: graded Ca^{2+} signals involvedk, Development 130 (2003) 3437-2446.
[31] S. Decary, V. Mouly, G.S. Butler-Browne, Telomere length as a tool to monitor satellite cell amplification for cell-mediated gene therapy, Hum. Gene Ther. 7 (1996) 1347-1350.
[32] A. Irintchev, M. Langer, M. Zweyer, R. Theisen, A. Wernig, Functional improvement of damaged adult mouse muscle by implantation of primary myoblasts, J. Physiol. 500.3 (1997) 775-785.
[33] M. Serrano, M.A. Blasco, Putting the stress on senescence, Curr. Opin. Cell Biol. 13 (2001) 748-753.
[34] S. Bortoli , V. Renault , E. Eveno , C. Auffray , G. Butler-Browne , G. Pietu, Gene expression profiling of human satellite cells during muscular aging using cDNA arrays, Gene 321 (2003) 145-54.
[35] S. Bortoli, V. Renault, R. Mariage-Samson et al., Modifications in the myogenic program induced by in vivo and in vitro aging, Gene 347 (2005) 65-72.
[36] H. Rubin, Cell aging in vivo and in vitro, Mech. Aging Dev. 98 (1997) 1-35.

[37] G.P. Dimri, X. Lee, G. Basile et al., A biomarker that identifies senescent human cells in culture and in aging skin in vivo, Proc. Natl. Acad. Sci. USA 92 (1995) 9363-9367.
[38] J. Campisi, From cells to organisms: Can we learn about aging from cells in culture?, Exp. Gerontol. 36 (2001) 607-618.
[39] S. Decary, V. Mouly, C. Ben Hamida, A. Sautet, J.P. Barbet, G.S. Butler-Browne, Replicative potential and telomere length in human skeletal muscle: implications for satellite cell-mediated gene therapy, Hum. Gene Ther. 8 (1997) 1429-1438.
[40] S.B.P. Charge, A.S. Brack, S.M. Hughes, Aging-related satellite cell differentiation defect occurs prematurely following Ski-induced muscle hypertrophy, Am. J. Physiol . Cell Physiol. 283 (2002) C1228-C1241.
[41] S. Machida, E.E. Spangenburg, F.W. Booth, Primary rat muscle progenitor cells have decreased proliferation and myotube formation during passages, Cell Prolif. 37 (2004) 267-277.
[42] A. Wernig, R. Schafer, U. Knauf et al., On the regenerative capacity of human skeletal muscle, Artif Organs 29 (2005) 192-198.
[43] L.E. Thornell, M. Lindstroem, V. Renault, V. Mouly, G.S. Butler-Browne, Satellite cells and training in the elderly, Scand. J. Med. Sci Sports. 13 (2003) 48-55.
[44] S. Sajko, L. Kubinova, E. Cvetko, M. Kreft, A. Wernig, I. Erzen, Frequency of M-caderin-stained satellite cells declines in human muscles during aging, J. Histochem. Cytochem. 52 (2004) 179-185.
[45] C. Berthier, A. Monteil, P. Lory, C. Strube, Alpha(1H) mRNA in single skeletal muscle fibers accounts for T-type calcium current transient expression during fetal development in mice, J. Physiol. 539 (2002) 681-691.
[46] E. Perez-Reyes, Molecular physiology of low-voltage-activated T-type calcium channels, Physiol. Rev. 83 (2003) 117-161.
[47] R.J. Przybylski , V. Szigeti , S. Davidheiser , A.C. Kirby, Calcium regulation of skeletal myogenesis. II. Extracellular and cell surface effects, Cell Calcium 15 (1994) 132-142.
[48] S. Seigneurin-Venin, E. Parrish, I. Marty et al., Involvement of the dihydropyridine receptor and internal Ca2+ stores in myoblast fusion, Exp. Cell. Res. 223 (1996) 301-307.
[49] A. Pisaniello, C. Serra, D. Rossi et al., The block of ryanodine receptors selectively inhibits fetal myoblast differentiation, J. Cell Sci. 116.8 (2003) 1589-1597.
[50] B. Constantin, C. Cognard, G. Raymond, Myoblast fusion requires cytosolic calcium elevation but not activation of voltage-dependent calcium channels, Cell Calcium 19 (1996) 365-374.
[51] O. Delbono, Molecular mechanisms and therapeutics of the deficit in specific force in aging skeletal muscle, Biogerontology 3 (2002) 265-270.
[52] D.R. Plant, G. Lynch, Excitation-contraction coupling and sarcoplasmatic reticulum function in mechanically skinned fibres from fast skeletal muscles of aged mice, J. Physiol. 543.1 (2002) 169-176.
[53] J. Nakai, R.T. Dirksen , H.T. Nguyen , I.N. Pessah , K.G. Beam , P.D. Allen, Enhanced dihydropyridine receptor channel activity in the presence of ryanodine receptor, Nature 380 (1996) 72-75.

[54] J. Nakai , N. Sekiguchi , T.A. Rando , P.D. Allen , K.G. Beam, Two regions of the ryanodine receptor involved in coupling with L-type Ca2+ channels, J. Biol. Chem. 273 (1998) 13403-13406.
[55] S. Sencer, R.V.L. Papineni, D.B. Halling, P. Pate, J. Krol, J-Z. Zhang, S.L. Hamilton, Coupling of RYR1 and L-type calcium channels via calmodulin binding domains, J. Biol. Chem. 276 (2001) 38237-38241.
[56] R. Squecco, C. Bencini, C. Piperio, F. Francini, L-type channel and ryanodine receptor cross-talk in frog skeletal muscle, J. Physiol. 555 (2003) 137-152.
[57] G. Avila, R.T. Dirksen, Functional impact of the ryanodine receptor on the skeletal muscle L-type Ca(2+) channel, J. Gen. Physiol. 115 (2000) 467-80.
[58] C. Cognard, M. Lazdunski, G. Romey, Different types of Ca2+ channels in mammalian skeletal muscle cells in culture, Proc. Natl. Acad. Sci. U S A 83 (1986) 517-521.
[59] R. Mejia-Alvarez, M. Fill, E. Stefani, Voltage-dependent inactivation of T-tubular skeletal calcium channels in planar lipid bilayers, J. Gen. Physiol. 97 (1991) 393-412.
[60] G. Cota, E. Stefani, Voltage-dependent inactivation of slow calcium channels in intact twitch muscle fibers of the frog, J. Gen. Physiol. 94 (1989)937-951.
[61] S. Hering, S. Berjukow, S. Sokolov et al., Molecular determinants of inactivation in voltage-gated Ca^{2+} channels, J. Physiol. 528 (2000) 237-249.
[62] M. Morad, N. Soldatov, Calcium channel inactivation: Possible role in signal transduction and Ca^{2+} signalling, Cell Calcium (2005) 223-231.
[63] S. Welle, A. Brooks, C.A. Thornton, Senescence-related changes in gene expression in muscle: similarities and differences between mice and men, Physiol. Genomics. 5 (2001) 67-73.
[64] R. Shirokov, G. Ferreira, J. Yi, E. Rios, Inactivation of gating currents of L-type calcium channels. Specific role of the alpha 2 delta subunit, J. Gen. Physiol. 111 (1998) 807-823.
[65] T. Nabhani, T. Shah, J. Garcia, Skeletal muscle cells express different isoforms of the calcium channel alpha2/delta subunit. Cell. Biochem. Biophys. 42 (2005) 13-20.
[66] D. Freise, B. Held, U. Wissenbach et al., Absence of the γ subunit of the skeletal muscle dihydropyridine receptor increases L-type Ca2+ currents and alters channel inactivation properties, J. Biol. Chem. 275 (2000) 14476-14481.
[67] C.A. Ahern, P. Powers, G.H. Biddlecome et al., Modulation of L-type Ca^{2+} release by the gamma1 subunit of the dihydropyridine receptor of skeletal muscle, BMC Physiol. 1 (2001) 8.
[68] N.L. Brice, N.S. Berrow, V. Campbell et al., Importance of the different beta-subunits in the membrane expression of the alpha1A and alpha2 calcium channel subunits: studies using a depolarization-sensitive alpha1A antibody, Eur. J. Neurosci. 9 (1997) 749-759.
[69] M. Beurg, M. Sukhareva, C.A. Ahern et al., Differential regulation of skeletal muscle L-type Ca2+ current and excitation-contraction coupling by the dihydropyridine receptor beta subunit, Biophys. J. 76 (1999) 1744-1756.

Table 1: Kinetic parameters of L-type Ca^{2+} current activation and inactivation in murine myogenic i28 cells during *in vitro* aging in culture (n°= number of cell divisions; n=number of cells; data are presented as mean ± SEM, note no significant changes due to aging).

	Activation			Inactivation		
n° of cell divisions	$V_{1/2}$ (mV)	k	n	$V_{1/2}$ (mV)	k	n
n°<30	-11.17±0.45	4.88±0.41	27	-19.50±0.75	7.79±0.67	21
30<n°<50	-8.54±0.35	5.87±0.31	29	-15.18±0.53	7.82±0.47	19
n°>50	-8.15±0.27	6.59±0.23	44	-16.04±0.48	7.35±0.42	29

Figure legends

Figure 1. The number of myotubes and the number of nuclei per myotube at different stages of *in vitro* aging in murine myogenic (i28) cells in culture. A) shows representative photomicrographs of patched myotubes, at 3 and 6 days in differentiating medium (DM), originating from the fusion of competent *young* (< 30 divisions) and *old* (> 50 divisions) myoblasts, and B) shows representative fluorescence and bright-field images of the same optical field (*old* cells, 3 days in DM) after DAPI staining (scale bar, 35 µm). The histogram in C) shows the drastic aging-related loss of multinucleated cells, and in D) the aging-related decrease of the number of nuclei per myotube, both comparing cells at the same day in DM (3 and 6 days) (n=number of optical fields, *= statistically extremely significant, $P<0.001$).

Figure 2. T- and L-type Ca^{2+} currents measured in myotubes during *in vitro* aging of i28 cells; A) current expression and B) current density. (A), left panel: representative maximum I_T and I_L currents recorded using the stimulation protocol indicated in the inset; right panel: percentage of cells exhibiting T-type and L-type currents at different days in differentiation medium (DM). In B) the decreasing densities of I_L and I_T with aging are shown; 3- and 6-day differentiated cells were grouped because of no significant differences (n=number of optical fields, *=statistically extremely significant, $P<0.001$).

Figure 3. Activation of L-type Ca^{2+} currents. (A) shows representative L- and T-type Ca^{2+} currents evoked in myotubes by the standard voltage protocol in the inset, and in B) the L-type current was isolated by applying a 750-ms prepulse to -30 mV. C) shows the averaged normalised L-type current-voltage (I-V) relationship and D) the activation curves in myotubes derived from i28 cells at different stages of replicative senescence (■= < 30 divisions; ○= 30< divisions <50; Δ= >50 divisions). Each point is the mean ± SEM and the best fitting parameters (see Material and methods) and the number of tested cells are summarised in Table 1. Note little or no change in the shape of the I-V or activation curves due to aging.

Figure 4. The voltage-dependent inactivation curves. A) Sample I_L traces from a double-pulse experiment covering the range of command potentials shown in the protocol above. B) The averaged relative voltage-dependent inactivation curves (data points are means ± SEM) in myotubes derived from *young* (■) and *old* (Δ) satellite cells (data means are significantly different, paired t-test with $P< 0.05$). Note upward shift of curve with aging.

Figure 5. The time course of inactivation of L-type Ca^{2+} currents**.** A) Sample I_L traces from double-pulse experiments from myotubes derived from *young* (upper trace) and *old* (lower trace) satellite cells displaying a different time course and voltage-dependent inactivation at a prepulse potential of 0 mV; superimposed are the exponential fits to the time course of inactivation, and the time constants of inactivation (ζ_i) of the sample currents are indicated. B) The mean ζ_i found in myotubes during aging (*=difference statistically extremely significant, t-test, $P<0.001$).

Figure 6. A) The averaged prepulse residual current at 1500 ms (r_{1500}) and B) the averaged voltage-dependent inactivation parameter (r_{inact}) during the *in vitro* aging (*=difference statistically significant, t-test, $P<0.05$).

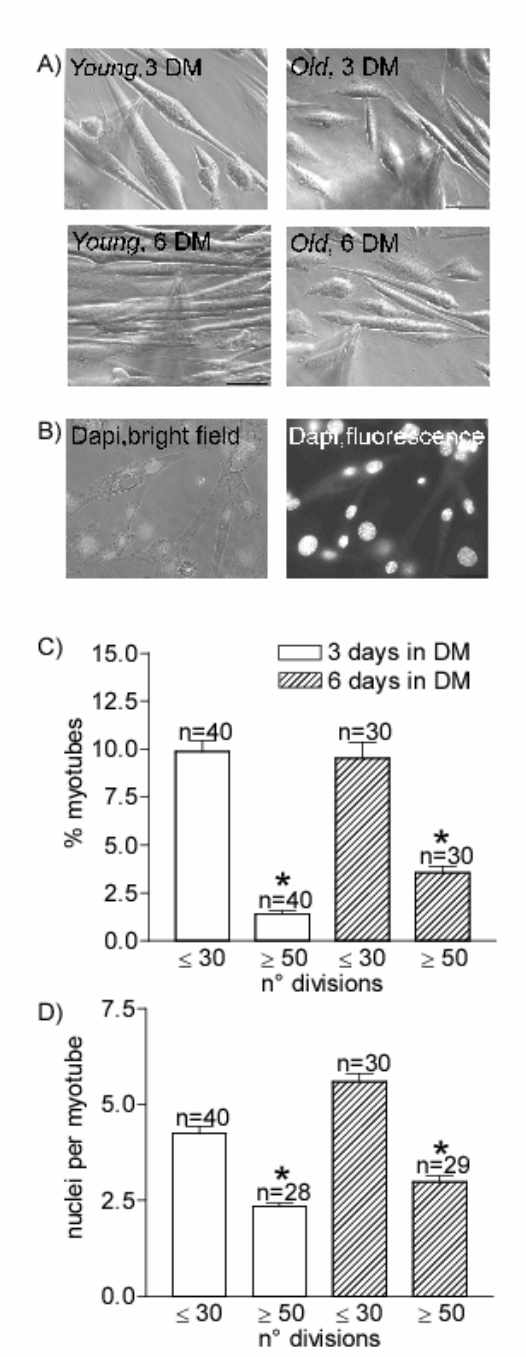
A)
Young, 3 DM
Old, 3 DM
Young, 6 DM
Old, 6 DM
B)
Dapi, bright field
Dapi, fluorescence
C)
3 days in DM
6 days in DM
% myotubes
15.0
12.5
10.0
7.5
5.0
2.5
0.0
n=40
n=40
n=30
n=30
*
*
≤ 30
≥ 50
≤ 30
≥ 50
n° divisions
D)
nuclei per myotube
7.5
5.0
2.5
0.0
n=40
n=28
n=30
n=29
*
*
≤ 30
≥ 50
≤ 30
≥ 50
n° divisions

Fig. 1

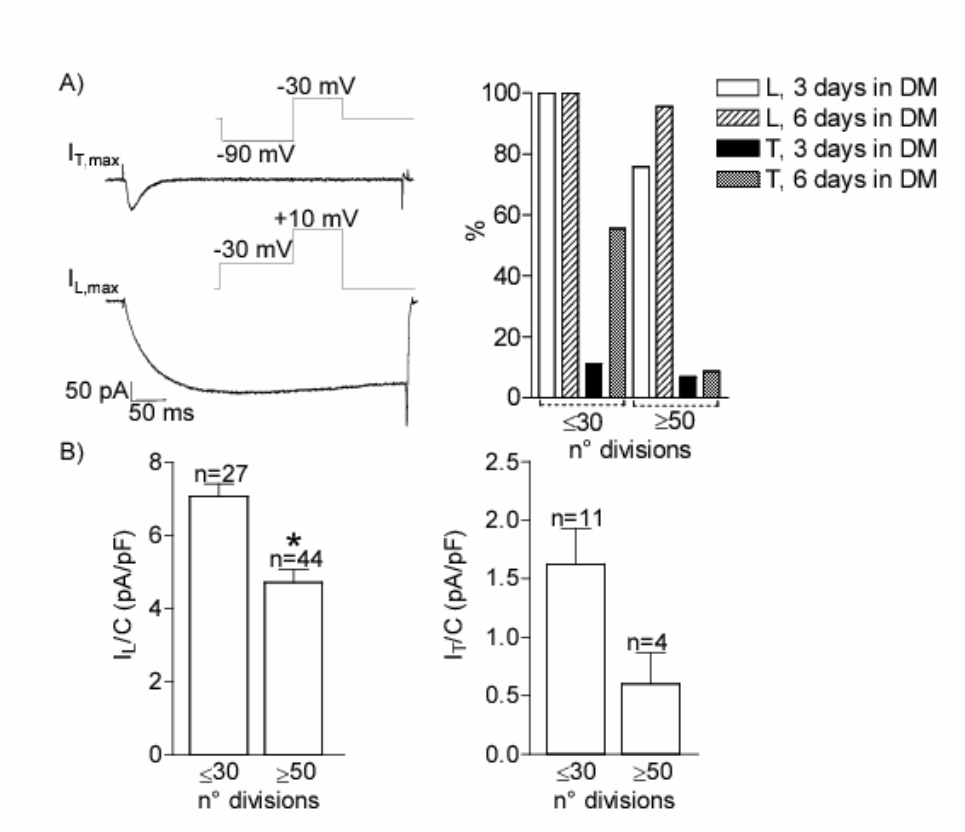
A)
-30 mV
-90 mV
$I_{T,max}$
+10 mV
-30 mV
$I_{L,max}$
50 pA
50 ms
L, 3 days in DM
L, 6 days in DM
T, 3 days in DM
T, 6 days in DM
%
≤30
≥50
n° divisions
B)
I_L/C (pA/pF)
n=27
n=44
*
≤30
≥50
n° divisions
I_T/C (pA/pF)
n=11
n=4
≤30
≥50
n° divisions

Fig. 2

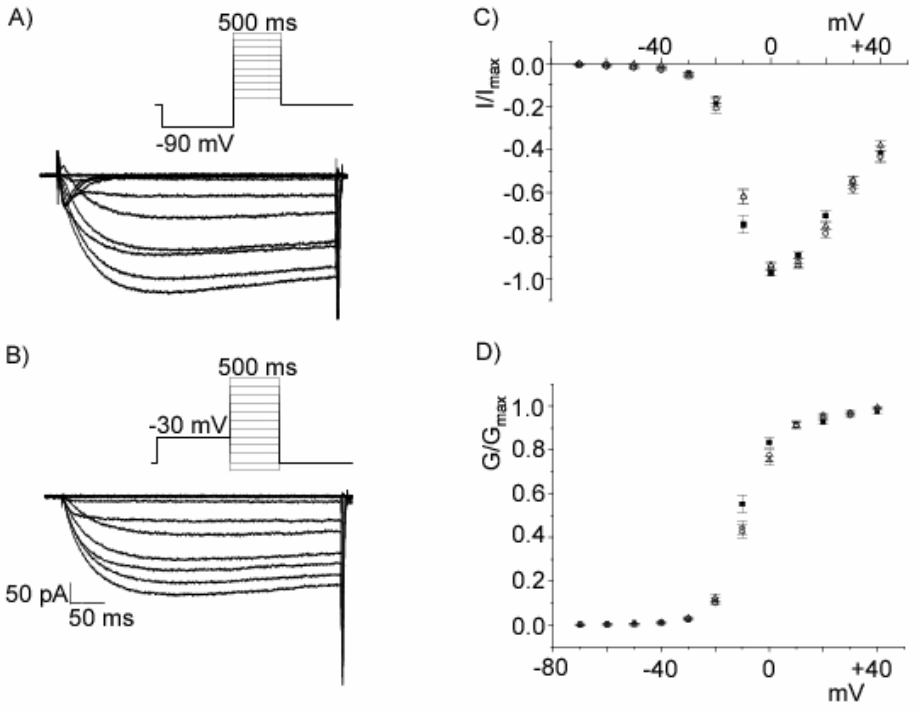
A)
500 ms
-90 mV
B)
500 ms
-30 mV
50 pA
50 ms
C)
mV
-40
0
+40
I/I_max
0.0
-0.2
-0.4
-0.6
-0.8
-1.0
D)
G/G_max
1.0
0.8
0.6
0.4
0.2
0.0
-80
-40
0
+40
mV

Fig. 3

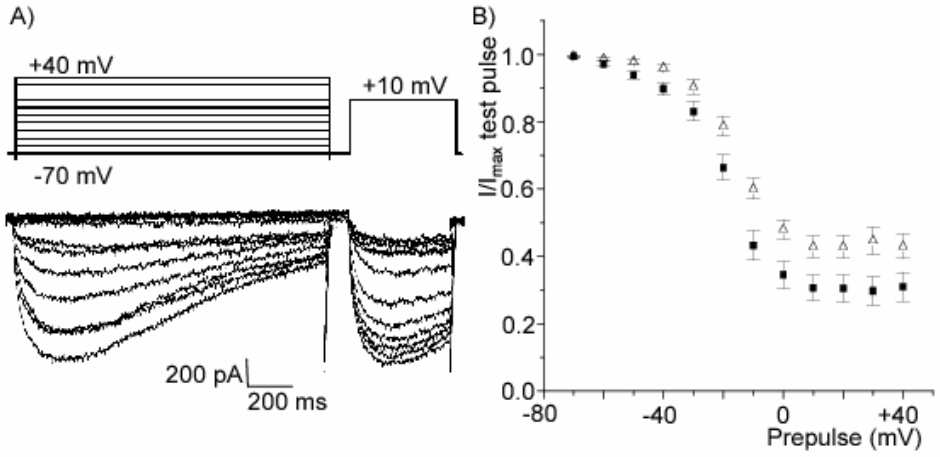
A)
+40 mV
+10 mV
-70 mV
200 pA
200 ms
B)
I/I_max test pulse
1.0
0.8
0.6
0.4
0.2
0.0
-80
-40
0
+40
Prepulse (mV)

Fig. 4

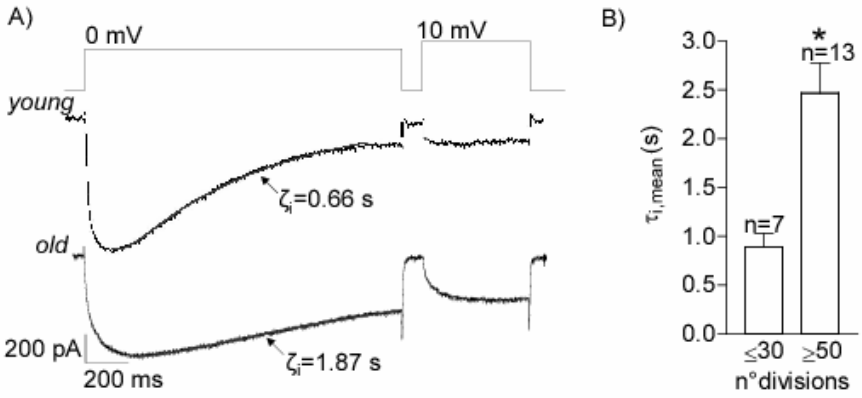
A)
0 mV
10 mV
young
old
ζ_i=0.66 s
ζ_i=1.87 s
200 pA
200 ms
B)
3.0
2.5
2.0
1.5
1.0
0.5
0.0
$\tau_{i,mean}$ (s)
*
n=13
n=7
≤30
≥50
n°divisions

Fig. 5

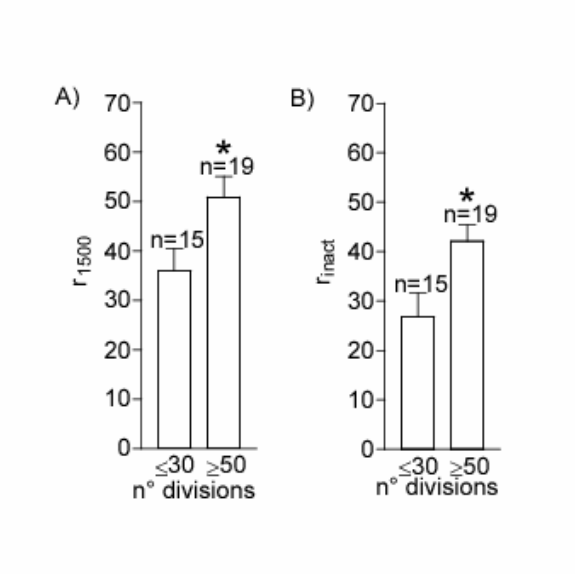
A)
70
60
50
40
30
20
10
0
r_{1500}
n=15
*
n=19
≤30
≥50
n° divisions
B)
70
60
50
40
30
20
10
0
r_{inact}
n=15
*
n=19
≤30
≥50
n° divisions

Fig. 6

7.2 Appendix 2

- ***E. Luin, P. Lorenzon, A. Wernig, F. Ruzzier "Calcium currents kinetics in young and aged human cultured myotube" Cell Calcium (2008), accepted with minor revisions.***

Calcium current kinetics in young and aged human cultured myotubes

Elisa Luin[1,*], Paola Lorenzon[1], Anton Wernig[2], Fabio Ruzzier[1]

[1]Department of Physiology and Pathology, University of Trieste, Via A. Fleming 22, I-34127 Trieste, Italy

[2]Department of Physiology, University of Bonn, Wilhelmstrasse 31, D-53111 Bonn, Germany

***Corresponding Author**: Tel: +39-040-5587182; FAX: + 39-040-567862; e-mail: elisaluin@dfp.units.it

Summary

There is evidence that the complex process of sarcopenia in human aged skeletal muscle is linked to the modification of mechanisms controlling Ca^{2+} homeostasis. To further clarify this issue, we assessed the changes in the kinetics of activation and inactivation of T- and L-type Ca^{2+} currents in *in vitro* differentiated human myotubes, derived from satellite cells of healthy donors aged 2, 12, 76 and 86 years. The results showed an age-related decrease in the occurrence of T- and L-type currents. Moreover, significant age-dependent alterations were found in L- (but not T) type current density, and activation and inactivation kinetics, although an interesting alteration in the kinetics of T-current inactivation was observed. The T-type and L-type Ca^{2+} currents play a crucial role in regulating Ca^{2+} entry during satellite cells differentiation and fusion into myotubes. Also, the L-type Ca^{2+} channels underlie the skeletal muscle excitation-contraction coupling mechanism. Thus, our results support the hypothesis that the aging process could negatively affect the Ca^{2+} homeostasis of these cells, by altering Ca^{2+} entry through T- and L-type Ca^{2+} channels, thereby putting a strain on the ability of human satellite cells to regenerate skeletal muscle in elderly people.

Keywords

Human satellite cells

Skeletal muscle aging

Ca^{2+} homeostasis

T- type Ca^{2+} channels

L-type Ca^{2+} channels

1. Introduction

The mechanisms involved in sarcopenia (the involuntary decline in muscle mass with aging, coupled with loss of force and function [1]), include both skeletal muscle intrinsic and extrinsic factors, and have been actively investigated in animal and human models over the last few years (for review see [2-5]). Indeed, age-related deterioration of muscle mass and strength has multifactorial causes, with no identifiable single mechanism or molecular event. In humans, some work has focussed on various extrinsic or environmental factors: lack of regular physical activity, alterations in various hormones and cytokine availability [6,7], and loss of neuromuscular function [8-10]. On the other hand, other studies have focussed attention on human muscle intrinsic factors: an aging signature in human muscle transcriptional profile [11-13], a change in protein structure and metabolism [14,15], and an altered redox modulation of muscle contraction and physiology ([16,17], reviewed also in [18]), partially also due to a decline in mitochondrial function ([19], but see [20]).

An important age-associated deficit (recently investigated by various researchers), that could be a cause or a consequence of some mechanisms underlying the decline in human skeletal muscle force, is the possible alteration of sarcolemmal excitability [21] and of the mechanisms controlling Ca^{2+} handling [22-25]. In particular, it is very important to consider an age-related impairment in the events that link the sarcolemmal depolarization and the action potential generated at a neuromuscular junction, to the release of Ca^{2+} from the sarcoplasmic reticulum (the so-called excitation-contraction (E-C) uncoupling [22]), events normally based on the mechanical interaction between the sarcolemmal voltage-dependent L-type Ca^{2+} channels and the ryanodine receptors located in the sarcoplasmic reticulum membranes [27].

Moreover, it has already been proposed that defective fibres in old humans could result from a reduced efficiency of aged satellite cells in properly differentiating into mature skeletal muscle cells, with a functional Ca^{2+} handling apparatus [23,24]. Satellite cells are a distinct muscle cell subtype, responsible for post-natal growth [28], and repair of damaged fibres throughout the entire lifespan (for recent reviews see [29,30]). Over the last 15 years, an idea is developing that age-related sarcopenia is associated with an impaired satellite cell regenerative response (reviewed in [5] and [31]). Despite some divergent opinions [32,33], one of the emerging hypotheses is that increasing human age is accompanied by a reduction in the satellite cell population [34-36], probably due to the age-related decline of satellite cell replicative capacity [37-40]. However, the muscle mass, endurance and force, might be related not only to satellite cell proliferation and availability, but also to their correct and complete differentiation. Our previous results [41], recently obtained using the model of *in vitro* aging of murine satellite cells, confirmed that there is an age-related decrease in the quality of fusion (see also [23,34]), and, more interestingly, an impaired handling of Ca^{2+} homeostasis in old satellite cells. In particular, the L-type and T-type Ca^{2+} current expression and kinetics were affected in myotubes derived from old cells. Taking into account that the L- and T-type Ca^{2+} currents are required to regulate Ca^{2+} entry during the satellite cell differentiation and fusion in myotubes [42,43], and that the L-type Ca^{2+} channels also underlie the skeletal muscle E-C coupling mechanism [27], we supposed that aging effects on these currents could be one of the causes of the inability of old satellite cells to efficiently counteract age-related impairment in muscle force.

During the physiological process of aging *in vivo*, both the intrinsic accumulation of cell generations (replicative senescence), and the muscle environmental age-related changes, might contribute to aging, which could lead to an altered satellite cell phenotype [44-46]. Considering that previous results in our laboratory showed that human satellite cells aged either *in vitro* or *in vivo* are unable to differentiate and fuse in culture in functional myotubes with a mature E-C coupling mechanism [23], the present study was conceived to explore the possibility to extend the results obtained with the *in vitro* aging of murine satellite cells model [41] to the physiological process of human aging *in vivo*, *i.e*. to investigate if satellite cells obtained from old donors could present the same important age-related alterations in voltage-dependent L-type and T-type Ca^{2+} channel properties that we found to occur in murine muscle satellite cells aged *in vitro*. For this purpose, the whole-cell patch clamp and the videoimaging techniques were employed to measure Ca^{2+} currents and transients respectively in myotubes derived from satellite cells obtained from human skeletal muscle tissue of different aged donors.

2. Materials and methods

2.1 Human muscle samples and satellite cell culture

All the human myogenic satellite cells used in the experiments were shipped seeded in growth medium in a culture flask or frozen in cryogenic vials on dry ice. The protocol to obtain the desmin positive-enriched culture of satellite cells, from human skeletal muscle tissue (used according to the Protocol of the Ethics Commission of the Medical Faculty of the University of Bonn and the Declaration of Helsinki), is described in [40].

More precisely, cells were obtained from tissue surgery remnants of otherwise healthy male donors, aged 2, 12, 76 and 86 years. They were then maintained as growing myoblasts at 37°C in a humid air atmosphere containing 5% CO_2, in HAM'S F-10 growth medium (GM) plus 20% fetal calf serum (FCS), L-glutamine (1 mM), penicillin (100 units/ml), and streptomycin (100 µg/ml). Whenever necessary, the mononucleated cells were sub-cultured and plated on matrigel-coated coverlips at a density of ~100,000 cells in 35 mm Petri dishes; to induce cell differentiation and fusion into multinucleated myotubes, 3 days after plating the growth medium was replaced with a differentiation medium consisting of DMEM supplemented with 10 µg/ml of insulin, 100 µg/ml of apotransferrin, penicillin (100 units/ml), and streptomycin (100 µg/ml). Both the growth medium and the differentiation medium were renewed every two days to avoid loss of nutrients and growth factors.

All the experiments were performed on multinucleated myotubes after 3-6 days of differentiation. Such myotubes were obtained from the differentiation and fusion of different age donors myogenic cells, all at the very beginning of the proliferative phase of the various cultures, between 3-20 (younger donors) and 6-10 (older donors) *MPDs* (mean population doublings, for details see [23-40-41]), well before the end of the replicative lifespan (proliferative senescence).

2.2 Electrophysiological recordings

T-type and L-type voltage-dependent Ca^{2+} currents were recorded at room temperature (20-24°C) by means of the whole-cell configuration of the patch-clamp technique using an Axopatch 200B amplifier (Axon Instruments, Foster City, CA). Patch pipettes were fabricated from borosilicate glass and fire-polished to a final tip resistance of 3-5 MΩ when filled with internal solution (see below).

All the 3 to 6 days human differentiated myotubes selected for the experiments had a compact shape, a smooth cell membrane appearance, non-branching geometry and small size, to avoid problems of space- and voltage- clamp. Moreover, the analog circuitry of the amplifier was used to reduce the capacitive transients as much as possible and to compensate the series resistance close to the point of amplifier oscillation. For subtraction of remaining linear leak and capacity, a standard P/4 protocol (leak holding potential –90 mV) was used in all recordings. Data acquisition and command voltage pulse generation were performed with a Digidata 1320 interface controlled by pCLAMP 8 software (Axon Instruments). Currents were filtered at 1 kHz and sampled at 5 kHz.

Cell membrane capacitance (C) was determined by integration of the capacity transient elicited in response to a 10 mV hyperpolarizing pulse from a holding potential of –60 mV and was also used to calculate the Ca^{2+} current density of each cell. The time constant for charging membrane capacity of each cell was calculated by fitting the capacity transient by a single exponential function.

To calculate the average passive membrane properties of the selected myotubes, we grouped together data from donors of different age, because they showed no significant differences. The average effective membrane capacitance (C) for all experiments was 212.2 ± 16.3 pF (*n*=82), the average series resistance (R_s) after compensation was 4.03 ± 0.22 MΩ (*n*=82) and the average time constant for charging the membrane capacity (calculated from $\tau=C^*R_s$) was 2.58 ± 0.18 ms (*n*=82); the average voltage error (V_e) due to uncompensated series resistance (from $V_e=R_s^*I_{Ca,max}$) was 1.06 ± 0.11 mV for L-type currents (*n*=55) and 0.77 ± 0.11 mV for T-type currents (*n*=56).

Both T- and L-type Ca^{2+} currents were activated from a holding potential of –60 mV, after a 750 ms hyperpolarizing stimulus (-90 mV) to remove inactivation. 500 ms test pulses were applied in 10 mV increments, ranging from –70 to +40 mV. L-type currents were isolated by using a 750 ms depolarizing (-30 mV) conditioning prepulse, that inactivated the T-type currents. T-type currents were then obtained by the subtraction of the recordings obtained with the prepulse from those obtained without it; in a few cases, only T-type currents were elicited, by blocking L-type currents with the specific L-channel blocker verapamil (20 μM) applied by a gravity-driven perfusion system. To determine current density-voltage (I/C-V) relationships, the peak T-type current, or the peak L-type Ca^{2+} current, normalised to C, was measured as a function of test potential.

Data were also transformed to a conductance-voltage [G-V] curve using the following equation:

$G(V) = I(V)/(V-E_{rev})$,

where E_{rev} is the reversal potential for the T-type, or for L-type Ca^{2+} current respectively, estimated by linear extrapolation of the I-V curve.

To compare the activation kinetics of the two types of Ca^{2+} current in myotubes derived from the differentiation and fusion of satellite cells from donors of different

age, the [G-V] curves of each group were normalised to the maximum conductance value (G_{max}), averaged and then fitted with the Boltzmann function

$G(V)/G_{max} = 1/(1+\exp[-(V-V_{1/2})/k])$

where $V_{1/2}$ is the voltage at which the conductance is half maximal and k describes the steepness of activation.

To promote and measure L-type current inactivation, cells were held at –60 mV, then *i*) stepped using a series of 1500 ms depolarizing voltages from –70 to +40 mV in 10 mV increments (prepulses) to promote inactivation, *ii*) stepped to –60 mV for 100 ms to close non-inactivated channels, *iii*) stepped for 500 ms to the test potential of +20 mV and finally *iv*) turned back to –60 mV to permit recovery from inactivation. The 1500 ms prepulse was the longest possible in this type of cells, in order to avoid membrane damage and consequent problems of voltage-clamp, that we experienced in longer recordings.

On the other hand, to promote and measure T-type current inactivation, we used a series of 300 ms conditioning voltages from -80 to -10 in 5 mV increments (prepulses), and a fixed test pulse of 500 ms to -30 mV.

To determine voltage-dependent inactivation, the peak L-type, or T-type Ca^{2+} current respectively, was normalised to the maximal current (I_{max}, generally observed with the prepulse at -80 or -70 mV) and measured as a function of prepulse potential. To compare myotubes from different age donors, the inactivation curves within each group were averaged and then fitted with the Boltzmann equation

$I(V)/I_{max} = 1/(1+\exp[(V-V_{1/2})/k])$

with $V_{1/2}$ being the voltage of half-inactivation and k a measure for the steepness. Moreover, to further analyze L-type Ca^{2+} current inactivation, recordings from double-pulse experiments, at the prepulse potential (usually +20 mV) which lead to maximal *prepulse* peak current and maximal *test pulse* current inactivation, were pooled and analysed to obtain other two indexes of inactivation [41]: 1) the rate of the L-type Ca^{2+} current inactivation (r_{1500}, or residual current at 1500 ms), expressed as the percent current reduction at the end of the *prepulse* (I_{1500}) compared to the peak *prepulse* current (I_{peak})

$r_{1500}\,[\%]=(I_{1500}/\ I_{peak})*100$

and 2) the degree of maximal voltage-dependent inactivation (called r_{inact}), determined as the ratio of the *test* current (at 0 or 10 mV) and the highest current measured during the set of test pulses (I_{max})

$r_{inact}[\%]=(I_{(20\text{-}30\ mV)}/\ I_{max})*100.$

2.3 Calcium imaging experiments

Calcium imaging experiments were carried out on myotubes plated on matrigel-coated coverlips loaded with the Ca^{2+} indicator Fura-2 pentacetoxymethylester (fura-2 AM). Cells were incubated for 30 min in the dark at room temperature in a physiological solution (NES, see below) supplemented with 10 mg ml^{-1} bovine serum albumin and 5 *μ*M fura-2 AM; after wash-out, cells were maintained in NES for 15 min in the dark at room temperature to allow de-esterification of the probe. All the experiments were performed at room temperature. Cells were alternatively

excited at 340 and 380 nm selected by a monochromator (Polychrome II T.I.L.L. Photonics GmbH, Martinsried, Germany) and fluorescence images were collected by a CCD camera (SensiCam; PCO Computer Optics, Kelheim, Germany) at image acquisition rate of 1 image /750 ms.

Intracellular Ca^{2+} ($[Ca^{2+}]_i$) transients in *coupled* myotubes were elicited by cell depolarisation with high $[K^+]$ (40 mM; 5 s superfusion by a gravity-driven perfusion system) in a Ca^{2+}-free solution (see below). The ratio was calculated off-line. The corresponding temporal plots (*i.e.* the variations in the mean value of fluorescence intensity) were calculated from ratio images in the areas of interest, and the fluorescence ratio at rest was conventionally assumed to be 1. Three experimental parameters were evaluated: *i*) the number of responsive myotubes, expressed as a percentage (%), *ii*) the peak of $[Ca^{2+}]_i$ transient , expressed as the maximum difference between the fluorescence ratio at rest and after the stimulus (ΔR), *iii*) the area of $[Ca^{2+}]_i$ transient, determined by integration of the transient itself.

2.4 Recording solutions and chemicals

With regard to the electrophysiological experiments, solutions used to record T- and L-type Ca^{2+} currents were as follows: the extracellular bathing solution contained (in mM): 145 TEA-Cl, 10 $CaCl_2$, 0.8 $MgCl_2$, 5.6 glucose and 10 Hepes (pH adjusted to7.4 with TEA-OH). The intracellular pipette solution contained (in mM): 140 CsCl, 0.005 $CaCl_2$, 1 $MgCl_2$, 5.6 glucose, 10 Hepes, 0.1 EGTA and 2 ATP (pH adjusted to 7.2 with TEA-OH). The physiological solution (NES), used for the Fura-2 loading of the cells before the videoimaging experiments, contained (in mM): 2.8 KCl, 140 NaCl, 2 $CaCl_2$, 10 Hepes, 2 $MgCl_2$, 10 glucose, pH 7.3); these experiments were then performed in a Ca^{2+}-free solution containing (in mM): 140 NaCl, 2.8 KCl, 5 $MgCl_2$, 2 EGTA, 10 glucose, 10 Hepes (pH adjusted to 7.4 with Na-OH). Fetal calf serum was purchased from Mascia Brunelli (Milano, Italy) and matrigel from Becton-Dickinson (NJ, USA). All the other chemicals, unless otherwise stated, were obtained from Sigma (St Louis, MO, USA).

2.5 Data acquisition and statistical analysis

For electrophysiological data acquisition, the pCLAMP software package (v. 8.0, Axon Instruments) was used, while fluorescent signals were acquired with a conventional system driven by Imaging Workbench software (v. 2.2, Axon Instruments). For data analysis Origin software (v. 7.0, Microcal Software, Northampton, MA) and Prism software (v. 3.0, Graph Pad Software, State of California, USA) were routinely used. All data, whenever possible, are presented as mean ± *SEM*, with *n* being the number of myotubes tested. Differences between data groups were evaluated by Student's t-test and a *P* value <0.05 was considered statistically significant.

3. Results

Electrophysiological and videoimaging experiments were performed on cultured multinucleated myotubes derived from young donors (2 and 12 years, called "young myotubes") and old donors (76 and 86 years of age, "old myotubes").

Due to the poor availability of human material, being aware of potential heterogeneity of the samples and knowing from literature that gender is important in muscle strength and aging (see also [47] and [48]), we focussed on healthy male human donors. Primary cultures obtained from muscle biopsies were expanded for a maximum of 6 passages.
After 3-6 days in differentiation medium, old myotubes were in general smaller and thinner than young myotubes, as shown in the representative examples in Fig. 1; this age-related difference in size is already known from previous work. In fact, both old myotubes (see [23,24,34]) and old myofibres (see [22]) were proved to be less differentiated.

3.1 T-type Ca^{2+} currents in human myotubes during the aging process

T-type Ca^{2+} currents evoked from -60 mV holding potential as explained in Section 2.2 (see Figs. 2A and 3), were detected in about 90% of the young human myotubes, but only in about 50% of the old myotubes analysed (Fig. 2B). The current density (I_T/C), calculated from the peak current values at different test potentials, was similar in both groups as judged from comparing the normalized and averaged (I_T*/C)-V* curves (Fig. 2C). Similarly, maximum peak current values (I_{Tmax}), generally detected at -30 or -20 mV holding potential, and normalized to the cell capacitance, were similar, thus confirming that there was no significant age-related decrease in T-type current density (Fig. 2D).

We next examined the voltage-dependence of the activation and inactivation of T-type Ca^{2+} currents. Using the subtraction method (see Section 2.2 and Figs. 3A-C), it was possible to separate the T-type current from the L-type current, and to determine the I_T-*V* relationship. The value of E_{rev} calculated for each myotube was used to estimate the voltage-dependence of activation (G, conductance), and, then, the normalized and averaged I_T-*V* and G_T-*V* curves were examined to compare the activation kinetics of T-type current (for further details see Section 2.2). The voltage-dependence of the T-type current is shown in Figs. 3D and E; no significant differences were found on comparing the two age groups, and this was also true for the best fitting parameters for $V_{1/2}$ and *k*, determined from the mean data points of the activation curves (see Section 2.2 and Table 1).

The voltage-dependence of the inactivation of the T-type current was studied using a double pulse protocol; the amplitude of each current elicited by the test pulse was normalized to the maximum current, usually obtained with the conditioning prepulse to -80 mV, and plotted versus the potential of the prepulse, for each myotube (see Section 2.2 and Fig. 4). The inactivation curves obtained in young and old myotubes respectively were then averaged, and the results are displayed in Fig. 4. The best fitting parameters for $V_{1/2}$ and *k*, determined from the mean data points of the inactivation curves, are presented in Table 1. Inactivation curve means, obtained in young and old myotubes, were significantly different (*paired t-test, P=0.0006)*, as was the best fitting parameter for $V_{1/2}$ (*t-test, P=0.0001,* Table 1). The ~4 mV shift of the inactivation curve of the T-type current towards more negative potentials in old myotubes exceeded the remaining voltage drop error, potentially induced by the uncompensated series resistance (see Section 2.2), so the noticed difference between the T-type current recorded in young and old myotubes can be considered a result of age-related alterations (see Section 4).

3.2 L-type Ca^{2+} currents in human myotubes during the aging process

L-type Ca^{2+} currents (I_L), evoked and recorded in human myotubes as explained in Section 2.2, are shown in Fig. 5A. We detected the L-type currents in almost 100% of the young and in about 50% of the old myotubes we recorded from (Fig. 5B). It is important to note that the majority of these old myotubes did not display voltage-dependent Ca^{2+} currents at all, since they did not display either T-type Ca^{2+} currents (I_T; see previous Section 3.1). In fact, these two types of Ca^{2+} current were typically detected together in the cells tested, and only in few cases we found either I_L or I_T. Interestingly, the L-type current density (I_L/C) also decreased significantly in an age-related manner; in fact, both the normalized and averaged (*I_L/C)-V* curves (Fig. 5C), and the maximum peak current value (I_{Lmax}), generally observed at +20 or +30 mV and normalized to the cell capacitance (Fig 5D), significantly differed in young and old myotubes. The normalized and averaged current – voltage relationship (*I_L-V*), and the normalized and averaged activation (*G_L-V)* and inactivation curves were then examined to compare the kinetics of L-type current at different ages (for further details on the protocols used to obtain the L-type current kinetics see Section 2.2 and [41]).

In Fig. 6, two representative recordings of I_L currents are shown, evoked and recorded at different potentials, respectively in a young myotube (Fig. 6A) and in an old myotube (Fig. 6B). Besides noting the clear decrease of I_L amplitude in old myotubes (already mentioned above), some additional differences became obvious when comparing the normalized and averaged *I_L-V* (Fig. 6C) and *G_L-V* (Fig. 6D) activation curves. Indeed, mean values of activation curve data (*G_L-V*), obtained in young versus old myotubes, were significantly different (*paired t-test, P=0.0188*), as was the best fitting parameter for *$V_{1/2}$* (*t-test, P<0.0001)*, provided in Table 2.

Recordings from double-pulse experiments allowed us to study the inactivation kinetics of the I_L current. On comparing the sample I_L traces from young and old myotubes (Fig.7A) and the relative normalized and averaged inactivation curves (Fig.7B), two different inactivation behaviours could be easily recognised. The first one was peculiar for young myotubes, which usually displayed a complete current inactivation; the second one was typically observed in old myotubes, which showed a greater resistance to inactivation. Data obtained from double-pulse experiments, at the prepulse potential (usually +20 mV) which lead to maximal *prepulse* peak current and maximal *test pulse* current inactivation, were pooled and analysed to obtain the two indexes of inactivation r_{1500} (residual current at 1500 ms) and r_{inact} (degree of maximal voltage-dependent inactivation; see Section 2.2 for details); this analysis indicated that r_{1500} increased during aging in a highly significant way ($r_{1500,young}$[%]=19.4±5.40, *n*=14; $r_{1500,old}$[%]=63.8±3.20, *n*=20; *t-test P<0.0001*), and that r_{inact} was also significantly higher in old myotubes ($r_{inact,old}$[%]=45.0±3.50, *n*=11) than in the majority of young myotubes, where it was close to zero (complete inactivation). In two out of 8 young myotubes however, we found an incomplete inactivation also (data not shown). Moreover, mean values of inactivation curve data obtained in young and old myotubes (Fig. 7B), were significantly different (*paired t-test, P=0.0077)*, as well as the best fitting parameter for *$V_{1/2}$* (*t-test, P=0.0014)* (Table 2).

3.3 E-C coupling mechanism in human myotubes during the aging process

In skeletal muscle, L-type Ca^{2+} channels, besides acting as ion-conducting pores, interact mechanically with the ryanodine receptors, and are involved in triggering Ca^{2+} release from the sarcoplasmic reticulum, even in the absence of extracellular Ca^{2+} (excitation-contraction (E-C) coupling mechanism [27]). In order to explore whether the age-related alterations of the L-type Ca^{2+} channels, highlighted by the electrophysiological experiments, had consequences on the excitation-Ca^{2+} release coupling mechanism, we performed videoimaging experiments on 3-6 days differentiated young and old myotubes. To distinguish between *coupled* and *uncoupled* myoubes, the cells were depolarized with high [K^+] (40 mM) in a Ca^{2+}-free solution, applied for 5 s by a gravity-driven perfusion system (see Section 2.3 and Figs. 8A and B for details). In every experimental field, only multinucleated myotubes were taken into consideration. While E-C coupling was detected in 86 % of young myotubes (*n*=189), only 44% of the old myotubes (*n*=138) were responsive to the depolarizing stimulus in the absence of extracellular Ca^{2+} (Fig. 8C).

On the other hand, the $[Ca^{2+}]_i$ transients elicited by depolarization were very similar in *coupled* young and old myotubes: both mean peak values and mean area of the $[Ca^{2+}]_i$ transient, were not significantly different when we compared young (*n*=154) and old (*n*=61) myotubes (Figs. 8D and E).

4. Discussion

We have recently shown that the inefficiency of *in vitro* aged murine satellite cells to generate functional myotubes could be partly due to defective voltage-dependent T-type and L-type Ca^{2+} currents. In particular, the expression and the amplitude of both currents decreased significantly when approaching replicative senescence, and the L-type current revealed significant alterations in the rate of inactivation [41]. Moreover, previous experiments on human myogenic cells in our laboratory, showed a delay in the establishment of the excitation-contraction coupling (E-C) mechanism, depending on the age of the donor, and this effect was reproducible in human myogenic cells from a young donor aged *in vitro* in culture [23].
Proceeding from these results, the present work has been specifically designed to investigate the possible age-related alterations of voltage-dependent T-type and L-type Ca^{2+} currents in myotubes derived from the differentiation and fusion of human satellite cells from donors of different age, in order to verify a possible involvement of these types of current in the intricate processes underlying human skeletal muscle loss of force and function with aging.

First of all, our experiments were aimed at confirming that human myotubes express T-type Ca^{2+} current and at exploring if the occurrence of this type of current decreases during aging. We have shown for the first time that the occurrence of T-type currents significantly decreased with aging, without any change in the current density (Fig. 2). These data are fully in accordance with those previously reported on murine myotube cells aged *in vitro* [41]. Whilst age-related changes in the voltage-dependence of activation were ruled out, a significant shift of ~4 mV in the inactivation curve towards more negative potentials with aging was revealed (see Fig. 4 and Table 1). Our results on T-type Ca^{2+}

currents demonstrate that, extensively, less Ca^{2+} would be available via T-type channels in the old human myotubes: either the T-type current would not present, or, if it is, it could inactivate at more negative potentials.

After the first recordings of a T-type current in starfish eggs in 1975, the research on this type of voltage-dependent Ca^{2+} current has advanced significantly over the last 20 years (reviewed in [49]). Today, T-type currents have many known or suggested functional roles in different types of developing and mature cells, and in several diseases (for recent reviews see [50] and [51]). T-type (or LVA (low voltage activated) Ca^{2+} channels), were distinguished, by electrophysiological studies, from the HVA (high voltage activated) Ca^{2+} channels by their low voltage thresholds for activation and inactivation, the smaller single channel conductance and their fast inactivation. Three pore-forming subunits (α_{1G}, $\alpha_{1H,}$ and α_{1I} (or $Ca_V3.1$-3.3)), have been recently cloned, characterized by several splice variants, and expressed in various cell types (for recent reviews see [52] and [53]). Interestingly, a correlation between LVA Ca^{2+} channel expression and skeletal muscle development was hypothesized several years ago (see [54],[55]), but the question of how T-type channels are involved in modulating human skeletal muscle differentiation has only very recently been addressed. Considering that these channels are functionally expressed only during myogenesis, several studies have been aimed at understanding the importance of this source of Ca^{2+} entry during the initial differentiation of myoblasts and the fusion into myotubes, the precursors of mature skeletal muscle fibres (see [42, 56-58]). The only T-type channel principal subunit found both in mouse and human skeletal muscle is the α_{1H} or $Ca_V3.2$ [42, 56]. Especially in humans, it plays a crucial role in generating the intracellular Ca^{2+} signal, triggering the myoblast differentiation and fusion ([42, 56-58], but see [57]). We have previously reported a correlation between senescence of satellite cells and defective T-type Ca^{2+} channels; we demonstrated that the occurrence of T-type current decreased during *in vitro* aging of murine satellite cells [41]. In the present study, we strengthen this age-related feature, by providing further evidence in human-derived cells. In addition, we report for the first time a possible age-related change in T-type current kinetics, by showing that these currents inactivate at more negative membrane potentials in old myotubes. The activation and inactivation parameters obtained both in young and old myotubes (see Table 1) are in the range of what has already been shown for T-type currents, considering the possible differences that can arise from different solution compositions and electrophysiological protocols, and different tissues or species analysed (for a review see [53]). The significant shift of the inactivation curve by ~4 mV towards more negative potentials induced by aging, could critically influence the steady-state "window" Ca^{2+} current through T-type channels, important in the differentiation of human myoblasts [42, 56-58]. In the 50% of old myotubes expressing functional T-type channels, this "window" Ca^{2+} current would be smaller, because of the age-related shift of the inactivation kinetics, thus less Ca^{2+} would be available for differentiation and fusion. This could possibly explain why senescent satellite cells fuse more slowly and less efficiently, leading to smaller and thinner myotubes [23,34,41].

The demonstrated changes in T-type current occurrence and kinetics in old myotubes, might arise from age-related alterations of the principal α_1 channel subunit expression or function, possibly due to aging-associated changes in genes transcription and protein expression, or modified post-translational processing (for

a review see [48]), or from alterations in intracellular signalling modulators, such as protein kinase C [60], Rho-associated kinase [61] or Ca^{2+}/calmodulin-dependent kinase and protein kinase II [62], and also in possible associated accessory subunits (reviewed in [52]). Unfortunately, none of these age-related hypotheses have been investigated to date, and in general, the studies on T-type channel modulation are just at the beginning, leaving open important possibilities for future research.

It has been proposed that human myoblasts in culture can change their preferred Ca^{2+} source for differentiation, if necessary [58]. Thus, Ca^{2+} entry via T-type channels is not the only means of increasing cytoplasmic Ca^{2+} concentration at the onset of myoblast differentiation and fusion into myotubes. An involvement of the HVA L-type voltage-dependent Ca^{2+} channels has been also proposed by several authors in different types of culture system [59,63,64]. In this study, we detected the L-type current in almost 100% of the young human myotubes, but the occurrence decreased to about 50% in old myotubes (Fig. 5B). Thus, we could hypothesize that less Ca^{2+} might be available for differentiation and fusion of old myotubes, even when myoblasts switch to this alternative source of Ca^{2+} influx (but see [42,65]). It is also important to consider the age-related decrease in the occurrence of L-type currents from another point of view. Besides producing a slow HVA Ca^{2+} current, L-type channels act as voltage-sensors to trigger the contractile machinery for excitation- Ca^{2+} release coupling in skeletal muscle [27]. In recent years, the contribution of alterations in E-C coupling to age-related mammalian muscle decline has been shown [66-70]. Our present results fit with the hypothesis that alteration of the mechanisms controlling Ca^{2+} handling, and particularly of different components of the excitation-contraction apparatus, could be one of the causes of the age-related decline in skeletal muscle strength [22-26]. In addition to the decrease in L-type current occurrence, the current density also significantly decreased in an age-related way (see Figs. 5C and 5D), as already seen by Delbono and colleagues in old human skeletal muscle fibres [22,71]. In these previous reports, the authors claimed a specific responsibility of the decrease of the L-type channel number and/or activity for the lowering of intracellular Ca^{2+} release, and so for the reduction in human muscle strength with old age. This would be supported also by strong evidence obtained in other mammals [66-70], but currently, there are some conflicting results about humans [47].

Our present electrophysiological results demonstrate an age-related decrease of the activity of L-type channels, and in the videoimaging experiments, a decrease in the occurrence of the E-C coupling mechanism from 86% in young myotubes to 44% in old myotubes (Fig. 8C). Similar results relative to age-related E-C uncoupling in humans have been obtained previously in old myotubes differentiated in culture, both in our laboratory [23] and by other researchers [24]. These results strengthen even more the possibility that the age-related absence of the E-C coupling mechanism could be due to the partial lack of L-type channel activity, as shown by Delbono and colleagues in old human skeletal muscle fibres [22,71]. On the other hand, in the present study, we also showed that the analysed Ca^{2+} transients were very similar in *coupled* myotubes derived from the differentiation and fusion of young and old satellite cells, since both the averaged peak and the averaged area of the Ca^{2+} transient were not significantly different when comparing young and old myotubes (Figs. 8D and 8E); this differs from the

significant reduction of maximum peak intracellular Ca^{2+} found by Delbono and his group in old human skeletal muscle fibres [22,71].
However, our results on Ca^{2+} transient kinetics and amplitude could be at least partially related to the different activation and inactivation kinetics we have found for L-type current at different ages. Analysing the activation and inactivation curve in young and old myotubes, we noted that the L-type current activation at more positive membrane potentials in old myotubes appeared to be accompanied by an age-related shift towards more positive potentials of the inactivation (see Figs. 6D and 7B and Table 2). However, what seems to be more relevant, is the greater resistance to inactivation, clearly demonstrated by both the L-type inactivation curve obtained in old myotubes (Fig. 7B), and the age-related increase of the two analysed indexes of the current inactivation r_{1500} (residual current at 1500 ms) and r_{inact} (degree of maximal voltage-dependent inactivation; see Section 2.2). We noted the lower susceptibility to inactivation of L-type current in myotubes derived from old cells also in our previous work on murine satellite cells aged *in vitro*, and we already hypothesized that this could be a sort of compensatory mechanism to hinder the age-related reduction of L-type current density and the lower availability of intracellular Ca^{2+}, indispensable for skeletal muscle contraction [41]. Here, we could also suppose a link between this result and the unchanged amplitude of the Ca^{2+} transients evoked in old myotubes, if compared with the transients obtained in the young ones (see above): in fact, if we also detected an age-related decrease in the L-type current density, the L-type channels available in old myotubes might remain open longer, and so, if coupled, they could enable a more prolonged Ca^{2+} release from the stores. Sure enough, this is only one of the hypotheses that could be taken into consideration; it would be also important to consider the possible age-related diminution in the open probability of the L-type channel, that could underlie the changes in the kinetics of activation (see Section 3.2 and Fig. 5) and inactivation (see Section 3.2 and Fig. 7), and possibly also the kinetics of the Ca^{2+} transient. Unfortunately it was not possible, at this stage, to analyse the single channel behaviour of the L-type Ca^{2+} channel.
The differences in L-type current occurrence and kinetics could arise, in general, from age-related alterations already hypothesized in our previous work (for details, see discussion in [41]). We were not able to find other previous studies in the literature about L-type current kinetics and possible changes during skeletal muscle aging in humans. However, there are some studies on L-type current activation and inactivation in healthy cultured human skeletal myotubes [72,73], and others in which changes in the L-type current kinetics in human myotubes were thought to be related to the development of a skeletal muscle pathology [74-76]; the activation and inactivation parameters that we obtained both in young and old myotubes (see Table 2) are comparable with those reported in literature, considering the possible differences that could arise from different solution compositions and electrophysiological protocols.

In conclusion, we confirm what has been observed in mammalian models [41] and in human-derived cells [22-24,34,71], that aged satellite cells may have a reduced efficiency to generate functional skeletal muscle fibres, and consequently this may be one of the causes of sarcopenia in old skeletal muscle. Moreover, we showed for the first time that in human myotubes derived from satellite cells of old donors, the functional expression and the biophysical properties of the T- and L-type voltage-dependent Ca^{2+} channels are somehow impaired. Even if there is still a lot

to explore and to explain about the complex mechanisms that underlie human skeletal muscle aging, this is further strong evidence that in humans, as in other mammals, the satellite cells and the regulation of Ca^{2+} homeostasis have a decisive role in this physiological process.

Aknowledgments

We wish to thank Dr. Daniela Pietrobon (University of Padova) for her valuable comments and helpful suggestions, and Dr Andy Constanti (School of Pharmacy, University of London) for critical reading of the manuscript and editorial assistance. This work was supported by grants from MIUR-Italy (PRIN and FIRB projects) to F.R..

References

[1] I.H. Rosenberg, Sarcopenia: Origins and Clinical Relevance, J. Nutr. 127 (1997) 990S.
[2] T.J. Doherty, Invited review: aging and sarcopenia, J. Appl. Physiol. 95 (2003) 1717-1727.
[3] L.J.S. Greenlund, K.S. Nair, Sarcopenia-consequences, mechanisms, and potential therapies, Mech. Aging Dev. 124 (2003) 287-299.
[4] A. Di Iorio, M. Abate, D. Di Renzo et al., Sarcopenia: age-related skeletal muscle changes from determinants to physical disability, Int. J. Immunopathol. Pharmacol. 19 (2006) 703-719.
[5] A.M. Solomon, P.M.G. Bouloux, Modifying muscle mass- the endocrine perspective, J. Endocrinol. 191 (2006) 349-360.
[6] W.J. Evans, Protein nutrition, exercise and aging, J. Am. Coll. Nutr. 23 (2004) 601S–9S.
[7] L.A. Schaap, S.M.F. Pluijm, D.J.H. Deeg, m. Visser, Inflammatory markers and loss of muscle mass (sarcopenia) and strength, Am. J. Med. 119 (2006) 526.e9-17.
[8] L. Larsson, T. Ansved, Effects of ageing on the motor unit, Prog. Neurobiol. 45 (1995) 397-458.
[9] O. Delbono, Neural control of aging skeletal muscle, Aging Cell 2 (2003) 21-29.
[10] E. Edstrőm, M. Altun, E. Bergman, Factors contributing to neuromuscular impairment and sarcopenia during aging, Physiol. Behav. 92 (2007) 129-135.
[11] S. Welle, A.I. Brooks, J.M. Delehanty, N. Needler, C.A. Thornton, Gene expression profile of aging in human muscle, Physiol. Genomics 14 (2003) 149-159.
[12] H.J. Stuerenburg, B. Stangneth, B.G. Schoser, Age related profiles of free amino acids in human skeletal muscle, Neuro. Eendocrinol. Lett. 27 (2006) 133-136.
[13] J.M. Zahn, R. Sonu, H. Vogel et al., Transcriptional profiling of aging in human muscle reveals a common aging signature, PLoS Genet. 2 (2006) e115.
[14] K. R. Short, J.L. Vittone, M.L. Bigelow et al., Changes in myosin heavy chain mRNA and protein expression in human skeletal muscle with age and endurance exercise training
J Appl Physiol 99 (2005) 95-102.
[15] E. Prochniewicz , L.V. Thompson, D.D. Thomas, Age-related decline in actomyosin structure and function, Exp. Gerontol. 42 (2007) 931-938.
[16] S. Fulle, S. Di Donna, C. Puglielli et al., Age-dependent imbalance of the antioxidative system in human satellite cells, Exp. Gerontol. 40 (2005) 189-197.
[17] B. Marzani, G. Felzani, R.G. Bellomo, J. Vecchiet, F. Marzatico, Human muscle aging: ROS-mediated alterations in rectus abdominis and vastus lateralis muscles, Exp. Gerontol. 40 (2005) 959-965.
[18] L.L. Ji, Antioxidant signaling in skeletal muscle: A brief review, Exp. Gerontol. 42 (2007) 582-593.
[19] K.R. Short, M.L. Bigelow, J. Kahl et al., Decline in skeletal muscle mitochondrial function with aging in humans, Proc. Natl. Acad. Sci. 102 (2005) 5618-5623.
[20] E. Hűtter, M. Skovbro, B. Lener et al., Oxidative stress and mitochondrial impairment can be separated from lipofuscin accumulation in aged human skeletal muscle, Aging Cell 6 (2007) 245-256.

[21] E. Nurowska, B. Dworakowska, M. Kloch, M. Sobol, K. Dolowky, A. Wernig, F. Ruzzier, Potassium currents in human myogenic cells from donors of different ages. Exp. Gerontol. 41 (2006) 635-640.
[22] O. Delbono, K.S. O' Rourke, W.H. Ettinger, Excitation-calcium release uncoupling in aged single human skeletal muscle fibers, J. Membr. Biol. 148 (1995) 211-222.
[23] P. Lorenzon, E . Bandi, F. de Guarrini et al., Aging affects the differentiation potential of human myoblasts, Exp. Gerontol. 39 (2004) 1545-1554.
[24] S. Beccafico, C. Puglielli, T. Pietrangelo, R. Bellomo, G. Fanò, S. Fulle, Age-dependent effects on functional aspects in human satellite cells, Ann. N. Y. Acad. Sci. 1100 (2007) 345-352.
[25] N. Weisleder, M. Brotto, S. Komazaki et al., Muscle aging is associated with compromised Ca^{2+} spark signaling and segregated intracellular Ca^{2+} release, J. Cell. Biol. 174 (2006) 639-645.
[26] S. Boncompagni, L. d'Amelio, S. Fulle, G. Fanò, F. Protasi, Progressive disorganization of the excitation-contraction coupling apparatus in aging human skeletal muscle as revealed by electron microscopy: a possible role in the decline of muscle performance, J. Gerontol. A Biol. Sci. Med. Sci. 61 (2006) 995-1008.
[27] B.A. Block, T. Imagawa, K.P. Campbell, C. Franzini-Armstrong, Structural evidence for direct interaction between the molecular components of the transverse tubule/sarcoplasmic reticulum junction in skeletal muscle, J. Cell Biol. 107 (1988) 2587-2600.
[28] A. Mauro, Satellite cell of skeletal muscle fibers, J. Biophys. Biochem. Cytol. 9 (1961) 493-495.
[29] J.E. Morgan, T.A. Partridge, Muscle satellite cells, Int. J. Biochem. Cell. Biol. 35 (2003) 1151-1156.
[30] J. Dhawan, T.A. Rando, Stem cells in postnatal myogenesis: molecular mechanisms of satellite cell quiescence, activation and replenishment, Trends Cell. Biol. 15 (2005) 666-673.
[31] R.T. Hepple, Dividing to Keep Muscle Together: The Role of Satellite Cells in Aging Skeletal Muscle. Sci. Aging Knowl. Environ. 3 (2006) pe3.
[32] R.S. Hikida, s. Walsh, N. Barylski, G. Campos, F.C. Hagerman, R.S. Staron, Is hypertrophy limited in elderly muscle fibers? A comparison of elderly and young strength-trained men, Basic. Appl. Myol. 8 (1998) 419-427.
[33] S.M. Roth, G.F. Martel F.M. Ivey et al., Skeletal muscle satellite cell populations in healthy young and older men and women, Anat. Rec. 260 (2000) 351-358.
[34] V. Renault, G. Piron-Hamelin, C. Forestier et al., Skeletal muscle regeneration and the mitotic clock, Exp. Gerontol. 35 (2000) 711-719.
[35] F. Kadi, N. Charifi, C. Denis, J. Lexell, Satellite cells and myonuclei in young and eldely women and men, Muscle Nerve 29 (2004) 120-127.
[36] S. Sajko, L. Kubinova, E. Cvetko, M. Kreft, A. Wernig, I. Erzen, Frequency of M-caderin-stained satellite cells declines in human muscles during aging, J. Histochem. Cytochem. 52 (2004) 179-185.
[37] S. Decary, V. Mouly, C. Ben Hamida, A. Sautet, J.P. Barbet, G.S. Butler-Browne, Replicative potential and telomere length in human skeletal muscle: implications for satellite cell-mediated gene therapy, Hum. Gene Ther. 8 (1997) 1429-1438.

[38] V. Renault, E. Rolland, L. Thornell, V. Mouly, G. Butler-Browne, Distribution of satellite cells in the human vastus lateralis muscle during aging, Exp. Gerontol. 37 (2002) 1511-1512.
[39] A. Wernig, R. Schafer, U. Knauf et al., On the regenerative capacity of human skeletal muscle, Artif. Organs 29 (2005) 192-198.
[40] R. Shafer, U. Knauf, M. Zweyer et al., Age dependence of the human skeletal muscle stem cell in forming muscle tissue, Artif. Organs 30 (2006) 130-140.
[41] E. Luin, F. Ruzzier, The role of L- and T-type Ca^{2+} currents during the *in vitro* aging of murine myogenic (i28) cells in culture, Cell Calcium 41 (2007) 479-489.
[42] P. Bijlenga, J. Liu, E. Espinos, C. Haenggeli, J. Fischer-Lougheed, C.R. Bader, L. Bernheim, T-type α1H Ca^{2+} channels are involved in Ca^{2+} signalling during terminal differentiation (fusion) of human myoblasts, Proc. Natl. Acad. Sci. U S A 97 (2000) 7627-7632.
[43] S. Seigneurin-Venin, E. Parrish, I. Marty et al., Involvement of the dihydropyridine receptor and internal calcium stores in myoblast fusion, Exp. Cell. Res. 223 (1996) 301-307.
[44] S. Decary, V. Mouly, G.S. Butler-Browne, Telomere length as a tool to monitor satellite cell amplification for cell-mediated gene therapy, Hum. Gene Ther. 7 (1996) 1347-1350.
[45] J. Campisi, From cells to organisms: Can we learn about aging from cells in culture?, Exp. Gerontol. 36 (2001) 607-618.
[46] S. Bortoli, V. Renault, R. Mariage-Samson et al., Modifications in the myogenic program induced by in vivo and in vitro aging, Gene 347 (2005) 65-72.
[47] M. Ryan, G. Butler-Browne, I. Erzen et al., Persistent expression of the α_{1S}-dihydropyridine receptor in aged human skeletal muscle: Implications for the excitation-contraction uncoupling hypothesis of sarcopenia, Int. J. Mol. Med. 11 (2003) 425-434.
[48] L.C. Vianna, R.B. Oliveira, C.G.S. Araùjo, Age-related decline in handgripstrenght differs according to gender, J. Strenght Cond.Res. 21 (2007) 1310-314.
[49] B. Nilius, K. Talavera, A. Verkhratsky, T-type calcium channels: The never ending story, Cell Calcium 40 (2006) 81-88.
[50] E. Perez-Reyes, Molecular physiology of low-voltage-activated T-type calcium channels, Physiol. Rev. 83 (2003) 117-161.
[51] P. Lory, I. Bidaud, J. Chemin, T-type calcium channels in differentiation and proliferation, Cell Calcium 40 (2006) 135-146.
[52] E. Perez-Reyes, Molecular characterization of T-type calcium channels, Cell Calcium 40 (2006) 89-96.
[53] K. Talavera, B. Nilius, Biophysics and structure-function relationship of T-type Ca^{2+} channels, Cell Calcium 40 (2006) 97-114.
[54] K.G. Beam, C.M. Knudson, Calcium currents in embryonic and neonatal mammalian skeletal muscle, J. Gen. Physiol. 91 (1988) 781-798.
[55] K.G. Beam, C.M. Knudson, Effect of postnatal development on calcium currents and slow charge movement in mammalian skeletal muscle, J. Gen. Physiol. 91 (1988) 799-815.
[56] C. Berthier, A. Monteil, P. Lory, C. Strube, Alpha(1H) mRNA in single skeletal muscle fibers accounts for T-type calcium current transient expression during fetal development in mice, J. Physiol. 539 (2002) 681-691.
[57] L. Bernheim, C.R. Bader, Human myoblast differentiation: Ca^{2+} channels are activated by K^+ channels, News Physiol. Sci. 17 (2002) 22-26.

[58] S. Arnadeu, N. Holzer, S. Kőnig, C.R. Bader, L. Bernheim, Calcium sources used by post-natal human myoblasts during initial differentiation, J. Cell. Physiol. 208 (2006) 435-445.
[59] I. Bidaud, A. Monteil, J. Nargeot, P. Lory, Properties and role of voltage dependent calcium channels during mouse skeletal muscle differentiation, J. Muscle Res. Cell. Motil. 27 (2006) 75-81.
[60] J. Park, H. Kang, H. Moon et al., Activation of protein kinase C augments T-type Ca^{2+} channel activity without changing channel surface density, J. Physiol. 577 (2006) 513-523.
[61] M. Iftinca, J. Hamid, L. Chen et al., Regulation of T-type calcium channels by Rho-associated kinase, Nat. Neurosci. 10 (2007) 854-860.
[62] J. Yao, L.A. Davies, J.D. Howard et al., Molecular basis for the modulation of native T-type Ca^{2+} channels in vivo by Ca^{2+}/calmodulin-dependentand protein kinas II, J. Clin. Invest. 116 (2006) 2403-2412.
[63] S. Seigneurin-Venin, E. Parrish, I. Marty et al., Involvement of the dihydropyridine receptor and internal calcium stores in myoblast fusion, Exp. Cell. Res. 223 (1996) 301-307.
[64] G.A. Porter, R.F. Makuck, S.A. Rivkees, Reduction in intracellular calcium levels inhibits myoblast differentiation, J. Biol. Chem. 277 (2002) 28942-28947.
[65] B. Constantin, C. Cognard, G. Raymond, Myoblast fusion requires cytosolic calcium elevation but not activation of voltage-dependent calcium channels, Cell Calcium 19 (1996) 365-374.
[66] O. Delbono, M. Renganathan, M.L. Messi, Regulation of mouse skeletal muscle L-type Ca^{2+} channel by activation of the insulin-like growth factor-1 receptor, J. Neurosci. 17 (1997) 6918-6928.
[67] M. Renganathan, M.L. Messi, O. Delbono, Dihydropyridine receptor-Ryanodine receptor uncoupling in aged skeletal muscle, J. Membrane Biol. 157 (1997) 247-253.
[68] Z. Wang, M.L. Messi, O. Delbono, L-type Ca^{2+} channel charge movement and intracellular Ca^{2+} in skeletal muscle fibers from aging mice, Biophys. J. 78 (2000) 1947-1954.
[69] A.M. Payne, Z. Zheng, E. Gonzàlez, Z. Wang, M.L. Messi, O. Delbono, External Ca^{2+}-dependent excitation-contraction coupling in a population of ageing mouse skeletal muscle fibres, J. Physiol. 560.1 (2004) 137-155.
[70] A.M. Payne, M.L. Messi, Z. Zheng, O. Delbono, Motor neuron targeting of IGF-1 attenuates age-related external Ca^{2+}-dependent skeletal muscle contraction in senescent mice, Exp. Gerontol. 42 (2007) 309-319.
[71] O. Delbono, M. Renganathan, M.L. Messi, Excitation- Ca^{2+} release-contraction coupling in single aged human skeletal muscle fiber, Muscle Nerve 5 (1997) S88-92.
[72] I. Sipos, C. Harasztosi, W. Melzer, L-type current inactivation in cultured human myotubes, J. Muscle Res. Cell. Motil. 18 (1997) 353-367.
[73] C. Harasztosi, I. Sipos, L. Kovacs, W. Melzer, Kinetics of inactivation and restoration from inactivation of the L-type calcium current in human myotubes, J. Physiol. 516 (1999) 129-138.
[74] J.A. Morrill, R.H. Brown, S.C. Cannon, Gating of the L-type Ca channel in human skeletal myotubes: an activation defect caused by the hypokalemic periodic paralysis mutation R528H, J. Neurosci. 18 (1998) 10320-10334.

[75] M. Rivet, C. Cognard, Y. Rideau, G. Duport, G. Raymond, Calcium currents in normal and dystrophic human skeletal muscle cells in culture, Cell Calcium 11 (1990) 507-514.

[76] N. Imbert, C. Vandebrouck, G. Duport et al., Calcium currents and transients in co-cultered contracting normal and Duchenne muscular dystrophy human myotubes, J. Physiol. 534 (2001) 343-355.

Figure legends

Figure 1. Representative photomicrographs of young and old human patched multinucleated myotubes, derived from the differentiation and fusion in culture, of satellite cells from a 12 year old (A) and a 86 year old donor (B). The arrow in (A) indicates some well-evident nuclei; scale bar, 35 µm.

Figure 2. T-type Ca^{2+} current (I_T) occurrence and density in human myotubes during the aging process: (A) shows representative I_T currents recorded in a young human myotube, obtained as explained in Section 2.2 (see also Figs. 3A, B and C). The histogram in (B) shows the percentage of young and old myotubes exhibiting I_T current (n=number of tested myotubes). In (C) the averaged current density-voltage (*(I_T/C)-V*) curves from young and old myotubes (each point is the mean ± *SEM*; ■= young, n=12; ○=old, n=8). Here and on the following I-V curves, superimposed are the fits of the I-V curves (continuous line=young, dash line=old), obtained with the formula $I(V) = G_{max}*(V-E_{rev})/(1+\exp[(V_{1/2}-V)/k])$; note that the high variability in the I_T current density probably was the cause of the apparent change (observable only in this figure) in the estimated E_{rev}. In (D) the histograms of T-type current density during aging, using only the maximum peak current value ($I_{Tmax,}$ n=number of tested myotubes).

Figure 3. Total Ca^{2+} currents, isolation of T-type (I_T) and L-type (I_L) Ca^{2+} currents and voltage-dependent activation kinetics in human myotubes during the aging process: in (A) representative I_T and I_L currents evoked in a young myotube by the standard voltage protocol in the inset; in (B), the same I_L currents, isolated by applying a 750-ms prepulse to -30 mV, and in (C) the I_T currents obtained by the subtraction of the recordings with the prepulse (B) from those obtained without it (A). (D) shows the averaged normalised T-type current-voltage (I-V) relationship and (E) the activation curves in young and old myotubes (each point is the mean ± *SEM*; ■= young, n=10; ○=old, n=8); here and on the following activation-inactivation curves, superimposed are the Boltzmann fits (continuous line=young, dash line=old). The best fitting parameters (see Section 2.2) are summarised in Table 1. Note very little or no age-related change in the shape of the I-V or activation curves.

Figure 4. The T-type current (I_T) voltage-dependent inactivation kinetics in human myotubes during the aging process: in (A), sample I_T traces from a double-pulse experiment covering the range of prepulse potentials shown in the protocol; in (B), the averaged normalised relative voltage-dependent inactivation curves (each point is the mean ± *SEM*; ■= young, n=12; ○=old, n=8). The best fitting parameters (see Section 2.2) are summarised in Table 1. Note the statistically significant shift (~4 mV) of the curve towards more negative potentials with aging.

Figure 5: L-type Ca^{2+} current (I_L) occurrence and density in human myotubes during the aging process: (A) shows representative I_L currents recorded in a young human myotube, isolated by applying a 750 ms prepulse to -30 mV (see Section 2.2 and Fig 3). The histogram in (B) shows the percentage of young and old myotubes exhibiting I_L current (n=number of tested myotubes). In (C) the averaged

current density-voltage (*(I_L/C)-V*) curves from young and old myotubes (■= young, n=16; ○=old, n=16); each point is the mean ± *SEM*; *= statistically significant difference, paired *t-test, P=0.0051*) and in (D) the histograms of L-type current density during aging, by considering exclusively the maximum peak current value (I_{Lmax}; n=number of tested myotubes, *= difference statistically significant, *t-test, P=0.0326*).

Figure 6: The L-type current (I_L) voltage-dependent activation kinetics in human myotubes during the aging process: (A) and (B) show representative I_L currents recorded respectively in a young and in an old human myotube (same scale, note the clear decrease of I_L amplitude in the exemplificative old myotube); (C) shows the averaged normalised L-type current-voltage (I_L-V) relationships and (D) the activation curves in young and old myotubes (each point is the mean ± *SEM*; ■= young, n=16; ○=old, n=16); the best fitting parameters (see Section 2.2) are summarised in Table 2. Note a significant age-related change in the shape of the I-V and activation curves, especially with test potentials ranging from -20 to +20 mV (see Section 3.2 for details).

Figure 7: The L-type current (I_L) voltage-dependent inactivation kinetics in human myotubes during the aging process: in (A) sample I_L traces from double-pulse experiments from a young (upper trace) and an old (lower trace) myotube, displaying a different time course and voltage-dependent inactivation; in (B) the averaged normalised relative voltage-dependent inactivation curves (each point is the mean ± *SEM*; ■= young, n=5; ○=old, n=5). The best fitting parameters (see Section 2.2) are summarised in Table 2. Note the upward shift of the curve with aging, which is indicative of a greater resistance to inactivation of the old myotubes (data means are significantly different, *paired t-test, P=0.0077*).

Figure 8: The E-C coupling mechanism in human myotubes during the aging process: in (A) four representative pseudocolor images of the $[Ca^{2+}]_i$ response elicited in one of the myotubes (*) of the optical field (scale bar, 35 µm). In (B) the corresponding temporal plot of the $[Ca^{2+}]_i$ response (the numbers indicate the timing of acquisition of the images shown in (A); the arrow head indicates the beginning and the bar the duration of stimulus application). In (C) the percentage (%) of responsive myotubes among young (white bar, n=189), and old (grey bar, n=138) myotubes; in (D) the averaged peak of $[Ca^{2+}]_i$ transients (R: young, n=154; old, n=61 myotubes), and in (E) the averaged area of $[Ca^{2+}]_i$ transients (young, n=154; old, n=61).

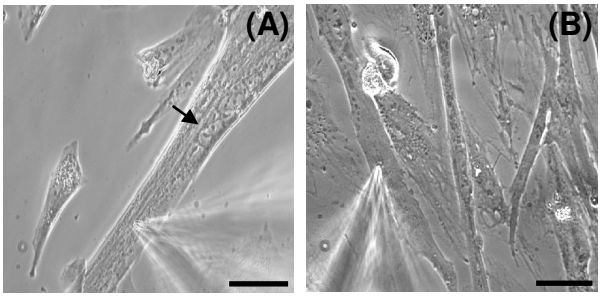

Fig.1

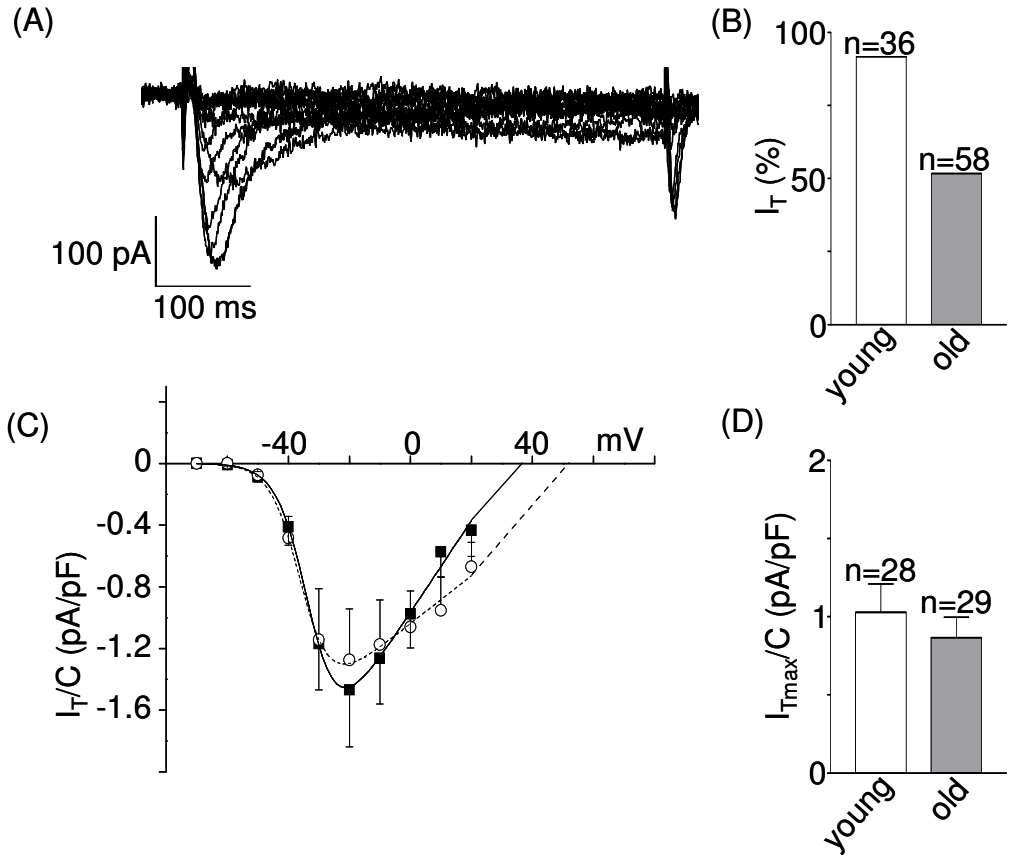
(A)
100 pA
100 ms
(B)
100
50
0
I_T (%)
n=36
n=58
young
old
(C)
-40
0
40
mV
0
-0.4
-0.8
-1.2
-1.6
I_T/C (pA/pF)
(D)
2
1
0
I_{Tmax}/C (pA/pF)
n=28
n=29
young
old

Fig.2

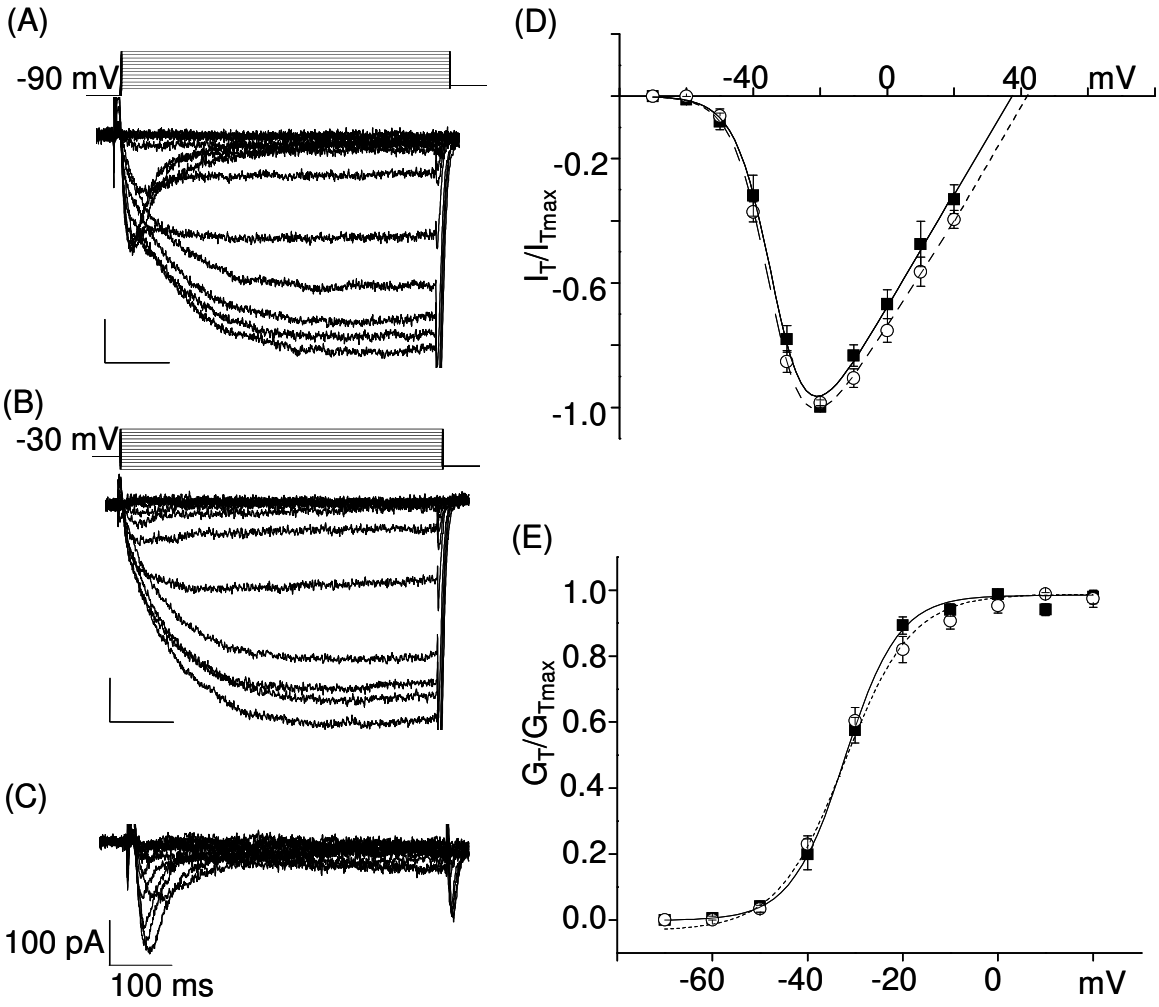
(A)
-90 mV
(B)
-30 mV
(C)
100 pA
100 ms
(D)
-40
0
40
mV
-0.2
-0.6
-1.0
I_T/I_{Tmax}
(E)
1.0
0.8
0.6
0.4
0.2
0.0
G_T/G_{Tmax}
-60
-40
-20
0
mV

Fig.3

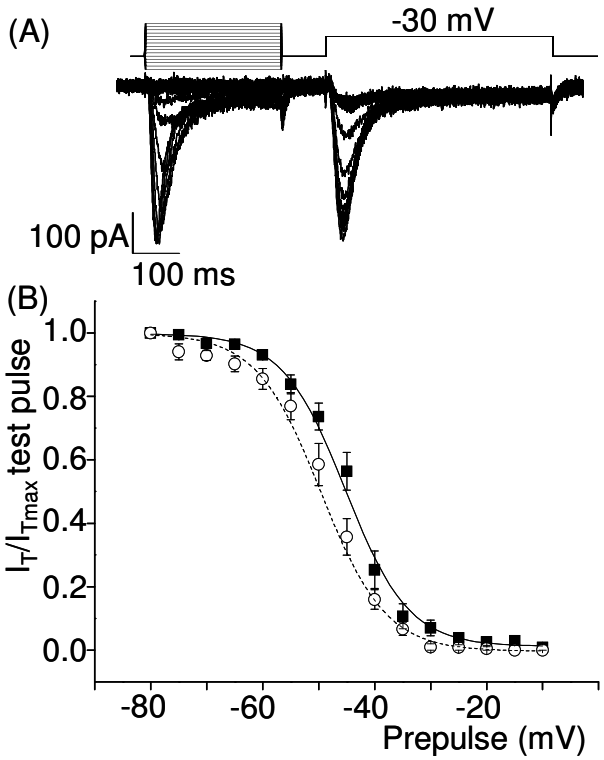
(A)
-30 mV
100 pA
100 ms
(B)
1.0
0.8
0.6
0.4
0.2
0.0
I_T/I_{Tmax} test pulse
-80
-60
-40
-20
Prepulse (mV)

Fig.4

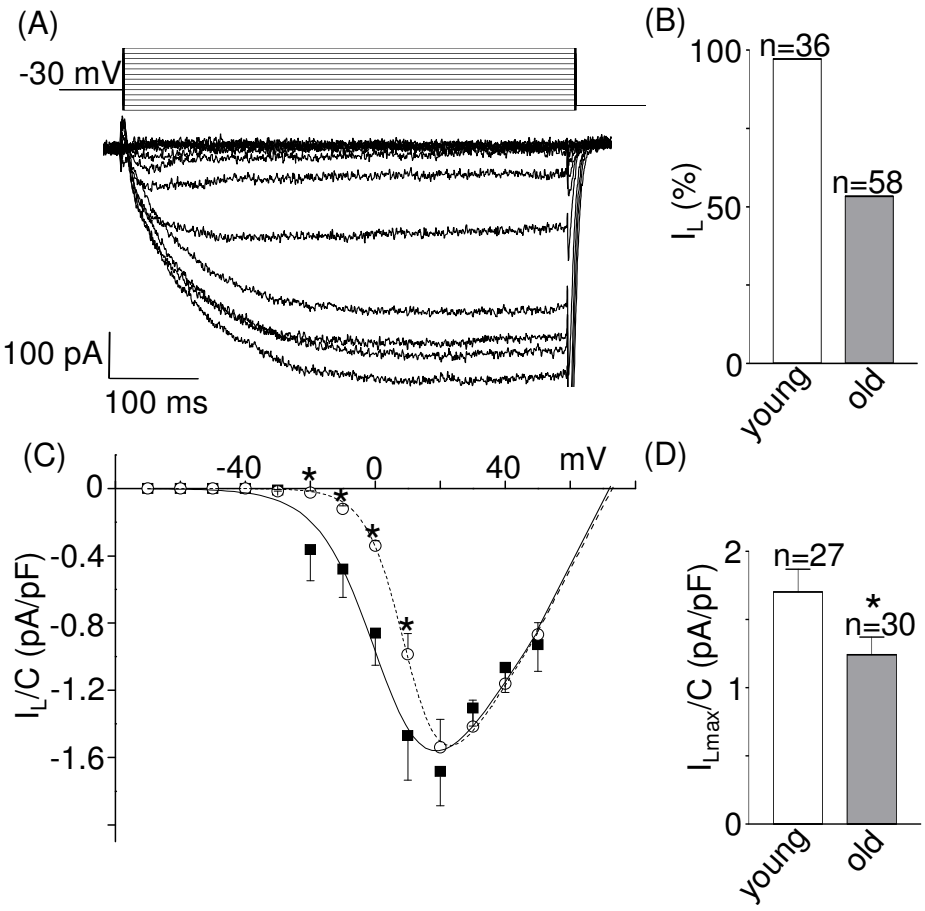
(A)
-30 mV
100 pA
100 ms
(B)
n=36
n=58
100
50
0
I_L (%)
young
old
(C)
-40
0
40
mV
0
-0.4
-0.8
-1.2
-1.6
I_L/C (pA/pF)
(D)
n=27
n=30
2
1
0
I_{Lmax}/C (pA/pF)
young
old

Fig.5

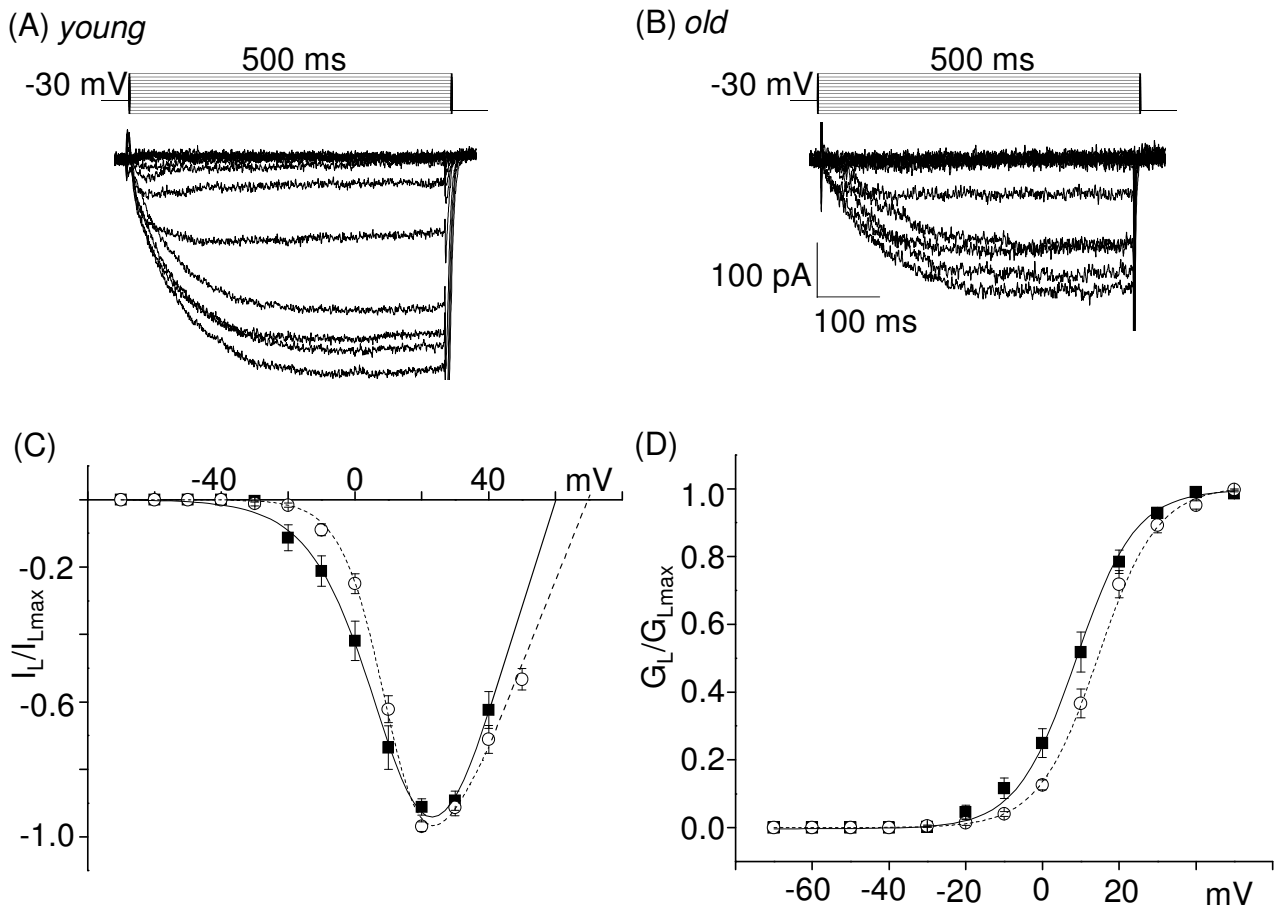
(A) young
500 ms
-30 mV
(B) old
500 ms
-30 mV
100 pA
100 ms
(C)
-40
0
40
mV
-0.2
-0.6
-1.0
I_L/I_{Lmax}
(D)
1.0
0.8
0.6
0.4
0.2
0.0
G_L/G_{Lmax}
-60
-40
-20
0
20
mV

Fig.6

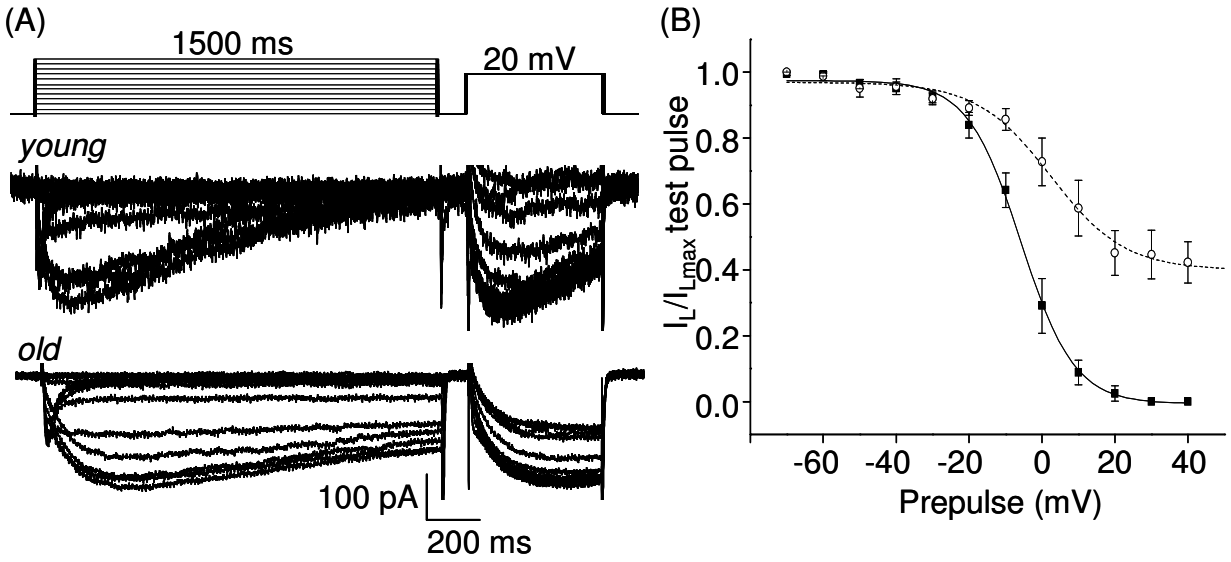
(A)
1500 ms
20 mV
young
old
100 pA
200 ms
(B)
1.0
0.8
0.6
0.4
0.2
0.0
I_L/I_{Lmax} test pulse
-60
-40
-20
0
20
40
Prepulse (mV)

Fig.7

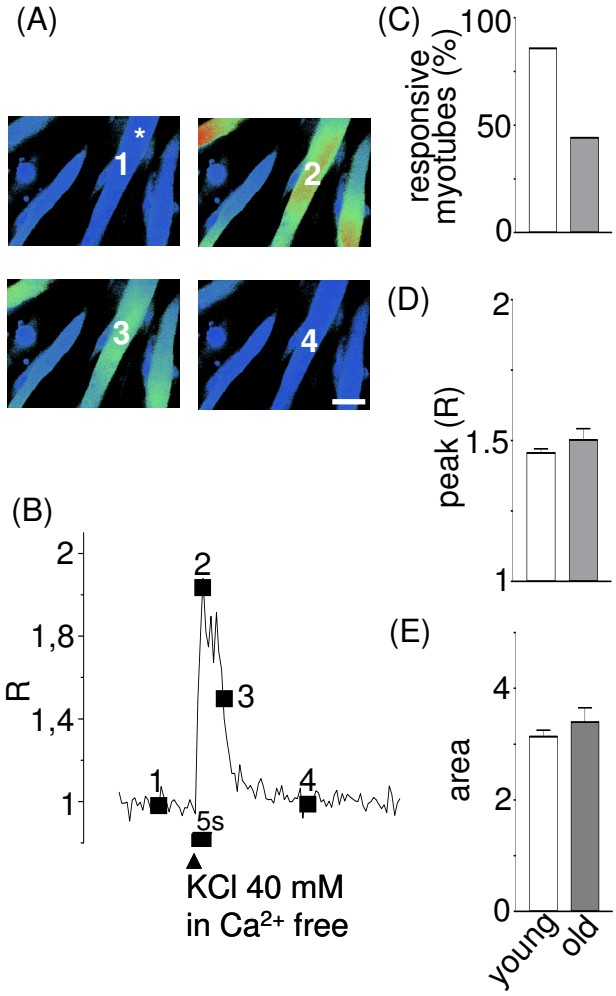
(A)
1
2
3
4
(C)
responsive myotubes (%)
100
50
0
(D)
peak (R)
2
1.5
1
(B)
R
2
1,8
1,4
1
1
2
3
4
5s
KCl 40 mM
in Ca2+ free
(E)
area
4
2
0
young
old

Fig.8

Table 1: Kinetic parameters of T-type Ca^{2+} current activation and inactivation in myotubes derived from the differentiation and fusion of satellite cells obtained from young and old donors (*n*= number of myotubes; data are presented as mean ± *SEM*, *** difference statistically extremely significant, *t-test, P=0.0001*; $V_{1/2}$ is the voltage at which the conductance is half maximal and k describes the steepness of activation of the fitted Boltzmann function: see Section 2.2).

T-type Ca^{2+} current	Activation			Inactivation		
	$V_{1/2}$ (mV)	k	*n*	$V_{1/2}$ (mV)	k	*n*
young	-32.14±0.75	5.66±0.55	12	-45.22±0.62	5.62±0.36	10
old	-32.25±0.79	7.04±0.62	8	-49.58±0.60 ***	5.76±0.34	8

Table 2: Kinetic parameters of L-type Ca^{2+} current activation and inactivation in myotubes derived from the differentiation and fusion of satellite cells obtained from young and old donors (*n*= number of myotubes; data are presented as mean ± *SEM*, *** difference statistically extremely significant, *t-test, P<0.0001,* ** difference statistically very significant, *t-test, P=0.0014*; $V_{1/2}$ is the voltage at which the conductance is half maximal and k describes the steepness of activation of the fitted Boltzmann function: see Section 2.2).

L-type Ca^{2+} current	Activation			Inactivation		
	$V_{1/2}$ (mV)	k	*n*	$V_{1/2}$ (mV)	k	*n*
young	8.73±0.93	7.72±0.49	16	-5.77±0.43	7.30±0.38	5
old	14.47±0.70 ***	7.74±0.45	16	2.38±1.65 **	10.1±1.46	5

8. Abstracts and Communications

- E. Luin, F. Ruzzier “Calcium currents during the in vitro ageing of murine myogenic cells” *56° Congresso Nazionale SIF (Società Italiana di Fisiologia) & Joint Symposium SIF-Physiological Society, Mondello (PA) (27-30.09.2005), poster*; published in Acta Physiologica, 188 (2006) S652, P173.

- E. Luin “Calcium currents and skeletal muscle aging” *13th Young Neuroscientists meeting (B.R.A.I.N. Centre for Neuroscience, Trieste (25.05.2006), oral communication*.

- E. Luin, F. Ruzzier “Calcium currents in human skeletal muscle during aging” *57° Congresso Nazionale SIF (Società Italiana di Fisiologia), Ravenna (25-27.09.2006), oral communication*; published in Acta Physiologica 188 (2006) S652,O17.

- E. Luin “L’omeostasi del calcio nella fisiologia dell’invecchiamento del muscolo scheletrico” *1° Riunione Nazionale dei Dottorandi di Fisiologia, Siena (17-21.07.2007), oral communication.*

- E.Luin, F. Ruzzier “L-type and T-type calcium currents kinetics during the aging process of human skeletal muscle satellite cells” *58° Congresso Nazionale SIF (Società Italiana di Fisiologia), Lecce (19-21.09.*2007), poster; published in Acta Physiologica 191 (2007) S657, P88.

- M. Sciancalepore, P. Lorenzon, E. Luin, F. Ruzzier “Properties and role of transient low voltage-activated Ca^{2+} channels during myogenesis” *IV Meeting Istituto Interuniversitario di Miologia (IIM), Roma (21-24.11.2007).*

9. Acknowledgements

I would like to thank some people for their contribution to this work, performed during my Ph. D. program, by mentioning them in the following.

I wish to thank Dr. Anton Wernig (University of Bonn) for the generous supply of i28 and human satellite cells, indispensable for carrying out my research on skeletal muscle aging, Dr. Daniela Pietrobon (University of Padova) for critical discussion, valuable comments and helpful suggestions, and Dr. Andy Constanti (School of Pharmacy, University of London) for critical reading, editorial assistance. and final revision of the two published manuscripts.

I have had the luck to work in Prof. Fabio Ruzzier's group since my undergraduate studies; I am grateful to him for this opportunity he gave me, and I would like to thank him for his personal help during these years and especially for the great friendship he showed to me. I also wish to thank all the people that I met in the lab in these years: Prof. Paola Lorenzon, especially for her affection, and for support during experiments and critical discussion of results; Dr. Marina Sciancalepore, for her friendship and for the enthusiasm she usually puts in doing research; Mihaela, Elena and Annalisa, companions of successful and unsuccessful experiments (and consolatory coffee-break!); Tamara, Vanessa and Arianna, for putting me in high spirits after a bad patch (a special thank to Vanessa, who helped me with the experiments on i28 myoblasts while working on her graduation thesis in the lab), and all the other undergraduate students.

I also would like to thank Alba and Gessica, Simona, Leo, Stefano, all the volleyball team-mates, and a lot of other friends, who did not contribute directly to this doctorate thesis, but had trust in my qualities, and brightened up the evenings after a day in lab in which the satellite cells had not cooperated in doing good patch-clamp experiments…

A special final thank to my father and my mother, who have always supported me lovely, and my brother and Piera, for their great affection and for sharing with me their love in doing research and in teaching respectively.

Last but not least Diego: THANK YOU for having been close to me during this Ph.D. experience and in every circumstance, and for having given me in these three years our marvellous dog Lampo first, and then the most wonderful present, our little Alessandro, who is smiling in my arms also while I'm typing these last words.